CHEMICAL REVIEWS

REVIEW

pubs.acs.org/CR

Metal−Organic Frameworks in Biomedicine

Patricia Horcajada,*[,†] Ruxandra Gref,[‡] Tarek Baati,[†] Phoebe K. Allan,[∥] Guillaume Maurin,[§] Patrick Couvreur,[‡] Gérard Férey,[†] Russell E. Morris,[∥] and Christian Serre*[,†]

[†]Institut Lavoisier, UMR CNRS 8180, Université de Versailles St-Quentin en Yvelines, 45 Avenue des Etats-Unis, 78035 Versailles Cedex, France

[‡]Faculté de Pharmacie, UMR CNRS 8612, Université Paris-Sud, 92296 Châtenay-Malabry Cedex, France

[§]Institut Charles Gerhardt Montpellier, UMR CNRS 5253, Université Montpellier 2, 34095 Montpellier cedex 05, France

[∥]EaStChem School of Chemistry, University of St. Andrews Purdie Building, St Andrews, KY16 9ST U.K.

CONTENTS

1. "BIOFRIENDLY" METAL−ORGANIC FRAMEWORKS

1.1. Influence of the Composition

Coordination polymers or MOFs (metal−organic frameworks) are the latest class of ordered porous solids.[1−5] Since their discovery in 1989 by Robson,[6] many potential applications have been proposed in strategic domains such as catalysis, separation, magnetism or others.[7,8] One of their key advantages compared to their organic (carbons) or inorganic counterparts (zeolites, silica), is the possibility to easily tune their composition through a change of the metal and/or the organic linker. Possible linkers are almost infinite, ranging from polycarboxylates, phosphonates, sulfonates, imidazolates, amines, pyridyl, phenolates. Thus, thousands of MOFs have been reported with at least a few hundreds of them being porous to nitrogen gas. Compared to zeolites, in addition to a wider chemical versatility, MOF structures exhibit a larger panel of pore sizes and shapes (tunnels, cages, etc), with sometimes a flexible porosity which allows to reversibly adapt the pore size to the adsorbate.[9,10] Functionalization of the organic linker represents another advantage of MOFs with the possibility of grafting during or after the synthesis various organic functionalities (polar, apolar), changing thus the physicochemical properties of the solid.[11]

However, the use of porous solids for biomedical applications requires a biologically friendly composition. So far, toxicity results dealing with MOFs or coordination polymers are very scarce. Data are mostly restricted to the toxicity evaluation of the metals and linkers taken individually. It is obvious to consider here only metals that exhibit an acceptable toxicity. One could argue that the decision to exclude one composition for biomedical application might depend on several parameters such as the application, the balance between risk and benefit, the kinetics of degradation, biodistribution, accumulation in tissues and organs and excretion from the body and so on. Thus, all metals and linkers could be used for such applications but at different doses depending on the above criteria. At first glance, most appropriate metals are Ca, Mg, Zn, Fe, Ti, or Zr whose toxicity, estimated by their oral lethal dose 50 (LD_{50}), range from few μg/kg up to more than 1 g/kg (calcium) (see Table 1). However, note that these values depend on the chemical formulation (salts, metal,

Special Issue: 2012 Metal-Organic Frameworks

Received: July 9, 2011
Published: December 14, 2011

Table 1. Oral LD_{50} (Rats) and Daily Requirements (Humans) of Selected Metals[a]

metal	LD_{50} (g/kg)	daily dose (mg)
Zr	4.1	0.05
Ti	25	0.8
Cu	0.025	2
Mn	1.5	5
Fe	0.45	15
Fe°	30	
Zn	0.35	15
Mg	8.1	350
Ca	1	1000

[a] Oral LD_{50}(in g/kg) for zirconyl acetate,[19,20] titanium dioxide,[21] copper(II)sulfate,[22] manganese(II) chloride,[23] iron(II) chloride,[24] zinc chloride,[25] magnesium chloride,[26] calcium chloride.[27]

counteranion, oxidation state ...). Another criterion concerns the metal daily dose, particularly if one considers the repetitive administration of the MOFs. If there is a need for daily doses of calcium, magnesium, and to a lesser extent zinc and iron, for titanium (or zirconium), if a very low daily dose is required (0.8 mg/kg per day), this metal is poorly absorbed (either by oral or dermal administration)[12] and is usually not considered as being toxic for specific applications, such as those related to cosmetics (LD_{50} > 25 g/kg). Concerning the linker itself, two possibilities are offered. The most common one is the use of exogenous linkers, synthetic or issued from natural compounds which do not intervene in the body cycles. Relevant exogenous MOFs for bioapplications are those built up from magnesium coordination polymers such as the magnesium 2, 5 dihydroxoterephthalate CPO-27(Mg) (CPO for Coordination Polymer from Oslo),[13] iron(III)polycarboxylates, such as MIL-100(Fe)[14] (MIL for Material from Institut Lavoisier) and zinc adeninate-4,4′ biphenyldicarboxylate BioMOF-1.[15] These solids exhibit large pore sizes (4−29 Å) and BET surface areas ranging from 1200 to 2200 $m^2 \cdot g^{-1}$, and in some cases exhibit accessible Lewis acid sites where biomolecules (NO, CO, H_2S, drugs,...) might coordinate strongly for a better control of the release.[16−18]

Here, to avoid possible toxic side-effects, exogenous linkers should be excreted from the body after in vivo administration of the MOFs. Toxicity data for a few specific organic linkers are available (LD_{50}) and indicate that typical polycarboxylic or imidazolate linkers are not very toxic at first sight, with rat oral doses of 1.13, 5.5 and 8.4 g/kg for terephthalic, trimesic, 2,6 napthalenedicarboxylic acid and 1-methylimidazole, respectively, because of their high polarity and a priori easy removal under physiological conditions.

Another possibility for MOFs based on exogenous linkers, concerns the use of functionalized linkers to tune their absorption−distribution−metabolism−excretion (ADME). Moreover, for adsorption and delivery of therapeutic molecules, the presence of functional groups within the framework can modulate the host−guest interactions allowing a better control of the release. The most common functionalized systems concern porous metal terephthalates based on iron or zinc whereas series of porous MOFs based on modified linkers that bear polar or apolar functional groups such as amino, nitro, chloro, bromo, carboxylate, methyl, perfluoro... have been reported (Figure 2).[11,28−31]One could also cite a recent series of organically modified porous Zn imidazolate solids.[32−36] In the case of functionalized flexible MOFs, please note that the functional group will not only modify the host−guest interactions but will also drastically affect the flexibility of the MOF during adsorption or delivery of the biomolecule.[29,30]

1.2. MOFs Built up from Endogenous Linkers

The second possible choice of linker concerns the use of endogenous organic spacers, that is, molecules that are constitutive part of body composition. Ideally, this would be the best case for the use of MOFs for bioapplications since the linker might be reused once administered in the body, which would strongly decrease the risk of adverse effects. A significant number of MOFs based on endogenous linkers have been reported so far.[40] For instance, the iron(III) gallate, fumarate or muconate MOFs exhibit either a rigid small pores structure or a highly flexible porous matrix.[41−43] A porous zinc aminoacid based MOF has also been reported that exhibit a flexible framework capable of accommodating carbon dioxide.[44] Series of cyclodextrin-based MOFs with rather large pore volumes have also been reported recently using however monovalent cations, which might restrict their practical use due to stability issues.[45] Finally, only a few of them are really porous and/or stable, i.e. capable of loading biological molecules of interest (Figure 3) and there is still a need to further develop new synthetic methods to produce endogenous porous and stable MOFs in a near future.

2. ADMINISTRATION: FORMULATION

The conditions required for a practical application of MOFs, for instance in the biomedical field, include the large scale production of suitable devices, adapted to each purpose. Scale-up synthesis of MOFs is a recent issue, which has emerged as a consequence of the increasing number of potential applications, mainly related to storage, separation or catalysis. New synthesis routes with appropriate space time yield (STY: kilograms of MOF product per cubic meter of reaction mixture per day), avoiding the use of expensive or dangerous reactants (toxic solvents, explosive precursors, acids, etc), and favoring low pressure conditions, are required.[49]Although most MOFs are produced at the (milligram−gram) laboratory scale, a few MOFs have been so far produced at the ton scale by BASF and are commercially available, such as the copper trimesate HKUST-1 (Basolite C300), the aluminum terephthalate MIL-53(Al) (Basolite A100), the magnesium formate (Basosiv M050), the zinc 2-methylimidazole (Basolite Z1200), or the iron trimesate Basolite F300.[50]

As mentioned above, the preparation of specific, practical and commercially marketable devices, suitable for each given application, is also required. This is a crucial step because it is well-known that shaping can sometimes reduce the performances obtained from the bulk solid. Specific formulations needed for bioapplication of MOFs include, between others, liquid, packed columns, tablets, suspensions, creams or nanoparticles.

2.1. Synthesis of Nanoparticles

Control of particle size is a key parameter because this dictates the chemical and physical properties of particles (rheology, reactivity, external surface, packing, etc.)[51−54] to obtain well-defined, reproducible and stable formulations. In addition, particle size is a limiting factor for some administration routes where very precise sizes are required. For instance, *parenteral route* requires stable solutions/suspensions of nanoparticles smaller than 200 nm to freely circulate through the smallest

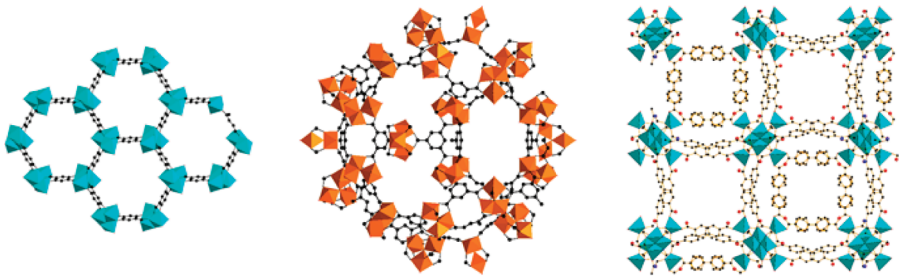

Figure 1. View of the structures of a few topical MOFs, here CPO-27(Mg, Zn)[13] (left), MIL-100(Fe)[14] (center)and Bio-MOF-1[15] (right), based on exogenous linkers for bioapplications. Metal Polyhedra and carbon atoms are in blue (Zn, Mg) or orange (Fe), and black, respectively.

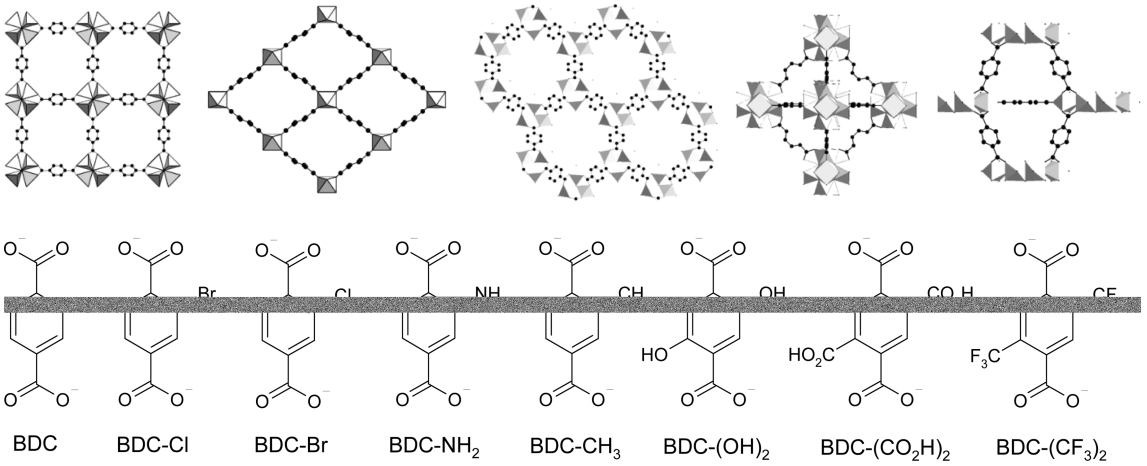

Figure 2. Top, from left to right, structures of MOF-5,[5a] MIL-53(Fe),[37] MIL-88B(Fe),[5j] UiO-66(Zr),[38] and MIL-125(Ti).[39] Bottom: selected modified terephthalic acids (BDC: 1,4 benzenedicarboxylic acid). Metal polyhedra and carbon atoms are in gray and black, respectively.

capillaries. As a consequence, preparation of homogeneous, monodispersed, and stable nanoparticles is an important issue tackled up to now through the following methods:

(i) The conventional **hydrosolvothermal** route playing on several parameters, such as the reaction time, temperature, stoichiometry, dilution pH, additives, etc. The flexible porous iron(III)dicarboxylates MIL-88A (150 nm),[55−58] MIL-88B_4CH_3 (40 nm),[55] or the porous zinc terephthalate MOF-5 (100−200 nm)[59] are topical examples obtained by decreasing reaction time or temperature, either using low temperature or atmospheric pressure conditions. Nanoparticles of the porous iron muconate MIL-89 (30 nm)[60] or the zinc imidazolate ZIF-8 (40 nm)[61]can also be obtained at low temperature using alcohols. Although particles diameters smaller than 100 nm are often obtained, the absence of an homogeneous and efficient heating usually leads to an important reduction of the yield and a high degree of polydispersity as a consequence of the lack of control of the nucleation and growth steps.[58] To tune the reaction kinetics or to slow down the nucleation−growth process, acidobasic or inhibiting additives (acetic acid, hydroxybenzoic acid, pyridine, ...)[60,62] are typically employed. Cho et al.[62]have proposed pyridine as an inhibitor in the solvothermal synthesis of porous indium terephthalate particles. Some of us have also used acetate ions as growth inhibitors for the preparation of small nanoparticles of the flexible porous iron muconate MIL-89 (30 nm).[60] Similarly, Tsuruoka et al.[63] have obtained nanorods of a porous Cu_2-(naphthalene dicarboxylate)$_2$(1,4-diazabicyclo(2,2,2)octane). Kerbellec et al. have also obtained very small nanoparticles of a luminescent terbium terephthalate (around 4−5 nm) by using a polyvinilpyrrolidone (PVP) polymer at ambient pressure and room temperature.[64] This method was further extended to other luminescent micro and nanoparticles of lanthanide (Tb, La, Tm, or Y) terephthalate MOFs.[65]

(ii) **Reverse-phase microemulsions**,[66−69] based on a metal source, an organic linker and micelles of cationic cetyltrimethylammonium bromide surfactant (CTAB) in an isooctane/1-hexanol/water mixture, led to nanometric nonporous Ln[66−68] or Mn[69] based polycarboxylates MOFs with interesting imaging properties (see section 8). This technique allows a control of particle size by tuning the dimensions of the micelles. However, very bad yields have been obtained because of the very large volumes of solvent required. In addition, the use of toxic compounds (CTAB LD_{50} (i.v. rats) = 44 mgkg^{-1},[70,71] isooctane LD_{50} (oral rats) = 3310 mg kg^{-1},[72] and hexane LD_{50} (oral rats) = 720 mg kg^{-1})[73] might strongly limit the biomedical applications of this kind of nanoMOFs.

(iii) **Sonochemical** synthesis, which is a rapid, facile and environmentally friendly method, which has recently been applied to the synthesis of micro and nanoscale MOFs. Ultrasonic irradiation leads to acoustic cavitation, associated to a collapse of bubbles, with localized hot spots and a very large gradient of temperature/pressure

dx.doi.org/10.1021/cr200256v |*Chem. Rev.* 2012, 112, 1232–1268

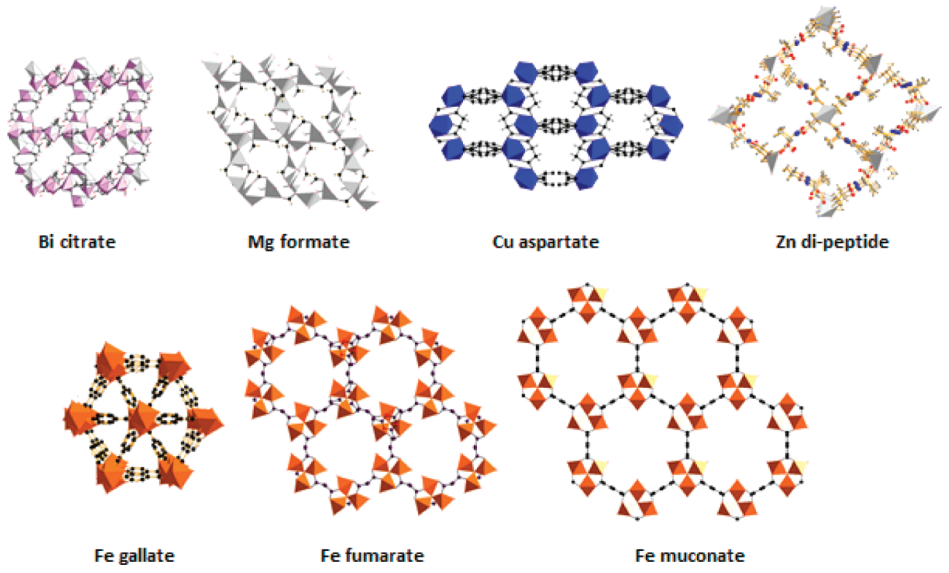

Figure 3. View of the structures of a few MOFs based on endogenous linkers (Bi citrate,[46] Mg formate,[47] Cu aspartate,[48] Zn-dipeptide,[44] Fe gallate,[41] Fe fumarate[42] and Fe muconate[43]). Metal polyhedral are in pink, gray, gray, blue, or orange (for Bi, Mg, Zn, Cu and Fe, respectively) and carbon atoms in black, respectively.

and a rapid mobility of the molecules. This favors the formation of high energy microreactors leading to the rapid crystallization of MOFs.[74,75] Microcrystals have been obtained for the microporous flexible iron(III) terephthalate MIL-53[76] and a rigid copper trimesate,[77] while other porous crystalline structures have been successfully prepared at the nanometric scale using ultrasonic conditions. Qiu's research group has described the ultrasonic synthesis at room temperature and ambient pressure of very high yields (75−85 wt %) nanoparticles of the porous copper trimesate HKUST-1 in DMF (10−200 nm)[78] and a zinc trimesate in ethanol (50−100 nm) with a selective sensing of organoamine.[79] Finally, particle size of the flexible porous iron fumarate MIL-88A can be modulated from 100 to 740 nm, the smallest particle sizes being obtained through the use of inhibitors, very high dilutions (0.01−0.008 M) or low temperatures (0 °C). As a consequence, only low yields are obtained (<5 wt %).[58]

(iv) **Microwave assisted** hydro/solvothermal synthesis, which is an efficient, homogeneous and faster method for the preparation of MOF nanoparticles. The high dielectric absorptivity of polar solvents leads to a highly efficient thermal conversion of the energy and thus to local superheated spots, favoring a fast and homogeneous nucleation over the crystal growth process.[80,81] The zinc terephthalate IRMOF-1, 2, and 3 (∼100 nm)[82] and the mesoporous chromium terephthalate MIL-101 (∼22 nm) were obtained using such a method.[83,84] More recently, some of us have successfully applied this concept to porous biocompatible MOFs, such as the flexible microporous iron terephthalate MIL-53 (350 × 1000 nm),[55] the mesoporous iron trimesate MIL-100 (∼200 nm),[55] the iron aminoterephthalate MIL-101_NH_2 (120 nm)[55,85] and the iron fumarate MIL-88A (∼20 nm; see Figure 4).[58]

Recent studies have compared different synthetic routes (hydro/solvothermal, ultrasonic, atmospheric pressure, mechanochemical, and microwave-assisted conditions) for the preparation of MOFs. The conclusion is that the best method to both obtain rapidly high yields and control the particle size, is the microwave irradiation solvothermal synthesis.[58,77]

Proposition: Regardless the method used to prepare the nanoparticles, the choice of the solvent is obviously crucial for biomedical applications. Indeed, the common frequently used solvents for the synthesis of MOFs are considered as toxic, with LD_{50} (oral administration in rats) values of 2800, 891, and 5628 $mg \cdot kg^{-1}$ for DMF,[86] pyridine,[87] and methanol,[88] respectively. Thus, such solvents shall be avoided as much as possible and hydrothermal synthesis routes should be preferred instead.

2.2. Shaping

Oral administration of MOFs can be also targeted, but requires chemically and mechanically stable formulations under the corresponding biological conditions (i.e., acidic stomach or basic intestinal conditions, intestinal motility, enzymes, etc.). Powders, pellets, tablets, or gels are some of the suitable formulations. To date, only tablets of ibuprofen-containing iron carboxylates MIL-53 and MIL-100, obtained using low pressures (0.5 Ton) without any binder but a correct stability under simulated body fluid conditions (SBF, 37 °C), have been proposed for controlled drug release.[27] However, several MOFs have been manufactured for catalysis or separation applications. Most of these shaping processes involve the use of binders to improve the stability. For bioapplications, the choice of the right additives for shaping will be restricted only to the biologically relevant excipients. However, several interesting concepts for the production of shaped MOFs have been reported in the literature. For instance, the chemical company BASF currently commercializes (through Sigma Aldrich) pellets and extrudates of several MOFs (MIL-53, iron trimesate, MOF-5 or HKUST-1)[89,90] using binders. Because of the lower mechanical or chemical stability of MOFs, there is however still an effort to further optimize the shaping processes.[91−93] Other interesting cases of shaped MOFs have been described, such as (i) the millimetric alumina beads of the zinc imidazolate MOF SIM-1,[94] (ii) the polyvinylalcohol-MIL-53(Al),[95] and (iii) the rubbery polydimethylsiloxane or polysulfone containing Cu-BTC MOFs.[96] Monolithic structures of

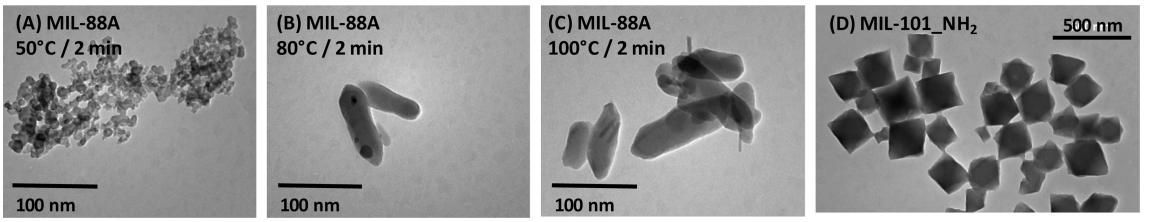

Figure 4. TEM images of nanoparticles made from microwave synthesis of MIL-88A at different temperatures (50 °C (A), 80 °C (B) and 100 °C (C)) and MIL-101_NH_2 (D).

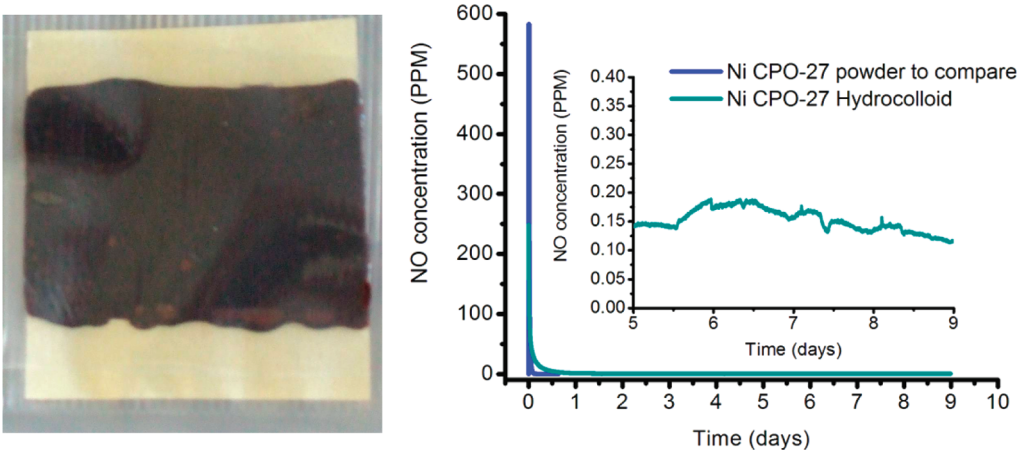

Figure 5. (Left): Photograph of a NO-loaded CPO-27(Ni) hydrocolloid. (Right): NO release curves for the CPO-27(Ni) hydrocolloid shown against a powder sample for comparison.

the copper trimesate HKUST-1 have also been obtained using methyl hydroxylpropylcellulose and methoxy-functionalized siloxane as additives using a two-step process including a molding batch in a lab-scale kneader followed by an extrusion process in a ram-extruder (Figure 5).[97]

Another novel approach for the synthesis of monolithic manufactured MOFs without the use of any binder or pelletizing processes is the sol−gel method.[98] For instance, the aging of a wet gel of the flexible microporous iron muconate MIL-89 in its mother solution led to a perfect monolithic xerogel.[60] Lohe et al. also obtained aero and xerogels of a quasi-amorphous porous iron trimesate with micro and macroporosity by a sol−gel method followed by supercritical CO_2 drying (Figure 6).[99] This kind of shaping could be appropriate in the biomedical domain to produce pellets, but also gels for oral, topical, or ocular administration, among others. Although the formation of such gels has been observed for many MOF systems, such as iron muconate MIL-89,[60] chromium terephthalate MIL-101,[84] copper or silver MOFs based on cyclotriveratrylene-type and trimesate ligands,[100] iron isophthalates,[101,102] and other manganese polycarboxylates,[103] the conditions required to obtain gelation over crystallization are still not fully sorted out.

Formulations, such as cream/ointment or patch/membrane, are needed for *topical administration* of MOFs. For instance, a wound healing antibacterial dressing based on NO-loaded nickel carboxylate CPO-27(Ni) particles (40%) and hydrocolloids (10% cellulose, 50% poly isobutanol (PIB)), widely used dressings in medicine,[104] have been prepared for the delivery of NO to the skin (Figure5). This composite patch is able to release NO over almost 10 days, which is extremely significant.

Making thin films or membranes of MOFs could also represent a suitable alternative to produce patches or composites. Homogeneous thin films of MOFs have been effectively prepared by simple and rapid wet methods (dip or spin coating) from stable colloidal solutions (Figure 6).[60,84,105] Thickness and packing of the film are easily tunable by multilayer deposition, control of the particle size and deposition conditions (extraction rate and solution concentration). Moreover, dense and continuous membranes of MOF-5,[106,107] HKUST-1,[108] Cu-(hfipbb)-(H_2hfipbb)$_{0.5}$ (hfipbb = 4,4′-(hexafluoroisopropylidene)bis(benzoic acid),[109] ZIF-8,[110−112] ZIF-7,[113,114] ZIF-90,[115] or MIL-53(Al)_NH_2[116] have been recently reported for gas separation. MOF membranes are prepared using a seeded surface by growing or deposing the MOF, or by producing a composite materials mixing MOFs with polymers such us polyimides (ZIF-90, MOF-5, Cu-4,40-bipyridine hexafluorosilicate)[115,117,118] poly(sulfone) (HKUST-1),[119] poly(vinyl acetate) (Cu-terephthalate),[120] or polyethyleneimine (ZIF-7).[114] However, for biomedical applications biologically acceptable polymers must be employed (polyvinylpyrrolidone, polyvinylalcohol, poly(lactic-co-glycolic acid), gelatin, etc.)

Finally, apart from composite devices made by mixing a MOF and an excipient (binder, polymers, ...), other complex MOF based materials have been prepared. The first method concerns the direct integration of a MOF into a polymer matrix. For instance, the copper trimesate HKUST-1 has been introduced within the monolithic macroporous hydrophilic polymer poly-HIPEs (Figure6).[121] Immobilization of MOF powders in easily flexible sheets of paper is also a convenient shaping method. Thus, from 6.5 to 14.6 wt % of the copper trimesate HKUST-1 has been unhomogeneously introduced in paper fibrous

dx.doi.org/10.1021/cr200256v |*Chem. Rev.* 2012, 112, 1232–1268

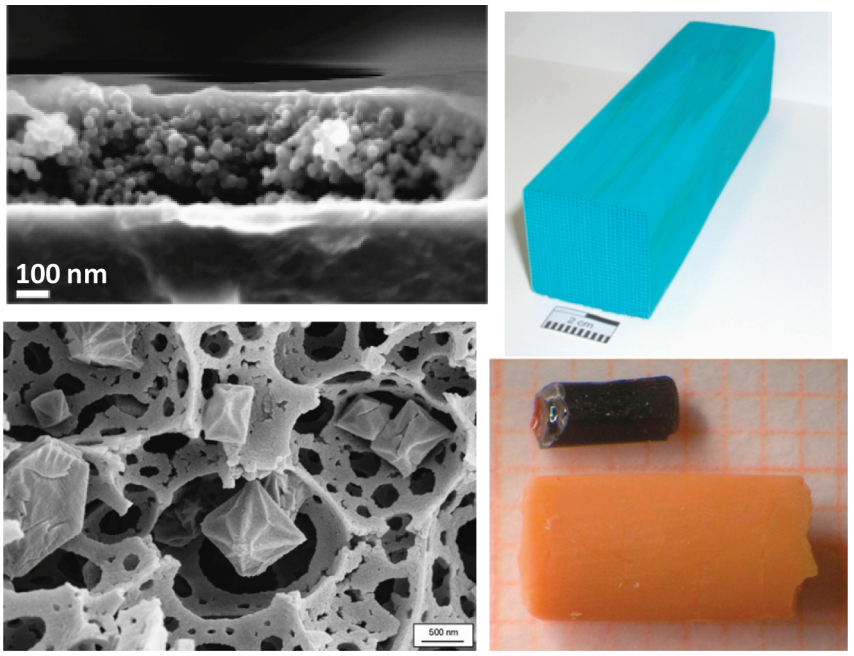

Figure 6. (Top left) FE-SEM images of the side view of a ZIF-8 thin film Reprinted with permission from Demessence et al.[105] Copyright 2010 Royal Society of Chemistry. (Bottom left) SEM image of HKUST-1 particles entrapped into a macroporous polyHIPE. Reprinted with permission from Schwab et al.[121] Copyright 2008 Wiley-VCH Verlag GmbH and Co. KGaA. (Top right) Monolith of HKUST-1. Reprinted with permission from Küsgens et al.[97] Copyright 2010 Wiley-Blackwell. (Bottom right) Aerogel obtained from 0.2 M trimesic acid solution in comparison with an air-dried xerogel of similar original size. Reprinted with permission from Aguado et al.[94] Copyright 2010 Royal Society of Chemistry.

networks.[122] A better method for the preparation of HKUST-1 containing sheets of paper has been obtained by direct growth of the MOF on the surface of pulp fibers,[123] improving the MOF-substrate adhesion by increasing the lignin content due to the presence of carbonyl or carboxylate groups.

Homogenous layers of the copper trimesate HKUST-1 and the iron trimesate MIL-100 have been obtained by electrospinning with a polymer as binder (polystyrene in tetrahydrofuran, polyvinylpyrrolidone in ethanol, or polyacrysonitrile in dimethylformamide). MOFs particles, arranged like a pearl necklace, were thus immobilized up to 80 wt % loading.[124] This is a promising shaping method for the production of MOF entrapped textiles clothing.

2.3. Surface Modification

The use of nanotechnology for drug delivery applications is widely expected to change the landscape of pharmaceutical and biotechnology industries for the foreseeable future, as by this way it might be possible to achieve: (i) targeted delivery in a cell- or tissue-specific manner, (ii) transcytosis of drugs across tight epithelial and endothelial barriers, (iii) delivery of drugs to intracellular sites of action, and (iv) visualization of sites of drug delivery by combining therapeutic agents with imaging modalities.

To achieve such challenging goals, an appropriate design of nanoparticulate systems is necessary. Indeed, the biophysicochemical properties of the nanoparticles, such as size, charge, surface hydrophilicity, as well as the nature and density of the ligands at their surface, are key factors which impact the circulating half-life of the particles as well as their biodistribution and targeting abilities. For instance, it has been shown that the ability of the nanoparticles to circulate in the bloodstream for a prolonged period of time is often a prerequisite for successful targeted delivery. To achieve this, hydrophilic "stealth" polymers, such as poly(ethylene glycol) (PEG), have been used as coating materials.[125] Such polymers shield the surface of the nanoparticle and thereby reduce opsonization by blood proteins and uptake by macrophages of the mononuclear phagocyte system.

Despite the tremendous interest in surface modification, there are only scarce examples of modified MOFs nanoparticles (nanoMOFs), certainly because of their novelty in the biomedicine domain. Recently, Gd-based nanoMOFs were prepared for theranostics and their surface was modified through the attachment of multifunctional polymer chains such as isopropylacrylamide and methacrylate derivatives.[126] In particular, PEG copolymers have also been coupled to these nanoMOFs.[127] However, there is a concern on the toxicity of the Gd-based materials and thus, iron-based nanoMOFs are a better alternative for such applications.[55−57]

In this case, a control of crystal growth has been achieved by adding PEG chains with only one terminal reactive group (amino or carboxyl) during the course of the nanoMOF synthesis, with a resulting 17 wt % of PEG attached to the nanoMOFs. The PEG chains have been assumed to form a superficial "brush" that would sterically protect the nanoparticles. PEG can be then removed only after nanoparticle degradation under serum conditions, in agreement with its strong binding to the nanoparticles through coordination of its amino or carboxyl end-group with the metal centers. Indeed, when PEG with two nonreactive monomethoxy end-groups has been added to the reaction mixture, a negligible incorporation has been observed. This method has been applied to other polymers such as chitosan grafted with alkyl side chains and dextran modified with biotin to modify the surface of iron carboxylate nanoMOFs.[55−57] However, investigations are still underway to further characterize the nanoMOF PEG shell and to check that it forms effective "brush"-like

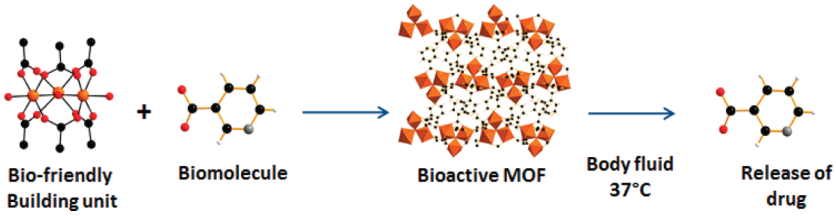

Figure 7. Schematic view of the formation of a BioMOF (Bio-MIL-1) built up from bioactive linker and its delivery. Here the bioactive linker is nicotinic acid. Iron, oxygen, nitrogen, and carbon atoms are in orange, red, gray, and black, respectively.

coatings able to prevent opsonin interaction, macrophage uptake, and thus to ensure prolonged blood circulation times.

Other interesting composite formulations consist in core−shell MOFs. For instance, PVP and silica were used to cover MOFs to control their degradation and delivery. Rieter et al.[68] have covered MOF nanoparticles made of a cisplatin derivative and Tb^{3+} ions with a shell of silica of around 7 nm. This improved the nanoparticle stability and allowed to control drug release by appropriately choosing the shell thickness.

Taylor-Pashow et al.[85] have covered postsynthesis with a silica coating nanoparticles made of iron terephthalate MIL-101 and modified with 17 mol % of amino-terephthalate ligands. A uniform layer of silica was obtained using Na_2SiO_3 as silica source. Interestingly, the release of the entrapped molecules was retarded presumably due to the slow diffusion through the shell. Moreover, the silica coated particles had adequate stabilities for biological applications, contrary to the uncoated ones, which readily decompose to presumably form amorphous iron hydroxide(oxide) phases.

3. BIOACTIVE MOFS

The most obvious use of a porous solid for bioapplications consists in benefiting from its pore volume to encapsulate an active molecule and deliver it through host−guest/diffusion/degradation considerations. This requires first a sufficient pore size and volume to optimize the cargo for a given biomolecule and second one has to load the cargo through an encapsulation step using a solution of the drug molecule followed by a cleaning step. This makes encapsulation success uncertain, in terms of loading, based on the size and the affinity of the molecule toward the porous matrix. In addition to the delivery of the biomolecule (see section 4), MOFs particles are likely to be degraded in the body fluid followed by a release of not only the metal but also the linker, often exogenous, raising additional toxicity concerns. If MOFs based on endogenous linkers and metals represent an acceptable alternative, only very few of them are really porous. Thus, another method will consist in complexing directly the active linker to a metal, which can also be active. So far, making cocrystals or complexes of active pharmaceutical ingredient (API) and low toxicity metals represents an easy method to tailor the dissolution kinetics of the API in the solution, resulting into improved administration conditions.[128−130] Modification of linkers and their hydrophobic character can also lead to a rationalization of the dissolution of the API-metal complex.[131] Recently, endogenous aminoacid and Zn- based MOFs that possess a therapeutic activity have been reported,.[132] Some examples are peptides, adenine, exonacin or norfloxacin drug based MOFs, but none of them was evaluated for a controlled released of the active molecule.[133−137] Recently, the proof of concept of "bioactive MOFs" for drug delivery applications, produced through the direct coupling of the biomolecule as the linker with a non toxic metal to prepare a MOF (Figure7), was reported.[138] The small pores iron(II/III) nicotinate BioMIL-1, based on nicotinic acid, also denoted niacin or vitamin B3, which possess pellagra-curative, vasodilating and antilipemic properties, is a rare example of bioactive MOF. Very high drug content, up to 71 wt %, was reached together with a fast release of the drug achieved through the degradation of the MOF in phosphate buffer solution (PBS) at 37 °C.

The rapid release of nicotinic acid from Bio-MIL-1 might be an issue for its practical use. However, it has been demonstrated that porous iron carboxylates based on the same trimeric secondary building units possess very different degradable characters. Indeed, the stability of a given MOF varies as a function of its composition (metal, number of complexing functions, hydrophobicity, ...). Thus, for a given bioactive linker, one could choose the right metal and structure for a suitable delivery. One could also point out that 80% of API possesses one or several complexing groups (carboxylates, phosphates, phosphates, amines or heterocycles, ...) that could be considered to build up a bioactive MOF with controlled degradation properties.

More recently, other iron or calcium based MOFs based on endogenous active dicarboxylic linkers have also been reported even if their degradability or their activity has not yet been disclosed (Figure 8).[139−142]One could cite either metal glutarates Bio-MIL-2 and −3, with glutaric acid as an experimental drug or metal derivated of azobenzenetetracarboxylates Bio-MIL-4 and Soc-MOF(Fe) or MIL-127 with an antimicrobial activity reported previously for azobenzene compounds.[143,144]

Another possibility for bioactive MOFs is to use an active metal. For instance, silver is well-known as an antibacterial agent, currently used for bioapplications. One could cite for instance the silver exchanged zeolites that are used in antibacterial systems.[145] So far, several nonporous silver coordination polymers have been intensively studied,[146] with antimicrobial properties.[147,148] Silver-based isonicotinate derivatives of bis-ethyleneglycol form a layered coordination polymer that, once deposited on a dental restorative material, using a flow chamber mimicking the oral cavity, kill bacteria upon contact with the substrate (Figure 9).[149] Authors mention that the activity is related to the release of silver and formation of nanoparticles from the coating.

The use of zinc as an antibacterial growth agent has also been reported,[150] and one can imagine that considering the huge number of existing Zinc based MOFs, interesting MOFs endowed with antibacterial activity might be found for adequate biomedical applications. Other MOFs based on active metals have also been reported, such as gadolinium, manganese, or iron polycarboxylates MOFs for their imaging properties. This part will be however detailed in section 8 of this article.

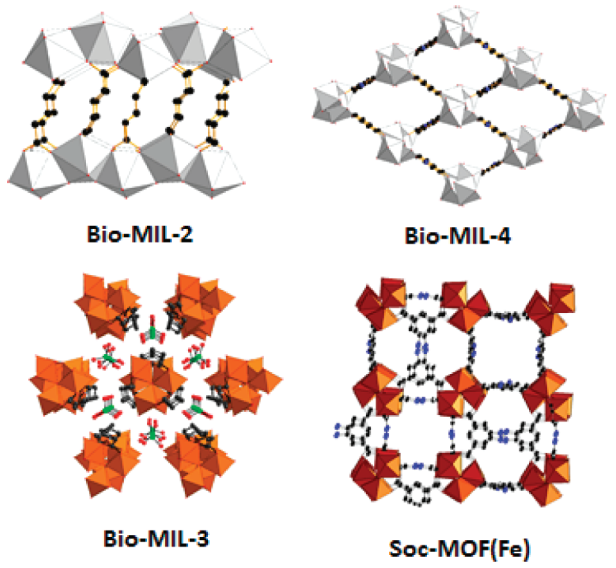

Figure 8. View of the structures of bioactive MOFs denoted Bio-MIL-2,[139] Bio-MIL-3,[140] Bio-MIL-4,[141] and Soc-MOF(Fe) or MIL-127.[142]

4. DRUG DELIVERY

4.1. Encapsulation and Delivery

Clinical use of many otherwise interesting APIs is severely limited if they suffer from important drawbacks such as low stability in biological conditions, poor solubility and/or inadequate ability to bypass natural barriers.[151] Since the 1970s, the biomedical development of drug nanocarriers has been pursued to find improved methods to protect both the organism from toxic side effects of the API from biological degradation, thus also increasing drug's efficiency and intracellular penetration.[152−154] In addition, the development of nanotechnologies has allowed specific targeting of tissues, cells and even subcellular structures.[155,156] Lipids or polymers are to date among the most studied drug nanocarriers.[157−160] Although therapeutic advantages reached by the use of drug nanocarriers have led to the commercialization of the first nanodrugs (Doxil, Abraxane, and Ambisome), there are still many potent drugs which have not yet been satisfactorily nanotransported, mainly because of the low drug loadings (<5 wt %) achieved, the presence of a burst release, poor biological barrier bypass and/or toxicity phenomena. Inorganic or hybrid porous materials have emerged as potential alternatives to organic nanocarriers. The high and regular porosity associated to important pore volumes and surface areas shall lead to an improvement of the drug loading capacities and ability to control drug release. Although interesting results have been obtained using purely inorganic zeolites,[161−165] they suffer from low loading capacities and toxicity concerns.[166] Other promising candidates are the ordered mesoporous silica materials,[167−172] which have shown interesting features such as high stability, important drug capacities and good biocompatibility.[171−175] In this context, MOFs which combine a highly regular porous crystalline hybrid inorganic−organic framework have been recently proposed as a new alternative.[18] First evidence of the high potential of porous MOFs for drug controlled delivery was given by some of us in 2006 by using a model drug, the anti-inflammatory and analgesic ibuprofen, and the model mesoporous rigid chromium carboxylates MOFs (MIL-100(Cr)[176] and MIL-101(Cr)[5h]). Despite the well-known toxicity of chromium

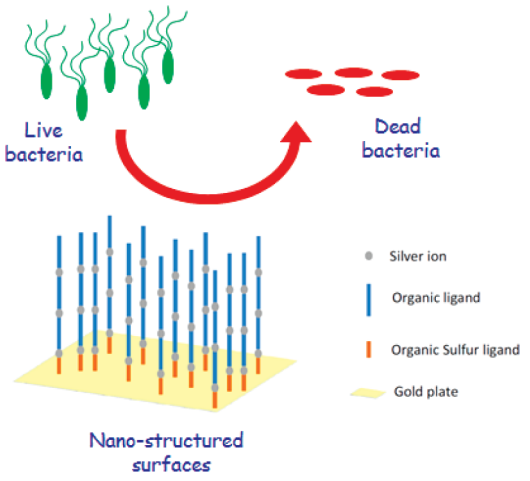

Figure 9. Schematic view of the use of an antibacterial silver based coordination polymers coated device (courtesy of Pr. K. Fromm (Friburg University, Switzerland)).

compounds, these MOFs have been chosen because of their (i) mesoporosity (cages of ø ≈ 25−34 Å) accessible from microporous windows (ø ≈ 5−16 Å) to permit the drug access, (ii) large pore volumes up to 2 $cm^3 \cdot g^{-1}$ and specific surface areas within the 2100−4400 $m^2.g^{-1}$ range (BET values), to ensure important drug loadings, and (iii) water stability, to avoid rapid degradation phenomena and drug release.

Ibuprofen has been encapsulated by a simple impregnation process into the porous MOFs. Exceptionally high drug loadings, up to 1.4 g of ibuprofen per gram of MIL-101(Cr), have been achieved, corresponding to ∼56 ibuprofen molecules in each smaller cage and ∼92 molecules in the larger cage. A comparison of the ibuprofen loading related with the pore size and volume of different porous solids, including MOFs, zeolites, and mesoporous silica, is given in Table 2. Ibuprofen loading in MIL-101 solid exhibits a loading capacity almost four and nine times higher than in mesoporous silica materials[171] and zeolites,[162] respectively. For zeolites, this is due to their smaller pore size and pore volumes. However, ordered mesoporous silica MCM-41 possesses a larger pore size and an important pore volume. Thus, the higher drug loading capacity of MIL-101 is probably the consequence of its higher surface area and the formation of specific interactions between the deprotonated ibuprofen molecules and the Lewis acid metal sites and the organic moieties of MOF, as supported by solid state ^{1}H NMR.[18] The much lower capacity of MIL-100(Cr) (0.35 g/g) in comparison with MIL-101(Cr) (1.38 g/g) is due to the non accessibility of Ibuprofen molecules (∼10 × 5 Å) to the smaller mesoporous cages, which are accessible only through narrow pentagonal windows (∼5 Å).

This approach has been extended in 2008 to the flexible microporous metal terephthalate MIL-53(Cr, Fe) solids,[37,177] which are able to reversibly modulate their pore size upon the application of an external stimuli (i.e., adsorption of gases,[178,179] liquids[180] or vapors,[181] as well as drug molecules[182]).[10] These solids adsorbed around 20 wt % of ibuprofen leading to an intermediate pore opening, consistent with the ibuprofen-containing MIL-53 form, as confirmed by X-ray powder diffraction (XRPD) characterization and computer modeling (see also section 4.2 below; Figure10). The lower capacity of MIL-53 solids in comparison with mesoporous MIL-100 and MIL-101 solids is due to its smaller pore volume (Table2). Interestingly, drug loading

Table 2. Pore Size and Pore Volume of Different Porous Solids, As Well As the Encapsulation/Release Results of Ibuprofen[a]

porous solid	pore size (Å)	V_p ($cm^3\ g^{-1}$)	S_{BET} ($m^2\ g^{-1}$)	ibuprofen loading (g/g)	time release (days)
MIL-101(Cr)	29−34[b]	2.0	4500	1.38	6
MIL-100(Cr)	25−29[c]	1.2	2100	0.35	3
MIL-100(Fe)	25−29[c]	1.1	2100	0.35	3
MIL-53(Cr)	8	0.5	1500	0.22	21
MIL-53(Fe)	8	0.5		0.21	21
Zeolite(Fau)	11	0.3	630	0.16	7
mesoporous silica (MCM-41)	36	1.0	1160	0.34	2
MCM-41_NH_2	28	0.4	780	0.22	5

[a] The release was achieved in SBF at 37°C. Table was reproduced with the permission of Wiley. [b] Accessible by microporous pentagonal (∼12 Å) and hexagonal (∼16 Å) windows. Smaller cages only accessible through pentagonal windows. [c] Accessible by microporous pentagonal (∼5 Å) and hexagonal (∼8.5 Å) windows. Smaller cages only accessible by pentagonal windows.

capacity does not depend on the nature of the metal (Fe or Cr), as similar capacities were found for the non toxic iron MIL-53 and MIL-100 analogues (for toxicity details see section 7; Table 1). This was an important result since similar exceptionally high loadings could be expected for the iron analogue of MIL-101.

In addition to the important drug loading capacities obtained using both rigid and flexible porous metal carboxylate MOFs, progressive release of ibuprofen has been achieved under biological simulated conditions (Figure 10). Pellets of the ibuprofen loaded MIL-100(Fe, Cr), MIL-101(Cr), and MIL-53(Fe, Cr) solids immersed at 37 °C in a simulated body fluid (SBF, pH 7.4), which possesses the same inorganic composition than human plasma, have fully released the drug cargo after 3, 6, or 21 days, respectively. In the case of rigid MIL-100 and MIL-101 materials, three different stages have been distinguished in the drug delivery profile according with the different adsorption sites of ibuprofen within the pores. Besides, the high stability of chromium solids in SBF enables us to conclude that the release of ibuprofen was mainly governed by diffusion processes combined with drug-matrix interactions.

On the other hand, the very long delivery of ibuprofen from flexible MIL-53(Fe, Cr) solids (3 weeks) is explained by the stronger drug confinement into the smaller one-dimensional pores and the specific hydrogen bonds between the carboxylic group of ibuprofen and the hydroxyl group of the solid, as confirmed by solid state ^{1}H NMR and DFT calculations (see more details in section 4.2).[177] Slow release profile of ibuprofen corresponded to a predictable and concentration independent zero order kinetic. This unexpected result makes the flexibility of MOFs an interesting property for the better control of the drug release by both the optimization of the drug-MOF interactions and the drug diffusion through the pores.

Later on, An et al.[15] reported an important encapsulation of the cationic antiarrythmic drug, procainamide, into the mono-dimensional pore system of the anionic zinc adeninate framework Zn_8(adeninate)$_4$(biphenyldicarboxylate)$_6O_2Me_2NH_2$.8DMF.11H_2O, so-called BioMOF-1. Noteworthy, the short in vivo half-life of procainamide necessitate to administer this compound every 3−4 h, making thus interesting the possibility of a controlled release of this drug.[183] Therefore, the loading of procainamide has been performed via a slow ionic exchange by single suspension of the solid into a drug solution, leading to a loading up to 22 wt % after 15 days (Table 2). This corresponds to approximatively 2.5 and 1 procainamide molecules per formula unit within the pores or at the outer surface, respectively. Note that the 8 toxic DMF molecules remaining in each cage of the as-synthesized solid have been substituted after the drug loading, leading to Zn_8(adeninate)$_4$(biphenyldicarboxylate)$_6O_{3.5}$(procainamide)-H^+)1.5Cl^-·16.5H_2O formula. Release of the procainamide has been achieved after 3 days in a phosphate buffer pH 7.4 (PBS). The stability of the Zn framework after release tests proves that procainamide delivery is governed by a cationic exchange. However, only 20% of the loaded procainamide was released using pure water, confirming the strong ionic interaction between procainamide and the anionic network. Ionic drugs can then be successfully entrapped and delivered from ionic MOFs.

Highly challenging drugs, such as the antitumoral busulfan (Bu) or doxorubicin (Doxo) and the antiviral azidothimidine triphosphate (AZT-Tp) or cidofovir (CDV), have also been recently entrapped into nanoparticles of different porous iron carboxylate MOFs.[55] These drugs suffer from important drawbacks such as poor solubility and/or stability in the biological aqueous media, often resulting in short half-lives, low bioavailabilities, and limited bypassing of biological barriers. Nontoxic porous iron(III) carboxylates MOFs nanoparticles have been recently proposed to circumvent these drawbacks.

The *amphiphilic* bifunctional alkylating agent busulfan, widely used in combination high-dose chemotherapy regimens in leukemias,[184,185] possesses a poor stability in aqueous solution and an important hepatic toxicity because of its microcrystallization in the hepatic microvenous system.[186] Although many drug nanocarriers have been attempted for entrapping busulfan, the low affinity of this amphiphilic molecule toward the nanocarriers has led to loading capacities lower than 5−6 wt %[187] and relatively fast release patterns[188] using polymeric nanocarriers. Using porous iron carboxylates MOFs, encapsulation of this challenging antitumoral molecule has been successfully performed with unprecedented loadings exceeding 25 wt %, which would allow the administration of high drug doses using low amounts of MOFs nanocarriers (Table 3).[55−57,189] Moreover, entrapping busulfan into porous nanoparticles not only protects this drug from biodegradation (as confirmed by liquid state ^{1}H NMR), but also from the microcrystallization likely responsible of hepatotoxic phenomena. Finally, although the release of busulfan seemed better controlled compared to polymeric systems,[188] it still needs to be improved (Figure 11). Thus, computer simulation has predicted that busulfan release might be further slowed down by the introduction of amino functionalized linkers (see section 4.2).

Nucleoside analogues such as AZT-Tp, used in the treatment of AIDS and HIV infection, or CDV, an antismallpox agent,

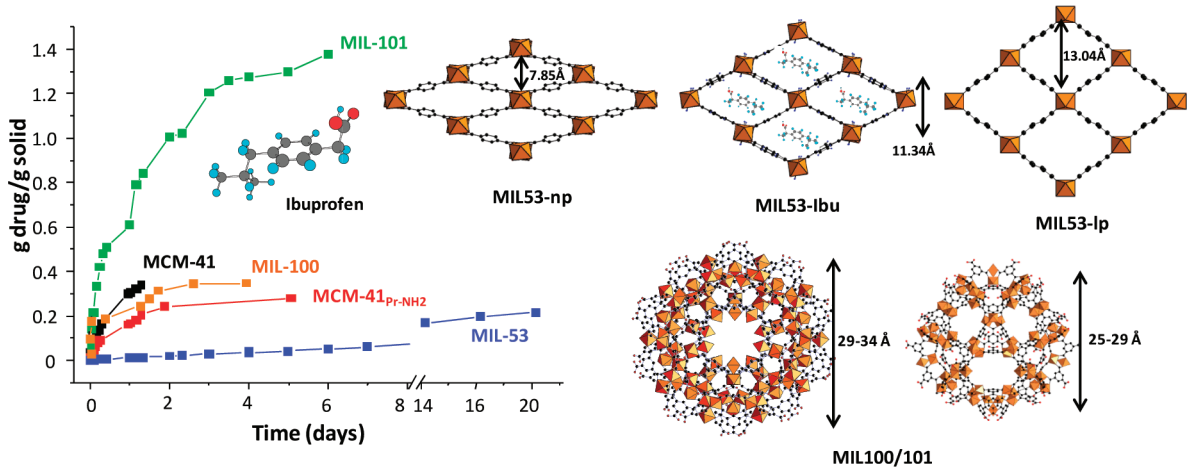

Figure 10. (Left): Kinetics of delivery of Ibuprofen from several porous MOFs carriers (SBF, 37 °C); (Top right): Pore openings of the MIL-53 solid: water (left), ibuprofen (center) and open form (right); (Bottom right): Schematic view of the larger cage (left) and the smaller cage (right) of MIL-100. Metal octahedra, oxygen and carbon atoms are in orange, red, and black, respectively. Reprinted with the permission from refs 18 and 177. Copyright 2006 Wiley-VCH Verlag GMBH and Co. KGaA and Copyright 2002 American Chemical Society, respectively.

Table 3. Drug Loading Capacities of Different Drugs on Several Porous MOFs

	drug loading (wt%)			
drug	BioMOF-1	MIL-100	MIL-101_NH_2	MIL-53
ethoxysuccinato-cisplatin			12.8	
procainamide	22			
busulfan		25.5		14.3
azidothimidine triphosphate		21.2	42.0	0.24
azidothimidine		6.1		
cidofovir		16.1	41.9	
doxorubicin		9.1		
ibuprofen		33		22
caffeine		24.2		23.1
urea		69.2		63.5
benzophenone 4		15.2		5
benzophenone 3		1.5		

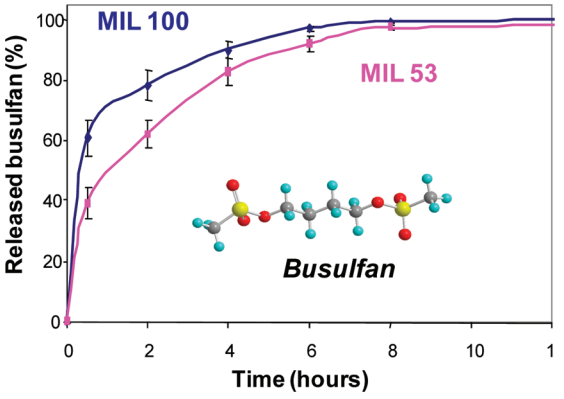

Figure 11. Kinetics of delivery of busulfan from MIL-100 (blue) and MIL-53 (pink) nanoparticles (PBS, 37 °C). Busulfan chemical structure: sulfur, oxygen, carbon and hydrogen atoms are in yellow, red, gray, and blue, respectively. Reproduced with the permission from Chalati et al.[189] Copyright 2011 Pan Standford Publishing Pte. Ltd.

exhibit similar challenges as Busulfan. Clinical use of nucleotide analogues is, indeed, limited by their poor stability in biological medium[190] and their limited intracellular penetration as consequence of their important *hydrophilic* character.[191,192] One of the main limitations in the use of nucleoside reverse transcriptase inhibitors (NRTIs) lies in their poor intracellular activation by cellular kinases into their active triphosphorylated form. Although the direct administration of triphosphate NRTIs has been considered for bypassing this metabolic bottleneck, these phosphorylated molecules do not diffuse intracellularly, due to their still more hydrophilic character than the parent NRTI.[191,192] Thus, nanocarriers have been developed to circumvent these inconveniences, but poor efficiencies together with "burst effects" have been observed.[193]

Once more, encapsulation of these highly hydrophilic nucleoside analogues (CDV and AZT-Tp) has been successful with encapsulation rates up to 42 wt % or 21 wt % using the iron aminoterephthalate MIL-101(Fe)_NH_2 or the iron trimesate MIL-100 nanoparticles (Table 3).[55−57,140] Remarkably, these unprecedented values exceeded by a forty or twenty factor the encapsulation rate in other systems.[193,194] Also, very high loading efficiencies (up to 90%), were achieved, explainable by the very high affinity of the drug with these hybrid nanoparticles. This could be due to the presence of free Lewis acid metal sites that can strongly interact with the phosphate groups of CDV and AZT-TP, as evidenced by solid state ^{31}P NMR.[140]

As expected, encapsulation of AZT-TP in flexible MOF nanoparticles (MIL-89, MIL-88A, and MIL-53) with pore sizes smaller than the drug dimensions have led to very poor loadings, not exceeding 2 wt % (Table 3).[140] This fact, together with the absence of any accessible (N_2, 77 K) porosity, is in agreement with the presence of the drug into the larger pores MOFs. Moreover, while a clear burst effect has been observed using the flexible nanoparticles of MIL-89, MIL-88A, and MIL-53 solids containing AZT-TP (only at the outer surface), the drug has been progressively released after 5 days from MIL-100 nanoparticles in PBS or in culture medium (RPMI 1640 supplemented with serum). This is related to the diffusion of the drug through the pores (Figure 11 and 12).[55,140] Drug release does not depend only on the diffusion rate, but also on the kinetics of material

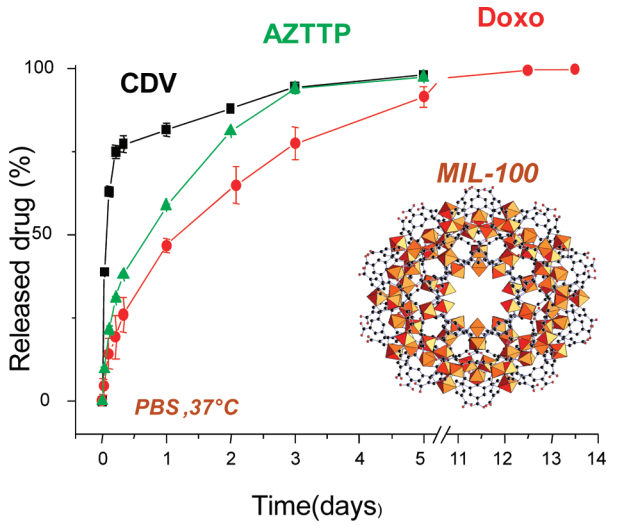

Figure 12. Kinetics of drug delivery in PBS, 37 °C of cidofovir (CDV; black), azidothimidin triphosphate (AZT-Tp; green) and Doxorubicin (Doxo; red) from nanoparticles of MIL-100(Fe). Reproduced with permission from Horcajada et al.[55] Copyright 2010 Nature Publishing Group.

degradation and on the drug-matrix interactions. Thus, the very large amount of AZT-TP entrapped into the MIL-101_NH_2 nanoparticles has been rapidly released in the PBS medium because of the lower stability of this solid. On the contrary, degradation of the MIL-100 nanoparticles did not significantly affect the release of the cargo since only 10% of MIL-100 solid was degraded under similar release conditions.[55] Finally, native non phosphorilated azidothimidine (AZT) has been encapsulated in the MIL-100 nanoparticles, showing a much lower loading capacity (6 wt %) and a faster release (more than 80% release in the first hour) than the phosphorilated AZT-TP (Figure 12).[140] Such differences in kinetics of release might be due to the presence of stronger interactions, as a consequence of the coordination of the polyphosphate groups of AZT-TP to the iron Lewis acid iron sites. In conclusion, the drug release can be modulated by controlling: (i) drug interaction with the matrix though the functionalization of the MOF, (ii) drug diffusion throughout the pores, by modulating pore size, connectivity, or morphology, and (iii) kinetics of degradation of the MOF.

Taylor-Pashow et al.[85] have reported the encapsulation of the *hydrophobic* ethoxysuccinato-cisplatin, a prodrug of the hydrophilic antitumoral drug cisplatin, with loadings up to 13 wt % into the silica covered iron terephthalate MIL-101 modified with 17 mol % of amino-terephthalate ligands (Table 3). Amino-terephthalate linker has allowed the grafting of the contrast imaging agent Br-BODIPY (1,3,5,7-tetramethyl-4,4-difluoro-8-bromomethyl-4-bora-3*a*,4*a*-diaza-*s*-indacene). Silica has been used to cover and protect the nanoparticles from fast degradation in presence of phosphate buffer which slowed down the drug delivery rate from 14 h in the pristine MIL-101 to 72 h in the silica coated nanoparticles.

Other interesting hydrophobic antitumoral drug, considered as one of the most effective drug in the breast cancer treatment, is the doxorubicin (doxo). This molecule suffers however from common resistance drawbacks.[195] Entrapment into nanocarriers has been found to overcome cancer multidrug resistance.[196] Thus, a similar approach has been developed with MIL-100 nanoparticles and a very high loading of doxo (up to 9 wt %) has been achieved.[55] Furthermore, doxo has been totally and progressively

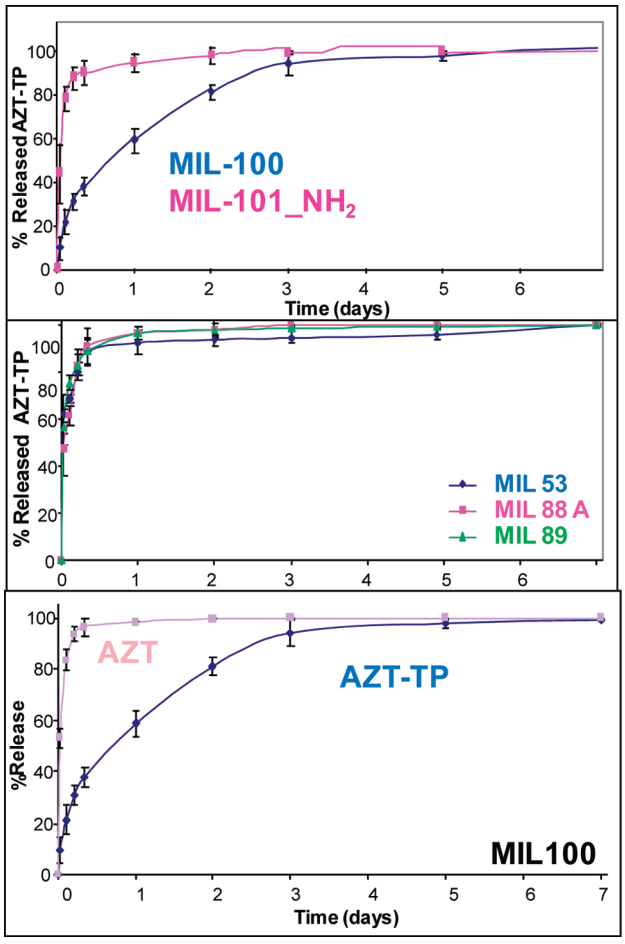

Figure 13. Kinetics of drug delivery in PBS, 37 °C of (i, top) azidothimidin triphosphate from MIL-100 (blue) and MIL-101_NH_2 (pink) nanoparticles; (i, middle) azidothimidin triphosphate from MIL-53 (blue), MIL-88A (pink) and MIL-89 nanoparticles (green); and (iii, bottom) azidothimidin triphosphate (AZT-Tp; blue) and azidothimidin (AZT; pink) from MIL-100 nanoparticles.

released in PBS from these nanoparticles after 2 weeks without any 'burst effect" (Figure 12).

Ke et al.[197] has recently reported the encapsulation and delivery of the hydrophobic anticancer drug, nimesulide, from a magnetic nanocomposite material made from the cupper trimesate HKUST-1 and Fe_3O_4 nanorods. The total amount of the loaded drug (0.2 g/g) was released after 11 days in physiological saline medium (0.9% w/v NaCl). This release time is however not comparable to other published values. Indeed, the choice of the release medium is essential, since the presence of highly complexant phosphates in the release medium (PBS) can compete for the metal sites and/or degrade the MOF, leading to a faster release.

Finally, other active molecules, either drugs or cosmetics, with different structures and physicochemical properties have been successfully encapsulated into different iron carboxylates MIL-53 and MIL-100 (Table 3), suggesting that the internal amphiphilic microenvironment is well adapted for the adsorption of a large number of guests.[55−57,198]

4.2. Computer Modeling

Molecular simulations are valuable tools to complement a large variety of experimental techniques (infrared, NMR, X-ray

diffraction) for not only probing the drug/porous host interactions but also exploring the dynamic properties of the drugs within the porosity. In addition, statistical approaches conducted from accurate sets of experimental data, are potentially very promising for rationalizing and further predicting several properties of porous materials including their drug uptake/release or their degradability. Up to now, semiempirical molecular orbital methods were first employed to elucidate the preferential geometries and conformations of a series of drug molecules confined in zeolite materials, further providing an estimation of the interaction energy in play.[199−201]

Density Functional Theory (DFT) calculations were also used for characterizing the structure of an antidepressant drug, the sertraline, within the interlayer of clay mineral and in the porosity of the MCM-41 mesoporous materials.[202] Beyond the quantum calculations, Molecular Dynamics simulations based on generic forcefields for representing the drug/porous host interactions have been further conducted to characterize the behavior of some drugs intercalated within the galleries of anionic clays.[203] Such a computational approach allowed to define the most stable arrangements and conformations of the confined biological molecules that have been further compared to those observed in the gas/liquid state. While the literature reporting modeling studies on the drug/porous solid systems is rather scarce, it is even more crying when one looks specifically at the family of the hybrid porous MOF type materials. Apart from our studies that will be summarized in this section, the only investigation reported so far was performed by Babarao et al.[204] who have explored the structural and dynamic behavior of ibuprofen in two MOF type materials, MIL-101 and UMCM-1. While the host/drug binding energy was estimated by means of DFT calculations, Monte Carlo simulations were able to both predict the drug uptake and further bring some insight into the microscopic adsorption mechanism in play. Molecular Dynamics simulations were also employed to follow the mobility of ibuprofen within the MOF cavities, with the crude approximation of neglecting the role of the physiological body fluid, which is expected to drastically underestimate the mobility of the drugs in play during the real in vivo release process.

4.2.1. Density Functional Theory Calculations. Our computational effort was first concentrated on probing the drug/MOF interactions by means of DFT calculations in conjunction with several experimental techniques. Such a joint experimental-computational approach is a powerful tool to elucidate the geometric and energetic behavior of the drugs confined within the porosity of MOFs that can further bring some insight into not only the adsorption mechanism but also the first step of the release kinetics. One challenge was to tackle the encapsulation of both amphiphilic (caffeine, busulfan) and hydrophobic (ibuprofen) drug molecules in the highly flexible iron terephthalate MIL-53(Fe)[37] that is known to adapt its pore size to the nature of the guest as already discussed above.

As a first step, a computational assisted structure determination approach has been employed to solve the structure of the hybrid porous framework in presence of ibuprofen[182] and busulfan.[189] Such a strategy that has been successfully used for solving the complex hybrid structures including flexible MOFs,[29,205,206] consisted of starting with the atomic coordinates of the empty MIL-53(Fe) form and imposing the lattice parameters obtained in presence of each drug from the refinement of the experimental ex situ X-ray powder diffraction patterns. The structures were then energy-minimized using generic forcefield for describing the intra- and intermolecular interactions, with fixed lattice parameters. DFT calculations were further performed to optimize only the geometries of the drug molecules.

It has been shown that the most likely interaction for the ibuprofen molecule involves a strong hydrogen bonding between the oxygen of its carboxylic group and the μ_2-OH groups present at the surface of the MIL-53(Fe) material, consistent with Infrared spectroscopy measurements.[182] In addition, weaker van der Walls or CH$-\pi$ interactions were found between the hydroxyl and the methyl groups of the drug molecule and the inorganic/organic part of the matrix (Figure 14a). It has been further evidenced that the structure of the confined ibuprofen is only slightly perturbed compared to the bulk phase, with only a tiny reorientation of its carboxylic group resulting from the interactions with the pore wall. Such a behavior, which has been confirmed by ^{13}C NMR measurements, is consistent with those reported for the same molecule within the porosity of different microporous and mesoporous materials.[36,37]

The interactions between the busulfan and the host matrix were found to be also governed by the formation of strong hydrogen bonding between the μ_2-OH groups and the oxygen atoms of the sulfonate functions present in the drug molecule (Figure 14b).[189] Here, the two sulfonate functions can interact simultaneously via hydrogen bonds with the opposite pore wall of the MIL-53(Fe) that leads to a binding energy of -69.6 kJ·mol^{-1} slightly higher than those observed for ibuprofen (-57.4 kJ·mol^{-1})[41] where only one carboxylate group is involved. It was thus possible to emphasize that the pore contraction of the MIL-53(Fe) results from a critical interplay between energetic and steric considerations. Indeed, although the dimension of busulfan is larger (13.4×3.5 Å) than those of ibuprofen (10×5 Å), the stronger interactions with the pore wall evidenced by the DFT calculations tend to favor a larger contraction of the unit cell volume (1339 Å^{3}vs 1406 Å^3) as experimentally determined by ex situ X-ray diffraction.

In absence of ex situ X-ray diffraction data, a full relaxation of the system, including both the optimization of the pore opening for the host and the geometry within the porosity for the drug molecule, needs to be addressed. While, the highly flexible behavior of this family of MOFs, has been tackled from classical simulations based on specific derived forcefield,[207,208] only one attempt has been reported recently in the literature to look at this phenomenon using DFT calculations,[209] emphasizing the complexity of such problem when treated at the quantum level. In that context, the encapsulation of caffeine in the same MIL-53(Fe) material was investigated starting from scratch. The full energy optimization of this system has predicted a slightly larger contraction of the unit cell volume (1289 Å^3) than observed for the two above-mentioned drug molecules associated to a strong hydrogen bonding between the μ_2-OH groups and the oxygen of the carbonyl group of the caffeine (Figure 14c). The arrangement of the molecule within the pore significantly differs from busulfan and ibuprofen. While these latter molecules are aligned along the direction of the tunnel as shown in Figures 14a and 14b, caffeine because of its smaller dimension (6.1×7.6 Å) adopts an orientation at a slight angle to the channel axis (Figure 14c). The resulting geometry leads to a binding energy of -62.6 kJ·mol^{-1} significantly higher than for ibuprofen (-57.4 kJ·mol^{-1}) which involves the interactions between the same functions. This energetic difference is explained by the fact that the additional interactions between the atoms of the caffeine and both organic and inorganic parts of the MIL-53(Fe) correspond to short distances as the confinement is more pronounced than for ibuprofen. These

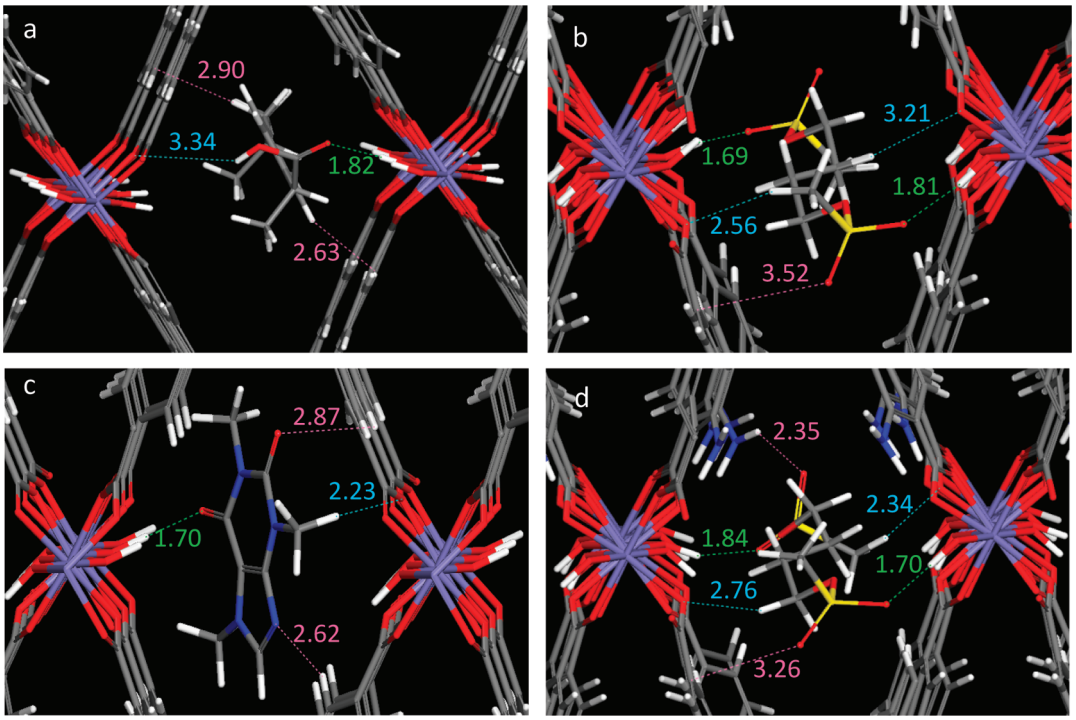

Figure 14. DFT optimized geometries of ibuprofen (a), busulfan (b), and caffeine (c) within the pores of the non modified MIL-53(Fe), and of caffeine in the functionalized MIL-53(Fe)-NH_2 (d). The different interactions between the drug and the host matrix are distinguished by colors (green, blue light and pink for the interactions with the μ2-OH groups, the inorganic nodes and the organic linkers respectively) and the distances are reported in Å.

predictions have been recently validated by experimental ex situ X-ray diffraction data.[140]

Indeed, it was clearly shown for each of the three investigated drugs, that the presence of the μ2-OH groups at the MIL-53(Fe) surface mainly governs the encapsulation mechanism, allowing a strong linking of the drug molecules to the pore wall, associated to high binding energies that would suggest a slow first step of the release in this material. A complementary exploration consisted of probing the influence of amine-functionalized organic linker on the structural and energetic features of the confined caffeine and busulfan molecules as it was widely reported in the literature that grafting such amino groups allows either to enhance the drug uptake or to slow down the release process.[210−212] It was thus observed that the -NH_2 functional group grafted on the organic linker serve as an additional anchoring points for both investigated drugs, leading to rather strong interaction with the oxygen atoms of the sulfonate and the carbonyl groups respectively with characteristic H(NH_2)-O distances ranging from 2.20 to 2.40 Å. In the meantime, the main hydrogen bonding interactions between the drugs and the μ_2-OH groups of the pore wall remain almost unchanged compared to the nonmodified MIL-53(Fe) form. An illustration of such geometry is provided in Figure 14 for the encapsulation of busulfan in this MOF type material. Further, while it has been shown that the pore size remains only slightly modified, the resulting interaction energies for both drugs were found to be between 5 and 7 kJ·mol^{-1} higher than in absence of functionalized linkers.[189,140] Such an enhancement of the drug/matrix interactions is expected to lead to an increase of the energy barrier required to be overpassed prior to triggering the delivery process, thus leading to a slower initial step of the drug release.

4.2.2. Quantitative Structure Activity Relationship Approach. The quantitative structure activity relationship (QSAR) approach can be seen as a "soft" computational method that aims at establishing a correlation between a property and some relevant descriptors that characterize the physicochemical features of the structure. While the previous DFT calculations would be too time-consuming for screening a wide range of structures, this method is based on a fast calculation of a large number of molecular descriptors that are further correlated to the property of interest. Although such a strategy has been intensively used in pharmaceutical drug design,[213] biology[214,215] and catalysis,[216] its application in the field of nanomaterials is relatively recent and remains relatively scarce. Recently, Leflaive et al. have employed such a method based on different statistical tools to predict the adsorption enthalpies of various alkanes on zeolites.[217,218] Regarding MOFs, the only investigation that was reported so far, comes from Kim et al.[219] who have built QSAR models by using linear regression analysis to predict the hydrogen uptake in a series of ten MOFs, which differ by their topologies.

Following the conclusions drawn from our DFT calculations which clearly stated that the drug/MOF interactions can be tuned by grafting amino functions, a QSAR approach has been conducted to rationalize the caffeine uptake measured experimentally by high performance liquid chromatography (HPLC) in a series of flexible iron terephthalate MIL-88B(Fe) materials wherein functional groups of various polarity, hydrophilicity and acidity (−Br, −F, −CH_3, −NH_2, −NO_2, −OH, −CF_3) have been introduced through the aromatic linker.[220] Indeed, the corresponding set of experimental data was an ideal starting point for performing such statistical strategy since it covers a broad chemical space and it is obtained from a rigorous chemical analysis based on the same methodology applied for all samples. A large variety of molecular descriptors has been first calculated to describe the topological, chemical and electronic features of each functionalized organic linker. A forward selection was then

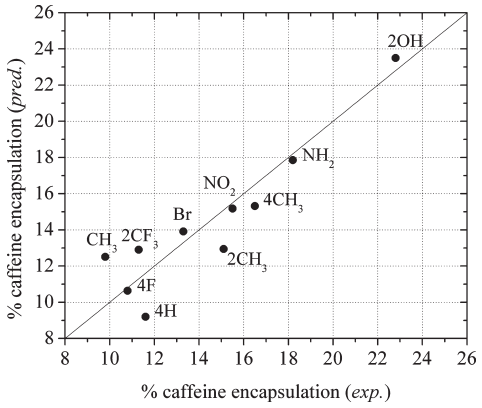

Figure 15. Predicted versus observed caffeine uptake rate for the set of functionalized MIL-88B(Fe) materials (n = 10) based on a validated QSAR model.[220]

applied to identify the most correlated descriptors to the caffeine uptake. The QSAR model constructed using a multiple linear regression method, consists of a linear combination of three descriptors that represents the predicted drug uptake. Figure 15 ompares the so-predicted caffeine encapsulation rate with the experimental value for each functionalized MIL-88B(Fe). The resulting cross-validation correlation coefficient Q^2 of 0.84 ensured a reasonable quality of the model, considering the limited set of data.

Further, it was possible to identify the main variables that impact the caffeine uptake in this series of MIL-88B(Fe) from a careful analysis of the three considered descriptors. It came that the polarity, polarizability and the H-donor capacity of the organic ligand are the key factors that boost the caffeine uptake in this material. Indeed, the highly polar and hydrogen donor $-$2OH, $-NH_2$ grafting functions lead to the highest performance of this material, that can be related to their abilities to form hydrogen bonds with the carbonyl group of the caffeine molecule as evidenced by DFT calculations for the amino-modified MIL-53(Fe) system. In contrast, the functionalization with monosubstituted apolar groups such as $-CH_3$ tends to lower the caffeine loading as these groups cannot form additional strong interactions with the drug molecules. In a same way, the derivation of QSAR models is in progress to predict the influence of the functionalization on the release of various drugs in MOFs.

4.3. In Vitro Activity Tests

Once MOFs have demonstrated to possess interesting features for biomedical applications, in vitro assays are required to confirm the activity and to determine possible limitations in the use of these nanocarriers. In vitro tests provide precious information related with cytotoxicity, cell uptake, intracellular distribution and/or degradation, bypassing of biological barriers and understanding of possible cell $-$ nanoparticles interactions. However, one must remind that the study of isolated cells must be completed with in vivo studies (see section 7), which take into account the complexity of the whole organism.

Using an angiogenic human colon carninoma cell line (HT-29), Rieter et al. have assessed the cytotoxicity of silica-polyvinilpyrrolidone (PVP) covered terbium(III) disuccinatocisplatin(IV) (DSCP; prodrug with an antitumoral activity) nanoparticles ($Tb_2(DSCP)_3(H_2O)_{12}$).[68] The delivery of the prodrug was modulated by controlling the degradation of the silica cover, from 1 h without coverage to 5.5 and 9 h for nanoparticles with respectively 2 or 7 nm silica layer thickness. These nanoparticles have, however, not shown any antitumoral activity since presumably DSCP released from the silica-coated Tb-DSCP nanoparticles was not able to enter into the cells and because the activation of the prodrug into the active cisplatin is only feasible in intracellular conditions. As HT-29 cells overexpress $\alpha_v\beta_3$integrins on their cell membrane, the nanoparticles' surface have been grafted with a c(RGDfK) peptide, which target these $\alpha_v\beta_3$integrins. The 50% inhibitory concentration ($IC_{50}\sim10$ μM) was slightly lower than the free cisplatin (13 μM), suggesting that the c(RGDfK)-silica-PVP-coated Tb nanoparticles were probably internalized into the cells, where the prodrug is released and further reduced into active Pt(II) species. In contrast, surface modification for targeting purposes was not necessary when cytotoxicity was evaluated using other carcinoma cell lines, such as human breast carcinoma MCF-7 cells, in which silica-PVP-coated Tb-DSCP nanoparticles showed similar activities as free cisplatin. Similar tests were performed on the silica-PVP-covered MIL-101 nanoparticles containing the prodrug ethoxisuccinate cisplatin.[85] In vitro cytotoxicity was slightly lower than free cisplatin (IC_{50} = 29 and 20 μM, respectively). By functionalizing the surface of nanoparticles with the c(RGDfK) peptide, similar cytotoxicity values were found, confirming that cisplatin prodrug was released and reduced into its active form with no loss of activity.

Apart from the previously mentioned exceptional capacities of the challenging antitumoral busulfan to loaded into the porous iron trimesate MIL-100 nanoparticles and their ability to release this compound in its intact form, MTT cytotoxicity assays were carried out on three different cells lines (human leukemia CCRF-CEM, human multiple myeloma RPMI-8226 and human macrophages J774) to confirm the preservation of the busulfan pharmacological activity (Figure 16).[55,189] Thus, the nanoparticles loaded with busulfan have found to possess a pharmacological activity comparable to the free drug in the three tested cell lines. Moreover, the empty MIL-100 nanoparticles were very well tolerated with IC_{80}> 5000 μg/mL for J774 and RPMI-8226 cells, and $IC_{80} \approx$ 1000 μg/mL for CCRF-CEM cells, corroborating their previously reported lack of in vivo toxicity (see results below).

The promising results obtained with the antiretroviral AZT-TP drug entrapped in mesoporous iron trimesate MIL-100 nanoparticles incited some of us to study their in vitro anti-HIV activity on HIV-1-LAI infected peripheral blood mononuclear cells (PBMC; Figure 17).[55,140] Here, one has to consider that (i) the high hydrophilicity of the triphosphorylated active form AZT-TP makes difficult the penetration of this compound into the cells and (ii) although non phosphorylated AZT can enter within the cell, the phosphorylation by intracellular kinases into its active form is a rate limiting step . Thus, cell uptake of the AZT-TP nanocarriers requires a specific formulation. The significant anti-HIV activity, observed only for the drug loaded nanoparticles (IC_{90} = 200 nM of AZT-TP into MIL-100), not only proves that AZT-TP was released in its active phosphorylated form, but also that the uptake of the AZT-TP loaded nanoMOFs effectively occurred inside the HIV-infected cells. Furthermore, the very low measured AZT-TP intracellular concentrations in PBMC cells clearly show that free AZT-TP can hardly penetrate the cell membranes (<3% after 24 h) because of its high hydrophilic character, as already explained before. In contrast, when AZT-Tp-containing MIL-100 nanoparticles were incubated with PBMC cells, much larger amounts of AZT-Tp were detected inside the cells (15, 23, and 26% at 2, 6,

and 24 h, respectively), confirming the nanoparticles uptake by these phagocyte cells.

Finally, several silver-based MOFs have been developed during the last two decades,[221] showing antimicrobial properties because of the silver release.[222,223] Therefore, Slenters et al.[224] have evaluated the antibacterial activity of dental restorative materials coated with a silver isonicotinate derivate of bis-ethyleneglycol by using a flow chamber mimicking the oral cavity. Although bacteria still adhered onto the coated surface they were killed upon contact with the substrate.

5. STORAGE AND DELIVERY OF GASOTRANSMITTER GASES

5.1. Gasotransmitter Gas Molecules

Gasotransmitter is a term coined to distinguish those biological signaling molecules which are freely permeable to cell membranes, and as such do not rely on the traditional cognate membrane receptor signaling mechanisms.[225] Ironically, considering this biological role, the three most important gases currently encompassed by this term are those that each have bad public images, nitric oxide, an atmospheric pollutant with a worldwide industry dedicated to its removal from exhaust fumes, carbon monoxide, dubbed the "silent killer", and hydrogen sulfide, a deadly gas characterized by its stench of "rotten eggs". Despite these bad reputations all three gases have been shown to be not only vital for life, but to be produced endogenously by the body in biologically active concentrations.

As well as their now relatively well-known endogenous function the three gases are of great interest for their use, and exogenous delivery of the gases from outside the body with a biological/medical target is a growing field of research.

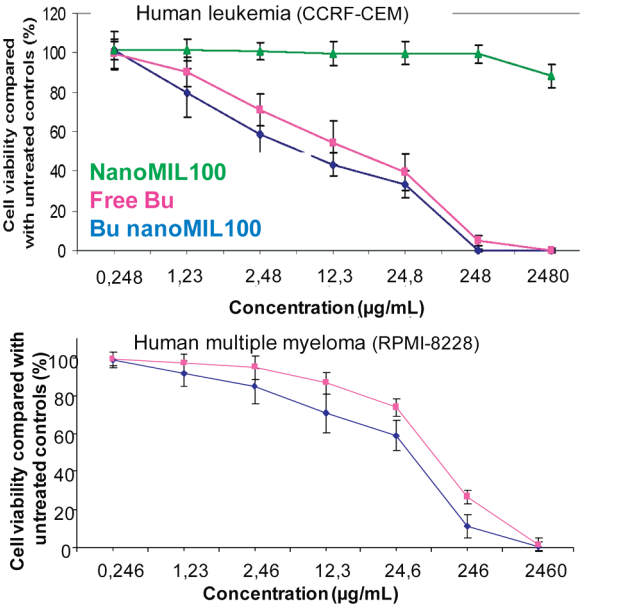

Figure 16. In vitro cytotoxicity activity of empty MIL-100 nanoparticles (green), free busulfan (pink), and busulfan-loaded in MIL-100 nanoparticles (blue) on (top) CCRF-CEM and (bottom) RPMI-8226. Reproduced with the permission from Chalati et al.[189] Copyright 2011 Pan Standford Publishing Pte. Ltd.

5.2. Nitric Oxide

Nitric oxide (NO) is a colorless, diatomic molecule was the first small molecule gas to be termed a gasotransmitter, and the discovery of its endogeneous production in 1987 led to an explosion of NO research.[226] NO is a radical species, meaning it is extremely reactive; it can both lose and gain electrons easily to form $[NO]^+$ and $[NO]^-$ respectively. Hence, it is lifetime in air (it is rapidly oxidized to NO_2) and in vivo is very small, at most a few seconds.[227] NO diffuses easily through the body, and the effect on the body is highly dependent on the concentration and location of the gas. Too high a concentration can lead to hypotension, excessive bleeding and inflammation, while too low a concentration can lead to hypertension or fibrosis and reduced ability to fight bacteria.

With nitric oxide being such an active biological molecule, much research is directed at exploiting the properties of NO for medicinal purposes. Exogenous sources of NO have unwittingly been used for over a century in such drugs as nitroprusside, $[Fe(CN)_5(NO)]^{2-}$, and since its discovery as a gasotransmitter, NO delivering agents has become an expanding area of research. Systemic release from soluble donors such as from glyceryltrinitrate often show unwanted side-effects[228] and simple gaseous inhalation using cylinders is only practical with such a toxic gas in very controlled situations. The short in vivo lifetime means that localized delivery of NO is only easily achieved by placing the NO donor near to the desired recipient organ and so NO gas delivery from materials is an expanding area of biological research.

Most work on such NO storage materials has concentrated on the use of polymers. Perhaps the chemically most advanced are those based on polymers functionalized with secondary

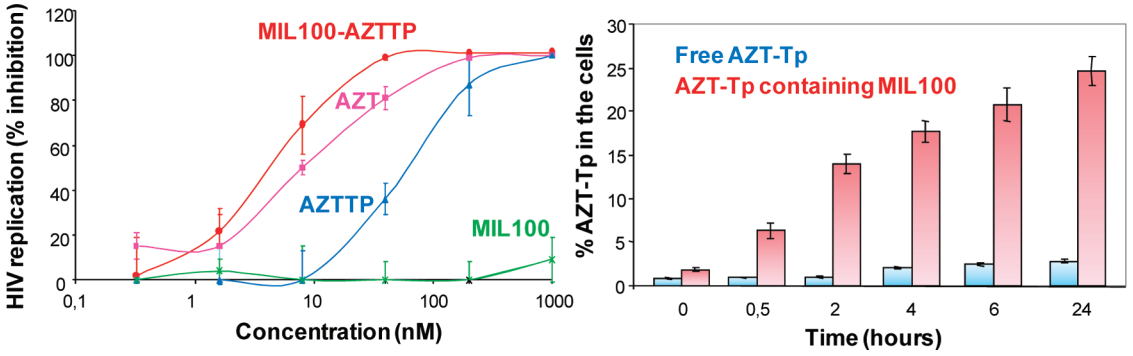

Figure 17. (Left) Inhibition of HIV-1-LAI replication in HIV-1-LAI infected PBMC in response to empty MIL-100 (green), free AZT (pink), free AZT-Tp (blue), and MIL-100 containing MIL-100 nanoparticles (red). (Right) Comparison of cell uptake of AZT-TP after incubation with PBMC cells of free AZT-Tp (blue) and AZT-Tp containing MIL-100 nanoparticles (red).

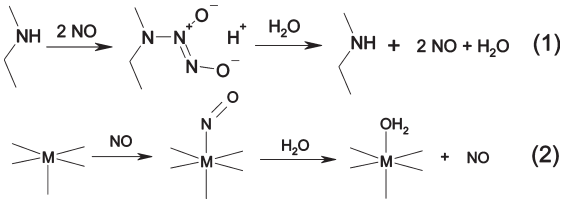

Figure 18. Two methods of storing NO on a material. (1) bydiazeniumdiolate formation and (2) by coordination to a metal ion. Both release nitric oxide on contact with water.

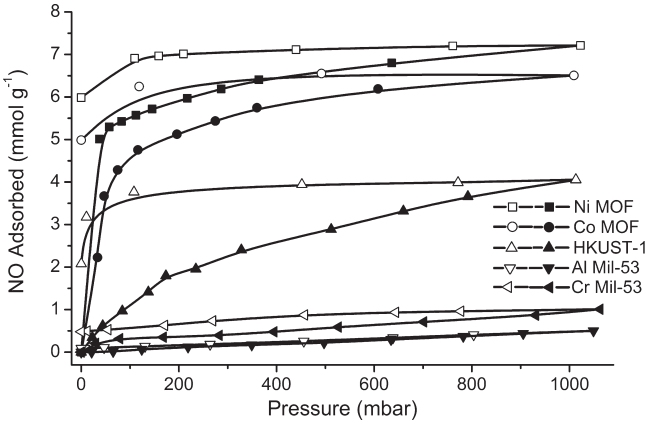

Figure 19. NO adsorption (closed symbols) and desorption (open symbols) isotherms into several MOFs at 298 K. The Ni-MOF (Ni-CPO-27 structure),[239] Co-MOF (Co-MOF-27 structure),[240] and HKUST-1 (Cu-BTC)[5k] all have open metal sites which interact strongly with the gas, leading to high uptake and hysteretic desorption. The two MIL-53(Al[243] or Cr[5g]) materials have no open metal sites and therefore have lower NO uptakes under the same conditions.[244]

amines, which on reaction with NO form ionic diazeniumdiolates (Figure18).[229,230]

Of more relevance to this particular review is the use of nanoporous zeolites to store nitric oxide. Such materials use the second storage mechanism from Figure 5, where the extraframework metal ions in a dehydrated zeolite coordinate the NO gas. As in the NONOate case the release of NO is triggered by exposure to moisture (or any other nucleophile of sufficient strength). NO-releasing zeolites show the expected biological activity.[231,232] Wheatley et al.[233,234] demonstrated antithrombosis activity on human platelet-rich plasma and Mowbray and coworkers have completed studies on human skin that show no significant inflammation on application of NO-releasing zeolites, in contrast to chemically produced NO (from acidified nitrite creams), which is a competitor to gas storage materials for topical delivery.[235] NO-loaded zeolites also showed excellent bifunctional antibacterial activity, consistent with the expected behavior of NO.[236]

5.2.1. Adsorption and Storage of NO on MOFs. As porous materials, MOFs clearly show some similarity to zeolites. However, the different chemistry of the framework structures means that the storage mechanism for NO is quite different to that shown by zeolites.[237] In fact, the versatility of MOFs has been exploited to adsorb and store NO using both mechanisms from Figure18, but this time the open metal sites in the MOF framework are utilized rather any extraframework sites as in zeolites. The importance of the open metal sites[238] for MOF

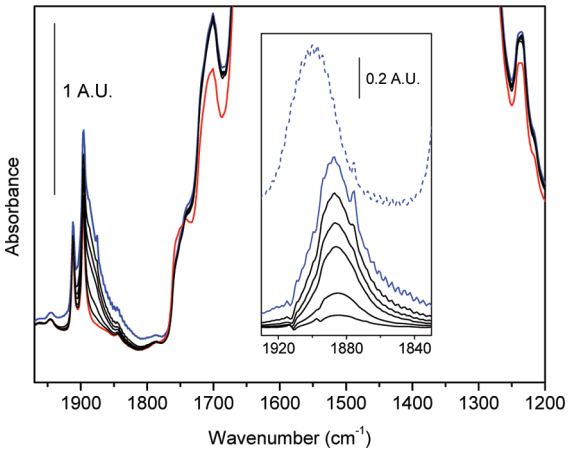

Figure 20. Interaction with NO monitored by IR spectroscopy. Red curve HKUST-1 outgassed at 180 °C. Blue curve: effect of 30 Torr of NO. black curves: effect of increasing pumping, residual pressure 10^{-3} Torr. The inset reports the background-subtracted spectra in the region of NO stretching (same color code). In the upper part of the inset (blue dashed curve), the spectrum of NO adsorbed at room temperature on a Cu-ZSM-5 zeolite is reported for comparison.

adsorption is clear from Figure19, where there are such sites (e.g., in HKUST-1[5k] or M-CPO-27[13,239,240]), there is a large adsorption capacity and a hysteresis, which is indicative of strong binding to a metal. This can be proven both structurally using X-ray diffraction or by infrared spectroscopy (Figure 20). Given the very large porosity of MOFs and their extremely well-known potential applications in gas handling it is not surprising that MOFs show very large adsorption capacities for NO,[241] with the CPO-27 structures[17] adsorbing upward of 8 mmol NO per gram of MOF, considerably more than other similar nanoporous solids, such as the zeolites. Other materials, such as the Fe-MIL-88,[5j] Fe-MIL-100,[14] and Fe-MIL-101 also show good uptake of NO.[141] These materials are particularly interesting because of the redox chemistry that occurs on activation of the solids, with changes in activation energy that strongly affect the interaction of the NO with the open metal sites in the structure.[242]

In general, every single MOF that has open metal sites seems to bind NO to a significant degree. However, the versatility of MOFs means that there are alternative methods of storing NO on these fascinating materials. Rosseinsky and co-workers[245] cleverly used postsynthetic functionalization techniques to engineer secondary amines inside the pores of the MOF HKUST-1, and then exposed the resulting compound to NO to form the NONOate compound, which was then characterized by IR spectroscopy. The key to the success of the method was the presence of enough proximal amine species in the cavities of the MOF, as a proton transfer reaction is required to successfully prepare the NONOate species, and this is turn requires a basic site relatively close to the amine that is interacting with the NO. Lower loadings of the 4-methylaminopyridine did not form any NONOate. Cohen and co-workers[246] used a similar strategy to form NONOates inside two other MOFs, IRMOF-3 and UMCM-1-NH_2.[236] However, rather than functionalize the open metal sites with an amine moiety here the organic linkers are functionalized with amines, but the overall effect of NONOate production is similar.

dx.doi.org/10.1021/cr200256v |*Chem. Rev.* 2012, 112, 1232–1268

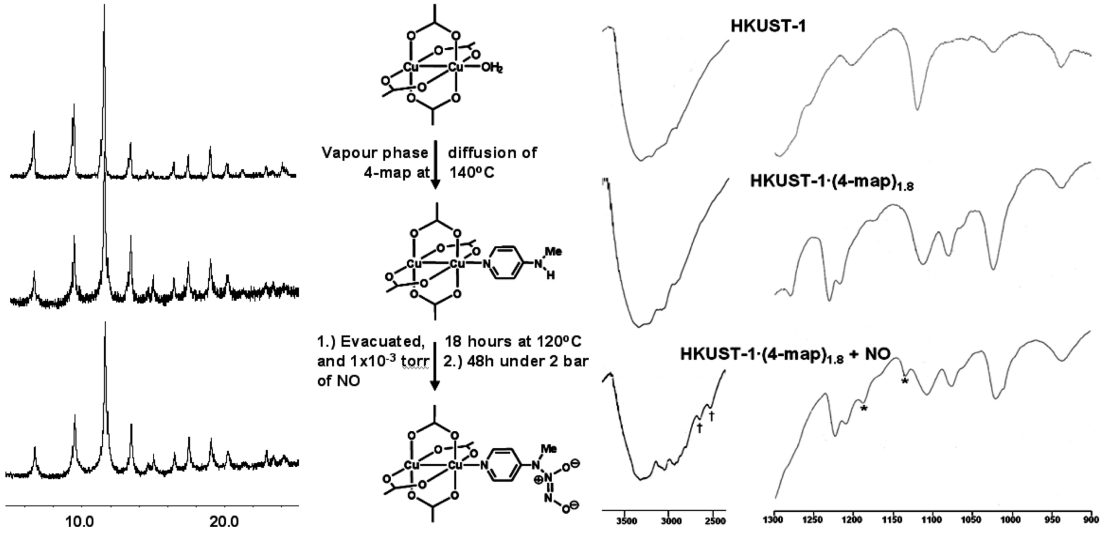

Figure 21. The formation of NONOate functionality in postsynthetically functionalized HKUST-1. (Left) Powder XRD before and after each functionalization (2θ range = 5−25) indicates the crystalline structure of HKUST-1 remains intact throughout the process. (Right) IR spectra (KBr disk) before and after each functionalization shows the presence of the NONOate (*N*-diazeniumdiolate) stretches at 1180 and 1129 cm^{-1}, which are marked by an asterisk.

NO, being a gas that interacts relatively strongly with atoms in the MOF framework, is a prime candidate for extremely selective adsorption. It is becoming more and more apparent that gases that interact relatively strongly with a MOF can, in the right circumstances with the right material, stimulate flexibility that can be termed ultraselective. In the case of the MOF Cu-SIP-3,[247−249] the activation process that removes the solvent water from the pores of the material causes a phase transition to an essentially nonporous MOF. This material does not adsorb any of the common gases tried. However, NO can interact strongly enough with the framework to reverse the phase transition, but only above a certain gating pressure of NO. Thus the material is effectively is ultraselective toward NO. In a similar vein, a zinc-TCNQ MOF structure prepared by Kitagawa and co-workers[250] is rendered flexible through an electron transfer reaction between the organic linker and the guest NO molecules.

Adsorption of NO, because of the strong interaction with open metal sites, can also be used as a good probe molecule for investigating the nature of pore surfaces in unusual MOFs. A prime example of this is in STAM-1, a MOF with two different channels that are lined by different chemistry, one pore is essentially hydrophobic and lined only by organic groups while the other is hydrophilic and lined by potential open metal sites.[251,141] Which channel is accessible can actually be controlled by changing the activation conditions and the adsorption between the two channels can be switched. Nitric oxide is an excellent probe for such switchable adsorption as its chemistry means it interacts relatively strongly with both types of surface, this is one reason why NO is such a good choice as a biological molecule as it can be effective in both aqueous and fatty tissue. Activation at low temperatures leaves the hydrophilic channel, which contains water in the as-made material, blocked. Activation at higher temperature then leads to loss of water from the hydrophilic channel to open this one up, but this is accompanied by a change in the framework structure that effectively closes the hydrophobic channel. This framework flexibility is reversible on re-exposure to water or methanol. The open channel is therefore switchable between the hydrophobic and hydrophilic pores: NO adsorption can be used to probe which pore is open as the strong interaction in the open metal sites that are available on leads to a steep increase in uptake at low pressure compared to that in the hydrophobic channel, which has no open metal sites (Figure 22)

5.2.2. Delivery of NO from MOFs. Of course, adsorption of a gas is all very well, but like any technology where the gas needs to be used after it has been adsorbed it is the delivery of the gas that is the most important aspect. The important questions regarding the delivery of potentially toxic gases in a biomedical context are how to control the rate and dosage of the delivery to match that required for beneficial actions of the gas, and how to ensure that such delivery consistent, both between batches of MOF and when the NO-loaded MOF has been stored for various lengths of time.

The first question to be answered is how to trigger the delivery of the gas. There are various options; one might use a reduction in pressure or an increase the temperature to desorb the NO, to photolytically release the gas or to use a chemical trigger. The rather strong binding of NO to metals in the systems, which leads to the large hysteresis on the desorption arm of the isotherm suggests that pressure reduction is not the most suitable method where MOFs have open metal sites, but might work well where physisorption is dominant mode of interaction in the NO-adsorbed material. An increase in temperature and light-induced breaking of the NO−metal interactions to desorb the gas would both likely work rather well in certain situations, although not practical in many others. Photolytic release of NO from metal-containing polymers has been shown to be a perfectly valid method of inducing NO delivery but this has not been applied to MOFs as yet. However, the method of choice in almost all NO-delivery systems using polymers, zeolites and MOFs is exposure to water, which acts to displace the NO from whatever species is present in the material. This is by far the simplest method as it needs no other external energy source, and works extremely well. The major criteria for such a method to be successful is that the NO-MOF must of course be susceptible to interaction with water, and that the NO-MOF must be stored under dry conditions until it is required for use. The second of these criteria is

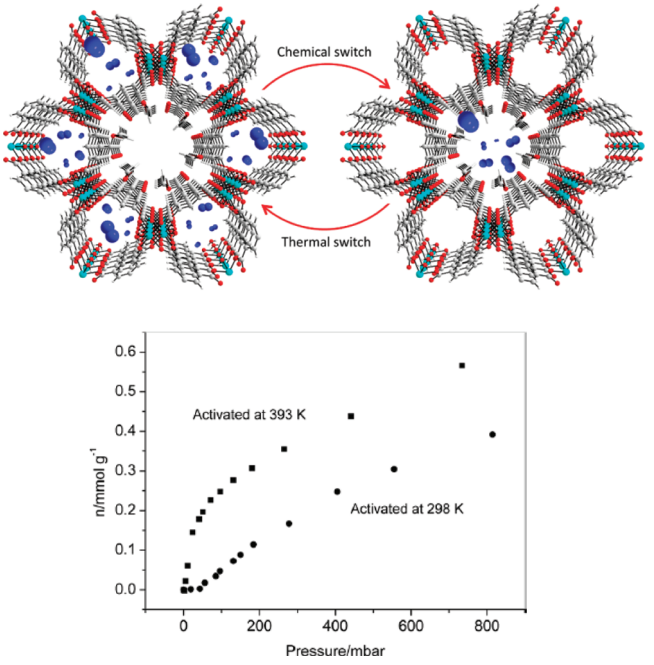

Figure 22. (left) Switchable adsorption in STAM-1.[251] A chemical switch can be used to open the central hydrophobic channel, while a thermal switch can be used to open the hydrophilic, open metal site-containing channels (right) NO adsorption into STAM-1 after different activation treatments. After room temperature activation, only guests in the organic-lined hydrophobic channels are removed, and NO is only adsorbed in this channel. After activation at high temperature, the water is lost from the hydrophilic channel, leaving open copper metal sites that interact more strongly with the NO, which can be seen in the steeper uptake at low pressure.

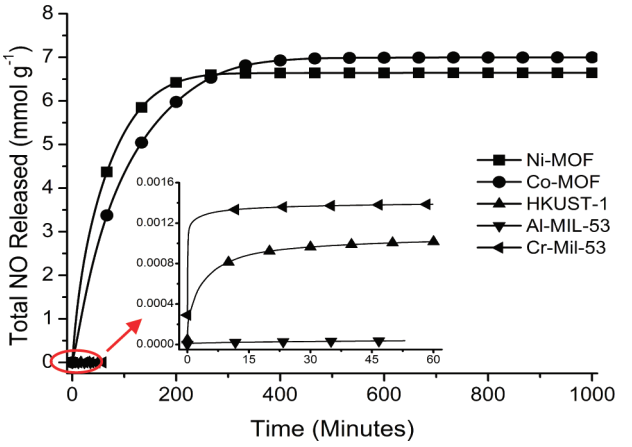

Figure 23. Wide range of deliverable NO capacity can be recovered from MOFs of different structures containing different metals. Ni-MOF and Co-MOF are the Ni-CPO-27 and Co-CPO-27 structures, respectively.

actually not all that much of an issue, as for medical applications that norm is that the materials have to be stored in sterile packages, which invariably prevent ingress of water from the outside environment. The first criterion is the key to a successful technology: how can we control the delivery of NO from a MOF using water as a triggering agent?

As stated above, the best MOFs for NO adsorption and storage are those containing open metal sites. Even within this subfamily of MOFs there is quite a range of chemistry available, and several of these have been tested for NO release. The first open metal site MOF to be characterized was HKUST-1, a copper benzene tricarboxylate MOF with a large porosity and open copper sites after dehydration/activation. As can be seen in Figure19 HKUST-15[k] adsorbs significant quantities of NO at room temperature, with the expected hysteresis on removing the NO pressure. However, this NO-loaded material is not very susceptible to water, and delivers only a very small fraction of the loaded NO in laboratory tests when contacted with moist gas over several hours (Figure23). This is not altogether surprising, there are after all many known stable metal nitrosyl complexes. However, other MOFs show very different behavior. The M-CPO-27 (M = Ni[239]or Co[240]) structure, for instance, shows exceptional reversibility of the NO-adsorption, taking up ~8 mmol of NO per gram of MOF and delivering it all back again under the same laboratory conditions used to test the HKUST-1 structure. Between these two extremes there are materials that deliver intermediate amounts of NO. Other MOF materials with open metal sites have been tested, including nontoxic iron-containing materials such as Fe-MIL-88, Fe-MIL-100, and Fe-MIL101.[141] None of these materials show the extremes of delivery properties of the CPO-27 or HKUST-1 structures, but lie somewhere in the intermediate region. Even within the same isotructural family, such as the M-CPO-27 structures, where M can be Mg,[13] Zn,[252] Co,[240] Ni,[239] and Mn,[253] there is a relatively wide range of delivery. As described above, the Co and Ni materials show almost perfect performance in terms of delivering the entire store of NO, while Zn and Mg materials deliver only about 10% of their capacity under the same conditions.

This deliverable NO actually correlates somewhat with the ease of dehydration/activation of the solids in the first instance, suggesting that the stability of the framework containing the open metal site is important in the mechanism of the NO delivery, but it is too early at the present time to make concrete conclusions surrounding the actual mechanism of this process and such work is currently still underway. However, what is true is the wide variety of MOF structures give an extremely wide range of deliverable capacities that we can tailor toward the potential biological applications (see section 5.2.3).

As well as tailorable delivery capacities, another important point is the stability and reproducibility of the delivery. The available adsorption capacity of MOFs is notoriously difficult to reproduce laboratory to laboratory, with some MOF materials being particularly bad. However, it seems that tightly defined protocols for the synthesis and activation procedures do indeed lead to very reproducible results. Like zeolites, the work to date shows that MOFs can have tight quality control parameters, which is a prerequisite for any commercial application. Similarly, the storage stability of the NO-MOF material has to be tightly controlled. The materials must have a suitable shelf-lifetime during which the deliverable capacity must not vary too much. Early indications are that MOFs have good stability for storage approaching that shown by NO-loaded zeolites which show little or no loss of NO capacity after storage for up to 5 years. In addition, it is also important that the material is "shaped" into a form that can be stored and applied successfully. Such work is forming an important part of current MOF research in many fields.[254]

5.2.3. Biological Activity of MOF-Delivered NO. The proof of the pudding, as the old English proverb goes, is in the eating. The overall target for these MOFs is application in biology, and in the longer term medicine, and so the obvious

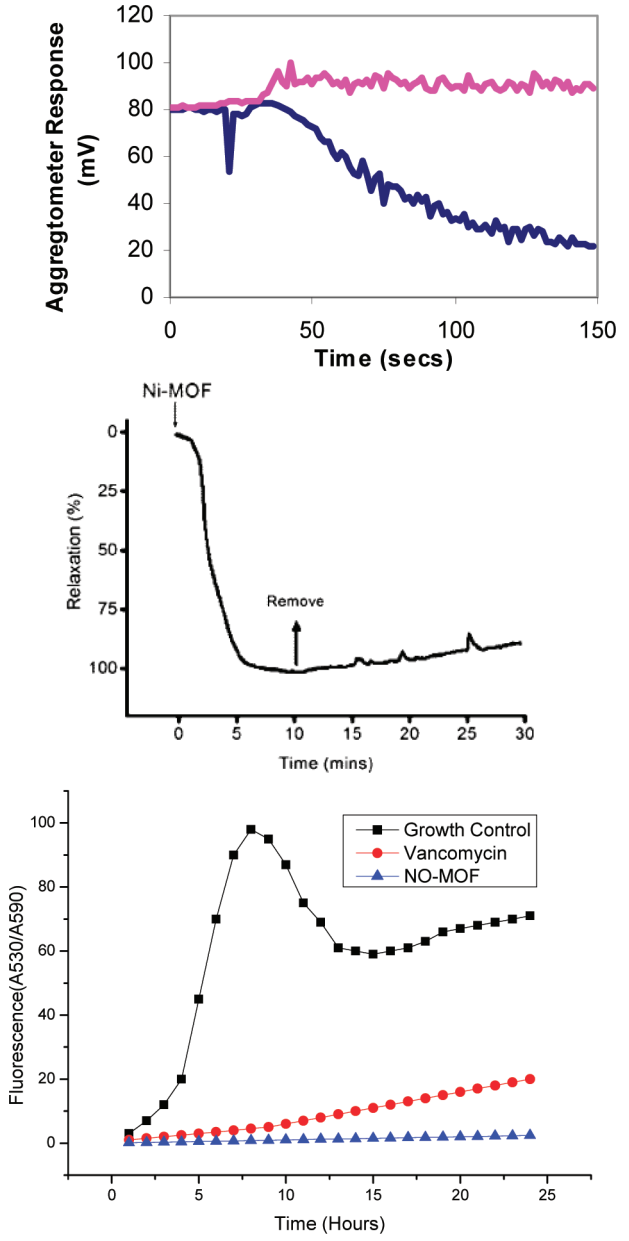

Figure 24. Biological effects of MOF-delivered NO. (a) The antiplatelet activity of NO delivered from HKUST-1 is demonstrated by complete inhibition of platelet aggregation when platelet rich human plasma is exposed to an activating agent (collagen). The response of the blue line is from the NO-free MNOF, while the pink line shows the response from the NO-loaded MOF (b) a representative trace of the relaxation of precontracted pig arteries when exposed to NO delivered from Ni-CPO-27 (c) the antibacterial effect of NO delivered from a MOF as a bactericidal agent inhibition of *S. aureus* DSMZ11729. MOF-delivered NO showed improved bactericidal effects against MRSA, which was significantly better than the vancomycin standard, which is itself significantly improved over the growth control. The bacterial colonization was measured using a fluorescence technique.

question is what sort of biological activity do the NO-loaded MOFs have? At the beginning of section 5.2, we discussed the potential biological applications of exogenous NO. To date the NO delivery from MOFs has concentrated on three in vitro experiments designed to test the antithrombosis (or rather more accurately the antiplatelet activation) action of NO-loaded MOFs, the vasodilatory (blood vessel relaxation) properties of NO-loaded MOFs and the antibacterial activity of NO-loaded MOFs. An important comparative feature of these three different biological tests is that they probably require different amounts of NO. Antiplatelet action requires relatively low concentrations of the gas, in the nanomole or picomole concentration range, while antibacterial activity requires a higher concentration. In human biology, the antiplatelet activity of NO arises from slow production of NO at low levels from the endothelial cells that line blood vessels, while antibacterial action occurs when NO production is induced by changing circumstances (such as wounding of the skin). This makes these tests extremely good for looking at the biological activity of the relatively wide-ranging NO delivery capacities shown by MOFs. Antiplatelet aggregation experiments using NO-loaded HKUST-1 showed that even the very low concentrations delivered by this particular MOF were biologically active, completely inhibiting the aggregation of platelets in human platelet rich plasma (PRP) after aggregation has been initiated using an exogenous agent. In contrast, the MOF itself had no effect on the platelets (Figure24a).

The rather larger flux of NO from materials such as Ni-CPO-27 offer a wider range of materials that can be used in applications. To this end, we investigated the impact of a pressed pellet of Ni-MOF (5 mg) on precontracted pig coronary arteries in vitro (Figure24b). Placement of pellets a distance of 2 mm from the vessel in the 10 mL organ bath resulted in rapid 100% relaxation of the vessel. The pellet could be seen to generate bubbles of gas for ~10 min of submersion, although the relaxation remained maximal for >1 h. In some experiments (Figure24b), the pellet was removed from the bath after 10 min and the relaxation was seen to gradually recover. Parallel control experiments with NO-free Ni-MOFs failed to cause relaxation and did not generate bubbles on exposure to the moisture and showed no relaxation effects. NO is one of the body's own signaling molecules for the control of blood pressure through relaxation of the muscles that surround arteries and veins, and this experiment shows that MOF-delivered NO is very much suitable for use in such a field. In fact, the formation of bubbles from the MOF indicates that the flux of NO is probably too great from the CPO-27 materials for optimum application.

The final biological experiment that has been carried out using MOF-delivered NO is antibacterial. The induced production of NO by the skin on wounding is one of the body's own defense mechanisms against bacterial infection, and it is known that NO is a strong antibacterial agent, especially so when it combines with superoxide species to form peroxynitrite, which is extremely toxic to invading pathogens. Investigation of NO-loaded MOFs against methicillin resistant *Staphylococcus aureus*, *Pseudomonas aeruginosa*, and *Clostridium difficile* all showed significant bactericidal effects (Figure 24c), indicating that NO delivered in this way is very much a potential method of developing new technologies in this increasingly important field.[141]

5.3. Hydrogen Sulfide

H_2S is now implicated in many biological processes and there is growing evidence of its importance in human physiology, stimulating great interest in understanding the endogenous actions of H_2S and in developing exogenous H_2S as a potential therapy. H_2S has been implicated in vasodilatation[255] and neurotransmission and also plays a role in neuroprotection.[256,257] In addition, a 2005 paper in *Science* reported the amazing property that H_2S induces a suspended animation-like state in mice[258] and has

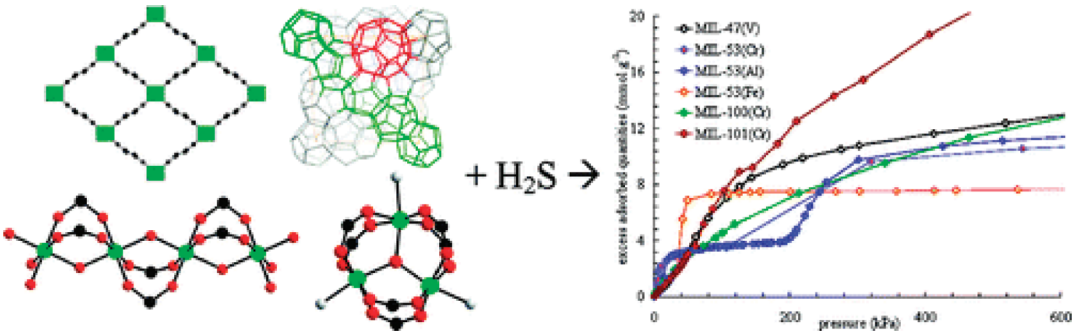

Figure 25. Hydrogen sulfide gravimetric isotherm adsorption measurements were carried out on MIL-53(Al,[243] Cr,[5g] Fe[37]), MIL-47(V),[269] MIL-100(Cr),[5i] and MIL-101(Cr)[5h] metal−organic frameworks (MOFs). A two-step adsorption mechanism related to a breathing effect was observed for MIL-53 terephthalate-based MOFs.

been hypothesized as a treatment to create a beneficial hypothermia/hypometabolic state in surgical situations, to benefit conditions such as ischemia/reperfusion injury, pyrexia and trauma,[259] and for the improvement of organ preservation.[260] It is suggested that as H_2S plays an important role in several other clinical conditions,[261] making delivery of it in biologically relevant amounts an attractive therapeutic target,[262] especially as an anti-inflammatory agent.[263] Recent work has indicated that it is important in the inflammation and remodelling stages in asthma, and that it could be a very exciting target for prevention and treatment.[264] In this report levels of endogenous H_2S were found to be decreased in pulmonary tissue in ovalbumin-treated rats. Exogenous delivery of NaHS as an H_2S donor reduced the inflammation and remodelling in the airways with several other positive markers (increase in peak expiratory flow, decrease in collagen deposition score etc). The conclusions were that NaHS treatment significantly reduced pulmonary iNOS activation in the asthma model, that H_2S plays a significant role in asthma pathogenesis and that H_2S is a very exciting potential therapy to prevent/reduce airway inflammation in asthmatic patients

The mechanism by which H_2S imparts vasodilator activity is seemingly different from NO, with possible contributions from K_{ATP} channels, activation of endothelial NO, voltage-gated Ca^{2+} channels, inhibition of respiration and central nervous system effects have all been suggested in the literature.[265] Moreover, the chemistry of the gases is quite different: NO is a free radical with a relatively short half-life (seconds) in the biological environment, H_2S partially dissociates at physiological pH to yield hydrosulfide and sulfide and interacts with Zn^{2+} in particular.[2] It is also more than likely that different mechanisms are evoked in different vascular beds and in different species, rat coronary arteries, for example, do not appear to be sensitive to H_2S.[266] Nevertheless, this study and others suggest that H_2S is protective against ischemia reperfusion injury.

The delivery of exogenous H_2S is dominated by NaHS, which rapidly equilibrates with the gas in aqueous and biological solutions. However, there are other organic compounds that can be employed, such as cysteine. The chemistry of these donors is not as easy to control as those of, the NONOates described above for NO, and are primarily systemic in nature. Recently, MOFs have become an interesting target for this area of research.

5.3.1. Adsorption of H_2S on MOFs. The field of H_2S adsorption is by no means as well developed in MOF terms as many of the other gases of interest for the many different gas handling applications that are of interest. Partly, this is because of the particular aggressive properties of this gas, especially when in contact with ferrous components of adsorption apparatus. However, given its toxicity and highly unpleasant odor there has been significant interest in removal of such sulfur-based contaminants from fuels and chemical feedstocks. Metal−organic frameworks have only recently been studied in this context, but not surprisingly MOFs do show good adsorption capacities. As one might expect, the interaction of H_2S with metal−organic frameworks can lead to invocation of flexibility in materials such as MIL-53[5g] with pronounced steps in the adsorption isotherms, while rigid structures such as MIL-101[5h] show more typical adsorption behavior (Figure 25).[10,267,268]

Even more recently, studies also aimed at removal of H_2S under ambient conditions using copper-based MOFs were carried out by Bandosz and co-workers.[270] Again, relatively good adsorption uptake was seen for the MOFs, which could even be improved by making composites of the MOFs with grapheme oxide. The CPO-27 materials that show such excellent behavior in NO adsorption/delivery systems have also been studied in this context, again showing good uptake behavior.

One striking feature of the H_2S adsorption isotherms that have been done to date is that the reversibility of the isotherms is not as good as it is for other gases. Again, this is not unexpected for a gas that can interact strongly with the frameworks. However, X-ray diffraction, further adsorption experiments (for example using methane) to test the effect of H_2S preadsorption on uptake capacities and other investigations indicate that for certain MOFs the adsorption of H_2S is so aggressive as to destroy the MOF framework completely. Clearly, this behavior is less than ideal if the MOFs are really to be used as the delivery agents in a biological context. Adsorption into the MIL-100 and MIL-101 structures was only partially reversible, and adsorption into copper based materials resulted in completed destruction of the MOF network. However, other materials including the CPO-27 and most of the MIL-53 did not show the same issues and these can be described as the more likely candidates for H_2S delivery materials. Adsorption onto the M-CPO-27 structures gave ~10 mmol H_2S per g of MOF. The structure of the H_2S-loaded could be determined from powder X-ray diffraction, and the interaction of the sulfur of the H_2S with the open metal sites in the framework confirmed using X-ray pair distribution functional analysis (Figure 26).[271]

5.3.2. Delivery of H_2S from MOFs. Given the discussion in the last section regarding the irreversibility of H_2S adsorption, delivery experiments to ascertain the amount of gas that is deliverable both from freshly made and from stored samples are required as a matter of urgency. As far as we are aware only one such set of experiments has been carried out to date. These

dx.doi.org/10.1021/cr200256v |*Chem. Rev.* 2012, 112, 1232–1268

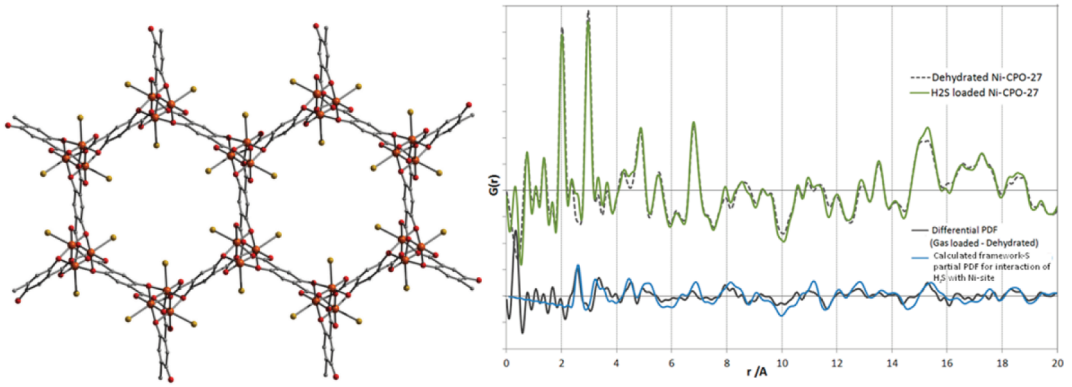

Figure 26. X-ray powder diffraction-derived structure of H_2S loaded Ni-CPO-27, showing the sulfur atom of the H_2S interacting at ~2.6 Å from the open nickel site in the structure, with the atoms pointing into the channel. This is confirmed by the X-ray pair distribution functional analysis (right) which shows a peak at about 2.6 Å that matches the diffraction structure.

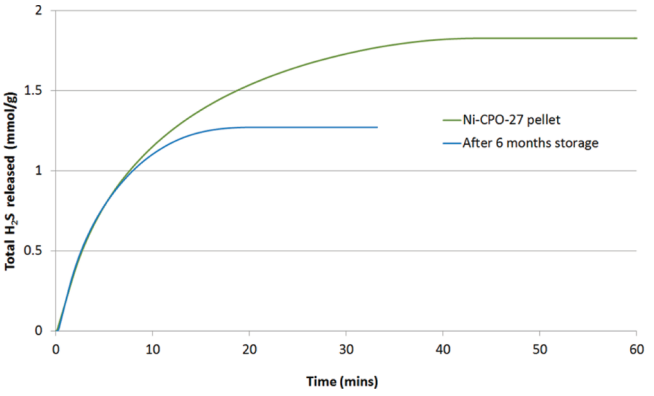

Figure 27. Delivery of H_2S from gas-loaded Ni-CPO-27 materials immediately after preparation and after six months storage. There is a loss in capacity on storage, but the delivery is still significantly above 1 mmol/g.

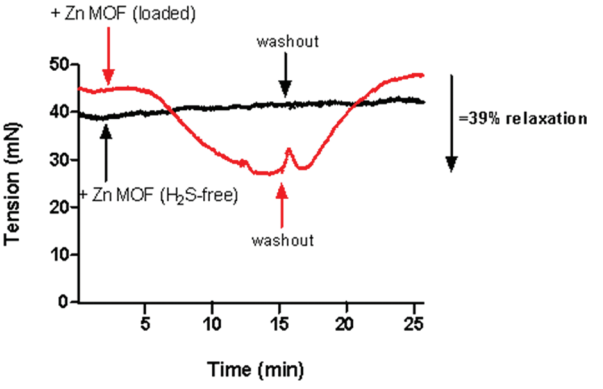

Figure 28. Exposure of precontracted porcine artery to a H_2S-loaded MOF (Zn-CPO-27) showed ~39% relaxation after about 15 min, which was reversed after the MOF was reversed using a washout procedure.

experiments were carried out on the Ni-CPO-27 and Co-CPO-27 structures that show such exceptional behavior for NO delivery experiments. This experiment used approximately the same conditions as those used for the NO delivery mechanism, using water as a trigger for the release of the gas. The releasable capacity under these conditions was good, but there was not the exceptional performance of the CPO-27 solids that was seen in the NO experiments, but there was still a significant delivery of >1 mmol H_2S per g of solid over the first 30 min or so. This certainly seems promising, and led directly to the preliminary biological activity tests described below. However, storage of the H_2S-loaded CPO-27 material for six months showed a slight loss in deliverable capacity, indicating a limited shelf life for this material (Figure 27).

5.3.3. Biological Activity of MOF-Delivered H_2S. In biological testing, we expect that H_2S can be used in many similar ways to NO, although as a much less active signaling molecule. The only biological activity test for MOF-delivered gas so far known is a similar vasodilation test to that described for NO in section 5.2.3, using myography to measure the relaxation of porcine arteries (Figure 28). As expected, the relaxation induced by the H_2S was less than that seen in the NO experiments, but whether this is entirely because of the lower activity of H_2S compared to NO, or whether it is simply because less H_2S is delivered is as yet unknown.

5.4. Carbon Monoxide

The final gasotransmitter molecule that could be stored in MOFs in carbon monoxide. Its actions mirror those of NO relatively well the mechanism by which they impart their vascular activity are not necessarily via the same routes although NO and CO both activate soluble guanylatecyclase (sGC) to generate cGMP. The chemistry of the two gases is similar in many ways, but while CO is relatively unreactive, except in the presence of Fe^{2+}, for which it has a very high affinity and binds irreversibly. Carbon monoxide is an odorless, colorless gas. Often dubbed as "the silent killer", the toxicity of carbon monoxide has been extensively studied. In 1857, Claude Bernard reported carbon monoxide could bind to hemoglobin (Hb), the oxygen carrier in blood.[272] The binding affinity of carbon monoxide and iron is approximately 220 times larger than that of iron and oxygen.[273] Consequently, the presence of carbon monoxide in the bloodstream can lead to competitive binding of carbon monoxide to the haem moiety to form carboxy-hemoglobin (HbCO) instead of the oxy-hemoglobin (OxHb) required to transport oxygen.[274] Further to this, binding of one molecule of carbon monoxide reduces the capacity of the other three sites of hemoglobin to bind to oxygen leading to a significant reduction in the oxygen carrying capability of the blood, interrupting oxygen delivery to organs ultimately leading to tissue hypoxia and poisoning.[275]

Research has shown that the body itself produces carbon monoxide, with as basal production rate of approximately 1−6 mmol/day.[276] The main source, accounting for 86% of carbon monoxide produced endogeneously is the oxidation of haem by the enzyme hemoxygenase (HO).[277] Hemoxygenase is the body's haem degrading enzyme, which breaks down the porphyrin ring at the alpha-methane bridge via oxidation. This oxidation requires three equivalents of oxygen and NADPH as cofactors,[278] and produces Fe(II), carbon monoxide and biliverdin, a green pigment. Biliverdin is then quickly broken down to the yellow bilarubin by biliverdinreductase, and then removed from the bloodstream.

Current research centers upon delivering carbon monoxide though the inhalation of between 20 and 400 ppm gaseous CO, using orally dosed methylene chloride (MC) which releases CO when metabolized in the liver, or in soluble form through the use of so-called carbon monoxide-releasing molecules (CORMs).[279] A summary of delivery methods and experimental results can be found in the literature.[280] Porous materials could represent a good alternative delivery mechanism for gasesous CO, necessary due to the precautions needed with gas cylinders due to the toxic nature of the gas.

However, while it is a good and well-used IR probe for several different MOFs (see, for example, ref 281), at the time of writing this review there has been no report on the biological activity of MOF-stored CO, and even very little regarding adsorption of MOFs using NO. There is clear scope in this area to make further impact in MOF-delivered gasotransmitters.

6. BIODEGRADABILITY AND STABILITY OF MOFS

The use of MOFs for bioapplications will depend on its toxicity, host−guest interactions, pore size, hydrophobic/hydrophilic balance, and so on. However, the performances will also strongly rely on its (bio)degradable character. MOFs are indeed based on ionocovalent metal−ligand bonds and one expects, in solution, a continuous ligand exchange process between the complexing group and the water molecule from the metal centers. Thus, particularly in body fluid where pH and composition drastically change, one has to address the question of the stability of the MOF that will strongly affect MOFs bioerosion and drug release performances. Very little information has been gathered so far concerning this critical issue. It is currently well-known that microporous zinc terephthalate such as MOF-5, are highly unstable in the presence of water.[35,32] Other porous MOFs have been proven to be hydrothermally stable such as Zn imidazolate ZIF-8,[282] the zirconium terephthalate UiO-66[38] and the iron trimesate MIL-100(Fe).[283] However, systematic study of their liquid phase stability is still required. A first tentative rationalization of the hydrothermal stability of MOFs has been described by Low et al.[28] The main conclusions are that the most important parameters are the charge and coordination number of the cations, the chemical functionality of the organic linker, the framework dimensionality, and the degree of interpenetration. MOFs based on metal−oxygen bonds are more stable when the coordination and the charge increase, leading to reasonable stabilities for metal(III) polycarboxylates such as MIL-100(Cr), while Zn-imidazolate MOFs seem highly stable.[140] For bioapplications, if one could point out that the tunable character of the MOF composition and structure might offer quasi infinite possibilities in terms of kinetics of biodegradation, there is still a need to establish the real stability of MOFs in body fluids.

So far, it was shown that the iron(III) mono or dicarboxylates Bio-MIL-1,[138] and MIL-101(Fe),[85] degraded rapidly in phosphate buffer (pH = 7.4). Similarly, some of us have shown that nanoparticles of iron fumarate MIL-88A and iron trimesate MIL-100(Fe) totally degraded in phosphate buffer at pH 7.4 over a few days.[55] On the contrary, first stability tests of metal(II) hydroxoterephthalate M-CPO-27 (Ni,[239] Co[240]) resulted into a rather stable character in phosphate buffer supplemented with bovine serum, at 37 °C.[244] Interestingly, some MOFs have been observed previously as hydrothermally stable, such as UiO-66(Zr) or MIL-100(Fe). However, if these MOFs are rather stable in deionized water or even under slightly acidic conditions, they degrade within few hours (UiO-66)[55] or a few days (MIL-100(Fe)), or even weeks for the iron(III) tetracarboxylate Soc-MOF(Fe) or MIL-127 solid,[142] once dispersed in phosphate buffer solutions (Figure29). This is partially related to the pH value (PBS is at pH 7.4) regarding the pK_a of the carboxylic linkers (pK_a < 5.5), making easier a deprotonation of the linker and thus reducing the complexing power of the linker toward the metal. However, the presence of phosphate groups, which exhibit a strong affinity toward high valence metals such as Zr, probably rapidly displace the complexation equilibrium toward a formation of metal phosphate. Thus, one cannot predict the body fluid stability of MOFs relying only on their hydrothermal stability. Further studies are thus urgently required to rationalize this issue for future biomedical applications.

7. TOXICITY

The large range of chemical compositions might allow finding many toxicologically acceptable MOF candidates for their use in healthcare. Indeed, MOFs based on endogenous linkers and metals are still quite scarce in comparison with general MOFs (see section 3). Of course, the entire MOF composition has to be taken into consideration in toxicological assays since some of these MOFs may also possess various toxic molecules (ligands or solvents) within their structures. Therefore, the use of porous MOFs in biomedicine is conditioned to the toxicity of each of the MOF components. However, to the best of our knowledge, apart from our in vitro and in vivo toxicological studies that will be summarized here, there are no more investigations reported so far.

In vitro toxicity of two iron carboxylates nanoparticles, the iron trimesate MIL-100 and the iron fumarateMIL-88A, were assessed through MTT assay (3-(4,5-dimethylthiazol-2-yl)-2,5-diphenyltetrazolium bromide). Even at very high doses, no cytotoxic effects were observed for both types of nanoparticles in contact with mouse macrophages J774. A1, human leukemia (CCRF-CEM) or human multiple myeloma (RPMI-8226) cells.[55,189] Moreover, half maximal inhibitory concentrations (IC_{50}) are comparable with those of other currently available nanocarrier systems.[284]

Biomedical application of MOFs requires understanding their administration, distribution, metabolization (including biodegradation) and excretion (ADME), parameters strongly related with nanoMOFs toxicity. The most direct administration way is the intravenous (i.v.) route, where the total of the administered dose is in blood. Thus, acute in vivo toxicological studies were performed intravenously in rats, using very high doses (up to 220 $mg \cdot kg^{-1}$) of three different iron carboxylate nanoMOFs, with different structures and organic compositions, based on either endogenous or exogenous, hydrophilic or hydrophobic and aliphatic or aromatic linkers (MIL-88A,[58] MIL-100,[14] and MIL-88B_4CH_3).[55] It has to be noted that in rats, the injected

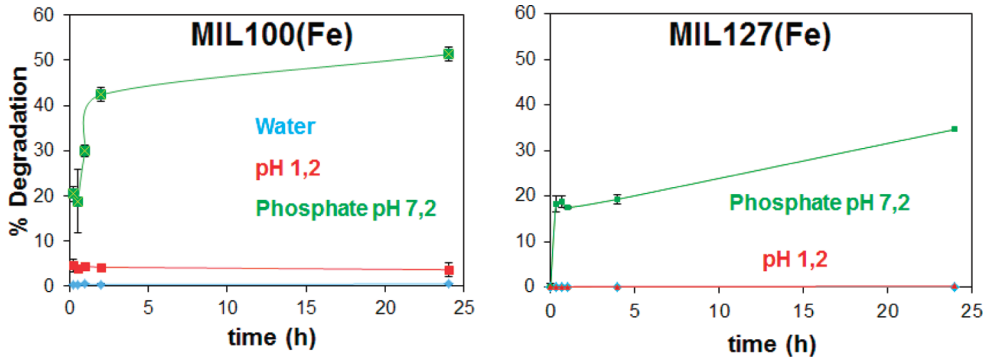

Figure 29. Percent degradation of MIL-100(Fe) (left) and Soc-MOF(Fe) or MIL-127 (right) under different simulated physiological conditions at 37 °C (estimated by % release of linker deduced from HPLC experiments).

Scheme 1. Biodistribution of Iron nanoMOFs According with the Iron Concentration

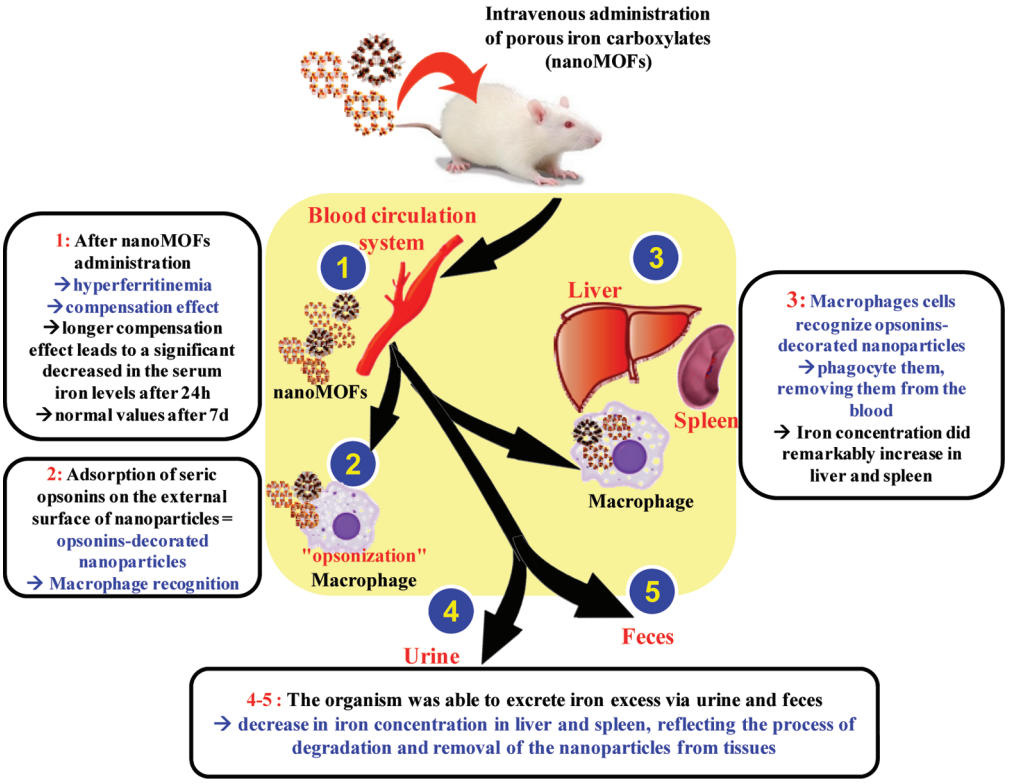

suspension volumes are limited and therefore, for stability reasons, it is impossible to concentrate more the suspensions and thus to administer higher nanoMOF quantities.

The toxicological investigation has been assessed during three months after the intravenous injection through the evaluation of different parameters such as animal behavior, body and organ weights, histology, enzymatic activity, and serum biochemistry.[55] Except for a slight increase in the spleen and liver weight, attributed to the fast sequestration by the reticulo-endothelial (RES) organs of the non surface engineered-nanoMOFs (see below), comparison with control groups did not show any significant difference. Normal organs weight was restored one to three months after the injection, confirming the reversibility of the phenomenon. On the other hand, the lack of inflammatory reaction, highlighted by the dosage of interleukine-6 levels (IL-6) after nanoMOFs administration, has confirmed the lack of toxicity of iron nanoMOFs.[55,140]

Biodistribution depends on the molecule/material properties such as composition (metal, linker, polarity, etc), surface characteristics (charge, accessible surface, porosity, reactivity, etc), particle size and shape,[285] which can affect the particle interactions with biological media (serum proteins-opsonization, lipids, sugars, etc), as reported for other materials.[286]

The first biodistribution studies on iron carboxylate nanoMOFs have been assessed by quantifying both iron and linker concentration in different tissues by atomic absorption spectroscopy (AAS) and high performance liquid chromatography (HPLC), respectively.[140] Serum iron concentration significantly decreased in comparison with control group the day following the intravenous administration of iron nanoMOFs, coming back to normal values

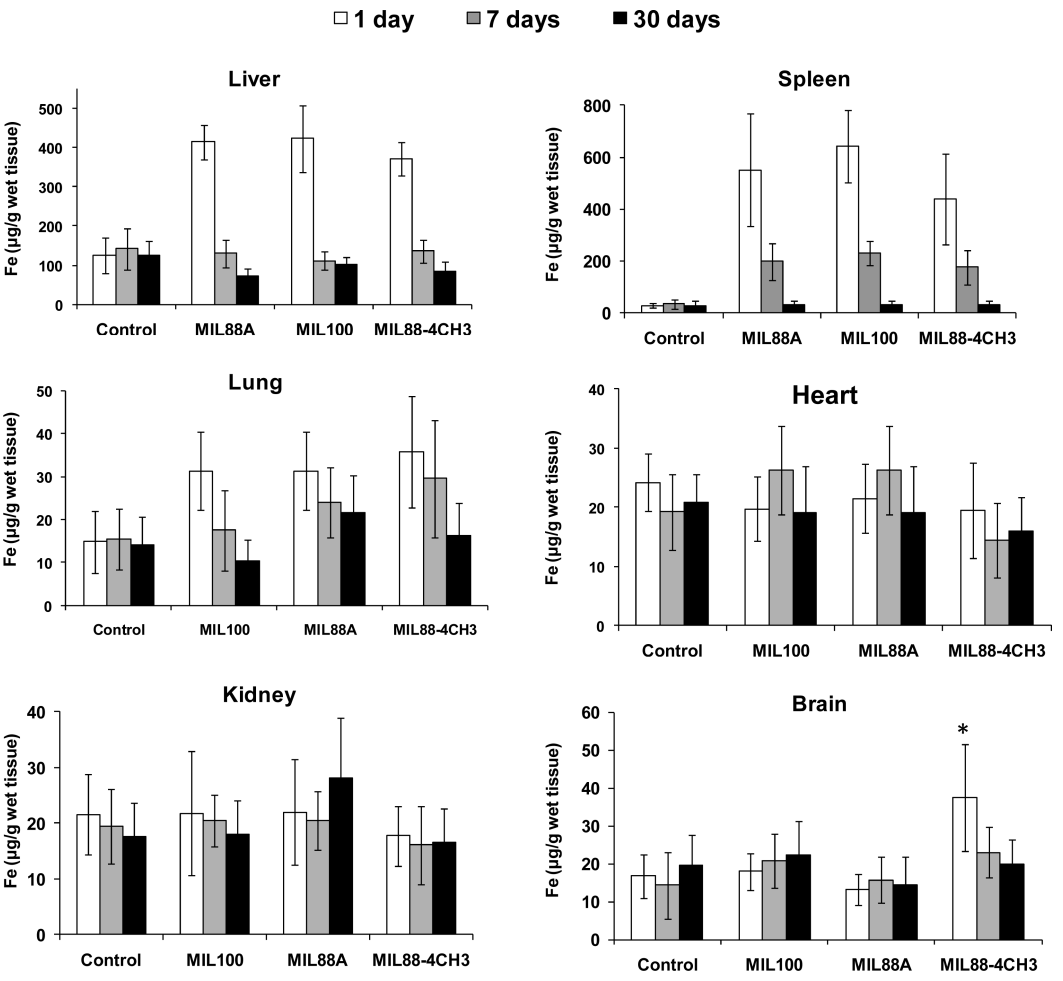

Figure 30. Iron levels in different tissues after 1, 7, and 30 days of the i.v.administration of nanoparticles of MIL-88A, MIL-100 and MIL-88B_4CH_3. Data are presented as mean ($n = 6$, * $p < 0.05$).

after 7 days (Scheme 1).[55,140] Noteworthy, in pathological situations, high serum iron concentration leads to a hyperferritinemia compensation effect in order to avoid toxic effects,[287] which induces a decrease in serum iron levels. However, this compensation process is usually longer than the iron overload, leading to a serum iron concentration even lower than the normal one.[288]

Concerning the iron concentration in other organs, no significant changes have been observed in heart and kidneys (Figure 30).[140] The slight increase in the iron concentration in lungs has been related to the accumulation of nanoparticles within the smallest capillaries of this highly irrigated organ, coming back to normal concentrations after 7 days, without any tissue damage as confirmed by histopathology. No significant changes in the brain iron levels have been observed after the administration of nanoparticles, with exception of a slight increase in the brain iron concentration after one day of the administration of nanoMIL-88B_4CH_3. Thus, the nanoparticles were not able to cross the blood brain barrier (BBB), probably because of their larger size (100−200 nm) and the hydrophilic character of the ligands. However, the presence of a small fraction of MIL-88B_4CH_3 within the brain was totally unexpected and, although the cross of the BBB could be related to the more hydrophobic character of the tetramethyterephtalate linker and to the smaller size of these particles (40−50 nm), the BBB crossing mechanism has not been investigated yet. This lack of behavioral changes in treated animals during the whole experiment as well as the normal activity of the biochemical marker for brain function, creatine phosphokinase (CPK), support that nanoMIL-88B_4CH_3 does not induce any brain toxicity but additional studies are required to understand in depth this phenomenon.

Iron concentration did remarkably increase in liver and spleen one day after nanoMOFs administration; then, progressively decreased up to normal levels after 7 days (Scheme 1). This may be explained by the well-known "opsonization" process, resulting from the adsorption of seric opsonins (which are immunologic proteins) at the surface of foreign particles. Blood is dispersed into the liver via a dense network of vessels (sinusoids), surrounded by a mixed layer of fenestrated endothelial cells and Kupffer cells.[289] These latter recognize opsonins-decorated nanoparticles and phagocyte them, removing them from the blood.[290] Rapid opsonization and phagocytosis by macrophages of many nanoparticles is well-known.[291] If the surface functionalization with polymers such as polyethyleneglycol may hinder the opsonins adhesion, promoting "stealth" properties, the rapid uptake by the liver upon i.v. administration of nanoMOFs is thus a consequence of fast opsonization because of the absence of surface modification and also to the rather large size of these particles (50−200 nm).

The highest level of hepatic iron concentration (1750 $\mu g.g^{-1}$), resulting from nanoMIL-88B_4CH_3 treatment, was however significantly lower than the values reported to induce hepatocellular damages (>4000 $\mu g.g^{-1}$ wet liver).[292,293] In addition, iron

dx.doi.org/10.1021/cr200256v |*Chem. Rev.* 2012, 112, 1232–1268

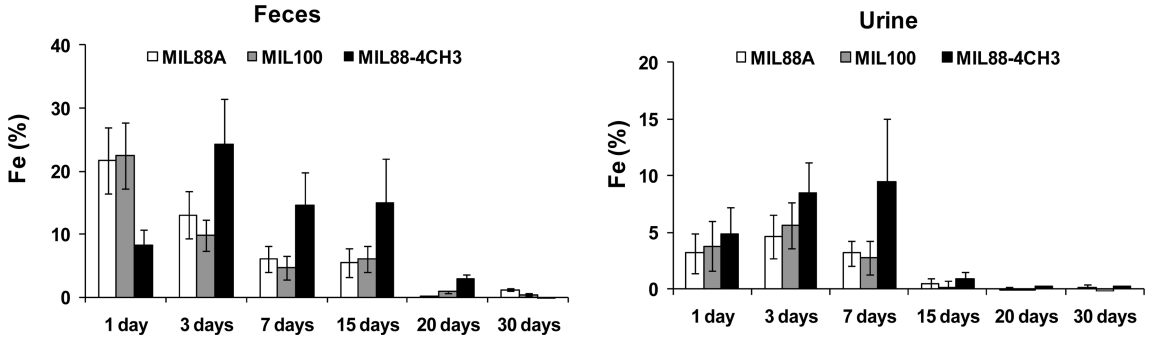

Figure 31. Excreted iron in urine and feces after administration of MIL-88A, MIL-100, and MIL-88_4CH_3 nanoparticles.

biodistribution analysis showed that about 26, 27 and 43% of the injected doses was localized in the liver after 24 h of the administration of MIL-88A, MIL-100, and MIL-88B-4CH_3 nanoparticles, respectively. Iron concentration in both liver and spleen then progressively decreased after 7 days down to 2%, 1%, and 4% in liver for nanoMIL88A, nanoMIL100 and nanoMIL88−4CH_3, respectively, and down to 3 wt % in spleen (Figure 30). This decrease in iron concentration reflects the process of degradation and removal of the nanoparticles from tissues, thus demonstrating that the organism was able to excrete both nanoparticles components (iron and ligand) via urine and feces, as also confirmed by the iron and ligand quantification in these media (Scheme 1).[140] Indeed, the amount of iron excreted by urine and feces after 15 days corresponds to about 40% of the administered dose (Figure 31). Interestingly, the kinetics profile of excretion strongly depends on the polarity of the ligands, related with their aqueous solubility. It was found that after nanoMOFs administration, iron regulatory systems needed around 3 weeks to achieve normal cells iron homeostasis,[294] which is faster compared to iron oxide nanoparticles (~20% of total administered iron removed after 7 weeks in different animal species).[294]

Furthermore, the histopathological examination of the liver revealed a normal parenchymal architecture without any inflammatory or fibrosis aspect with no apparent change in the cellular structures following the administration of nanoMOFs (Figure 32) or of their ligands, except MIL88-4CH_3 and its corresponding ligand (tetramethylterephthalic acid).[140] These latter exhibited a slight clarification of hepatocytes probably because the hydrophobic character of the linker, which probably possesses a higher affinity for the lipidic components of the liver. This clarification is, however, completely reversible after 7 days of the administration. Moreover, although nanoparticles can be detected inside the Kupffer cells by Pearls Prussian Blue staining, which colors specifically the iron in blue (Figure 32), microscopic observation of liver shows that nanoMOFs did not induce any hypertrophy or hyperplasia of peri-sinusoidal cells.

Regarding the spleen, a slight hypertrophy not associated with an important macrophagic activity has been revealed by microscopic examination, together with the presence of nanoMOFs-containing macrophages (Figure 32). Noteworthy, the amount of nanoparticles in liver and spleen decreased progressively at 7 days to completely disappear at 30 days, suggesting the total degradation and removal of nanoMOFs particles inside splenic and hepatic macrophages.

In parallel, the linker has been quantified by HPLC in liver, spleen and urine. The development on new extraction and HPLC procedures has allowed the determination of the organic linkers in different biological complex matrices.[295,296] The presence of ligand in liver, spleen and urine after the nanoMOFs injection suggests a *degradation/excretion* process, as reported for some iron oxide particles.[297] A progressive increase in ligand concentration in urine has, indeed, been observed up to 15 days following the nanoMOFs injection. Noteworthy, the excretion profile depends on the polarity of the ligand. At blood pH (7.4), all carboxylate linkers are deprotonated, favoring their removal from urine. More hydrophobic tetramethylterephthalate ligand led to a slower degradation of nanoMIL-88B_4CH_3 compared to MIL-100 and MIL-88A nanoparticles, probably because of its lower solubility in the biological medium. Note that fumaric acid is an endogenous molecule which can be reused in the Krebs cycle. Thus, only few traces of this linker have been detected in urine after the MIL-88A administration, in agreement with its biological reuse.[55,140] The dosage of the linkers in liver, spleen and urine after the administration of the organic ligand alone have shown that, in all cases, the linker is directly removed by urine without accumulation in the RES. In fact, while 90% of the injected trimesate has been rapidly removed by urine on the day following the injection, tetramethylterephthalate excretion occurred in more than 4 days. Interestingly, the absence of activation of cytochrome P-450 (Cyp3A4 and Cyp2E1 isoenzymes), an hepatic enzyme related to the metabolization of exogenous substance, rules out the metabolization of the organic linker and suggests a direct excretion of the polyacids, in agreement with the presence of the intact linker form in urine.

Serum levels of aspartate aminotransferase (AST), alanine aminotransferase (ALT) and alkaline phosphatase (AP) are frequently used as biochemical markers of the liver function. AST, ALT, and PA activity increased 24 h after administration of nanoMOFs, and were back to normal values after 7 days.[140] This probably results from the accumulation of iron issued from the biodegradation of the nanoMOFs, as previously deduced from iron quantification, since enzymatic activity remained totally normal after the administration of organic ligands alone. It is well-known that iron hepatic overload leads to a compensation phenomenon, characterized by a more or less longer overload depending on the intrahepatocytic overload, followed by either a reestablishing or a decompensate phase with cell damage and tissue necrosis (inflammation and fibroblast activation).[288] This suggests a latency time for the regulation of iron hepatic homeostasis, as observed experimentally.

Finally, the hepatic superoxide dismutase activity (SOD) and the glutathione levels (GSSG/GSH), commonly used as biochemical markers for oxidative stress, were evaluated after the nanoMOFs administration.[140] While the injected organic linker did not cause any modification on the antioxidant level, introduction of nanoMOFs produced a reversible increase in both the

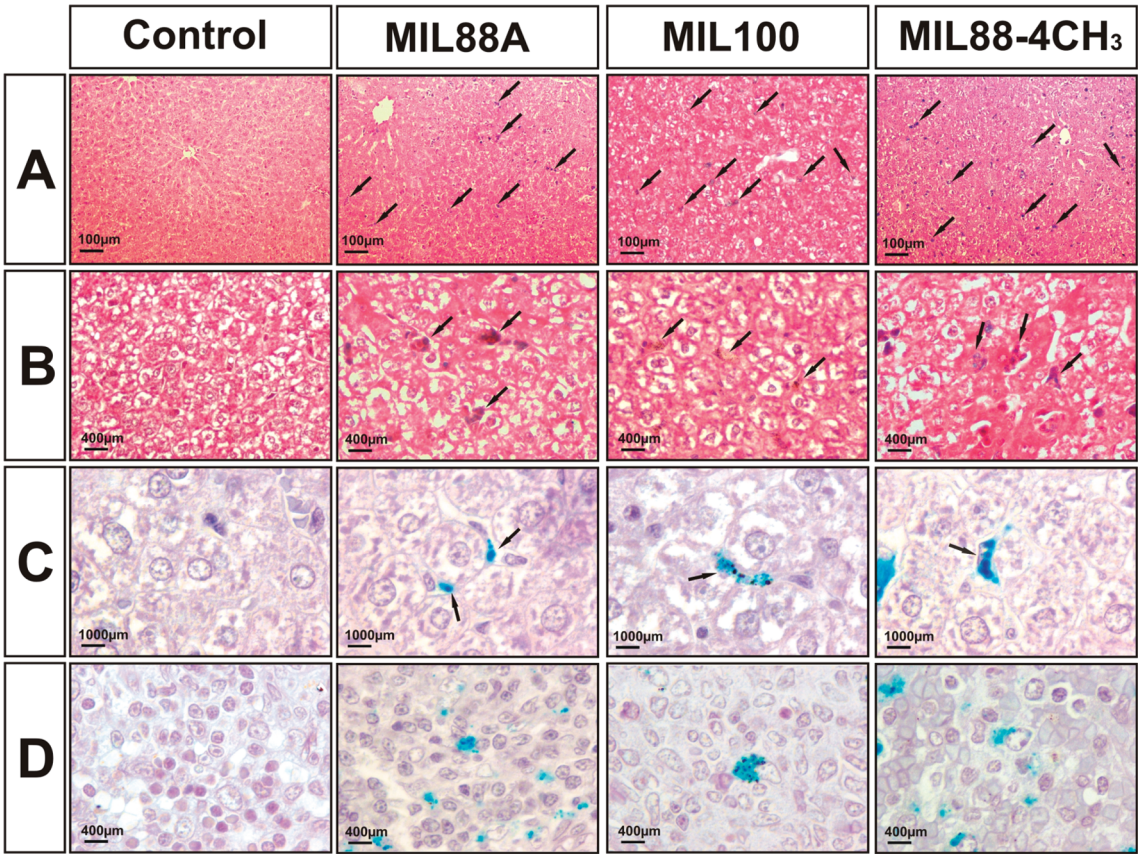

Figure 32. Histological sections of liver (A, B, C) and spleen (D) samples collected the day following injection of different nanoMOFs. (A,B) hematoxiline/eosin staining (Gx10(A) and Gx40 (B)); (C,D) Perls Prussian Blue staining (Gx100 (C) Gx40 (D)) of control, MIL-88A, MIL-100, and MIL-88B_4CH_3 groups.

activity of SOD and the GSSG/GSH ratio. This time depending effect (values increase up to 7 d and were back to normal values at 30 d) may be related with the high level of iron concentrations in the liver. If under physiological conditions, iron is present in the body, mostly associated with hemoglobin,[298] a high level of free iron has been previously associated with an increase in the oxidative stress.[299,300] Most of the iron might be incorporated to ferritin in Kupffer cells, as reported for other iron nanoparticles.[297] However, the rather good stability of iron carboxylates under acidic conditions could lead to a relatively slow degradation in the endosome.[140] Besides, in agreement with this, the neutral or negative surface charge of these nanoparticles in Kupffer cells might prevent their rapid clearance from the liver, as reported for some dextran-coated nanoparticles.[285] Iron resulting from a slight degradation in the endosome could be then transported from the endosome to the cytoplasm primarily by the iron transporter DMT1.[301]However, the endosomial degradation and the intracellular traffic studies are now required to clarify the biodegradation and biodistribution processes. Then, iron shall be reduced into Fe(II) by the Fenton reaction and incorporated to ferritin thought a ferroxidase center, which allows the iron oxidation and deposition in its cavity. Ferritin expression is regulated by iron homeostasis and by oxidative damage. Hence, this antioxidant reaction consumes Fe(II) and peroxides, producing toxic free radicals in the Fenton reaction,[302] which can consequently disturb the antioxidant balance.

Noteworthy, increase in SOD activity and GSSG/GSH levels did not significantly vary with the nature of the nanoMOFs tested and seem well correlated with the iron concentration. Hence, since one of the main roles of the liver is detoxification, hepatic cells are highly exposed to oxidative stress causes. However, histopathological examination of liver did not show any severe hepatic damage. Also, normal serum iron levels indirectly suggests that the total iron biding capacity of transferrin, parameter used as an indirect marker for the liver function,[288]is unchanged, explaining the preservation of the liver functions.

In a nutshell, these investigations have highlighted the lack of severe toxicity after intravenous administration of very high doses of iron carboxylate nanoMOFs. However, additional studies concerning biodistribution, cellular mechanism, subacute or chronic toxicity... are still needed. In this view, preliminary subacute in vivo toxicity assays have already been carried out by intravenous administration up to 150 mg of MIL-88A per kg and per day during four consecutive days and have revealed no sign of toxicity up to ten days after administration.[55]

8. DIAGNOSTICS

Magnetic resonance imaging (MRI) is a noninvasive diagnostic technique with high spatial resolution. The contrast in a MR image is the result of a complex interplay between instrument parameters and intrinsic differences in the relaxation rates of tissue water protons. Generally, the contrast can be improved by using a contrast agent (CA), such as a Gd^{III} chelate, which locally reduces the proton relaxation times. The magnitude of this effect on the longitudinal relaxation time T1 (or transverse relaxation time T2) is measured as the relaxivity r^1 (or r^2, respectively)

dx.doi.org/10.1021/cr200256v |*Chem. Rev.* 2012, 112, 1232–1268

normalized to 1 mM CA concentration at a given magnetic field strength. The relaxivity is used to evaluate the efficacy of the CAs.

However, most of the currently used CAs are nonspecific and far less efficient than predicted by theory.[303] Thus, a very active and challenging research is underway for targeting CAs, i.e. designing nanoparticulate systems able to delineate lesions in a given pathology. Reaching high concentrations of CAs enabling high relaxivity at the site of interest may be achieved mainly by: (i) using polymers with covalently bound CA units,[304,305] (ii) using noncovalent interactions between functionalized CA chelates and macromolecular substrates,[306,307]and (iii) using colloidal systems, such as liposomes and nanoparticles loaded with CAs.[308−311]

In particular, nanoparticles have received considerable attention because of their good entrapment properties offering the possibility to accumulate high amounts of the CAs in organs and tissues of interest (such as tumors) either by "passive targeting" taking advantage of enhanced permeability and retention (EPR) effect, or by "active targeting" using various target-specific ligands, such as monoclonal antibodies.[312]

The complexes of gadolinium (Gd^{3+}) are by far the most widely used CAs for MRI in clinic, because of their highest electronic spin value ($S = 7/2$) and slow electronic relaxation rate.[313] In the field of nanoMOFs for MRI,[314] first, a Gd^{III}-based nanoscale MOF has been reported.[66−69] High relaxivities have been obtained and were claimed to be of several orders of magnitude higher than those of other Gd^{III}-based MRI contrast agents. More recently, nanoMOFs for theranostics were prepared through the attachment of multifunctional polymer chains such as copolymers of poly(N-isopropylacrylamide)-co-poly(N-acryloxysuccinimide)-co-poly(fluorescein O-methacrylate) to the Gd III nanoMOF surfaces.[315]The succinimide functionality was utilized to attach both methotrexate, an active molecule, and a peptide for targeting purposes. Thus, the nanoparticles were endowed with bimodal imaging capabilities through both magnetic resonance and fluorescence microscopy. Besides, other polymers such as poly[*N*-(2-hydroxypropyl)methacrylamide], poly(*N*-isopropylacrylamide), polystyrene, poly(2-(dimethylamino)ethyl acrylate), poly(((poly)ethylene glycol) methyl ether acrylate), or poly(acrylic acid) could also be successfully coupled to these nanosystems.[316] The relaxivity rates of the surface-modified MOF nanoparticles were related to the molecular weight and chemical structures of the polymers and were significantly higher than both the unmodified Gd-nanoMOFs and the clinically employed contrast agents, Magnevist and Multihance.

However, although the Gd^{3+} ions are highly paramagnetic, their in vivo toxicity might be a concern.[317] To overcome this drawback, Mn(II)-based nano-MOFs have been developed based on the fact that Mn(II) is considered as much less toxic than its Gd(III) counterpart.[69] Although the relaxivities observed were modest, these studies have shown that site-specific imaging would be possible with the help of a silica-based coating at the nanoMOFs' surface to delay the leaching of metal ions until the nanoparticles reach their target site.

Other attempts to synthesize MOF materials endowed with imaging properties consisted in forming single crystalline materials by the reaction of the anhydrous chlorides of rare earth elements (Sm (1), Gd (2), Tb (3)) with a melt of 1,4-benzodinitrile in the absence of solvents. The dinitrile ligand was strongly coordinated substituting parts of the chlorine coordination. However, the largest cavities within the MOF structures had diameters of only 3.9−8.0 Å.[318] NanoMOFs consisting of Tb^{3+} ions and a cisplatin prodrug were surrounded by a silica shell and conjugated to a targeting peptide.[68] They showed good cytotoxicity against the colon adenocarcinoma cell line HT-29, comparable with that of cisplatin free in solution, whereas the untargeted nanoparticles did not exhibit significant cell death.

Relatively large crystals (400 nm to 1 μm) of Ln-MOFs were reported.[319] The values of r^1 were very small and varied only slightly with the effective magnetic moment of the lanthanide ions, while r^2 values were larger. The relaxivities of the nano-MOFs with smallest sizes were the most important. However, their relatively large size (>400 nm) is not optimal for intravenous administration.[320]

One of the most challenging objectives in drug therapy is "theranostics" or following both drug delivery within the body through the intrinsic imaging properties of the MOF and efficacy of the therapy. To reach this goal, the surface of the iron terephthalate MIL-101 nanoparticles has been modified post-synthetically through the use of amino terephthalate groups. Besides, an anticancer drug (12.8 wt %) and a fluorophore (5.6−11.6%) were then loaded onto the MOF in order to combine in the same nanoparticulate system the possibilities of optical imaging and anticancer therapy.[85] However, the nanoparticles had to be covered with a silica layer to increase their stability and control the drug and fluorophore release. The fluorophore agent is active only when it is free in solution, as a result of the quenching effect of Fe^{III}.[85]

In this context, a promising approach for theranostics is the use of non toxic porous iron(III) carboxylates,[55−57] able to load exceptionally high amounts of drugs with various physicochemical properties (hydrophobic, amphiphilic or hydrophilic) and have relaxivities adapted for in vivo applications.

Thus, MRI measurements have been performed on Wistar female rats 30 min after injection of suspensions of MIL-88A and MIL-100 nanoparticles. Both gradient echo and spin echo sequences clearly showed that the treated liver and spleen organs were darker than the normal ones, because of the preferential accumulation of the nanoMOFs in these RES organs.[55] The resulting aspects of the liver and the spleen are indeed different between control and treated rats (Figure 33A and B). However, three months after injection, the liver and spleen returned to a similar appearance to that of the untreated rats, in accordance with the temporary accumulation of the nano-MOFs in these organs. Moreover, it has been shown by Mössbauer spectroscopy that the contrast effect was because of the iron carboxylate matrix and not to the eventual presence of iron oxide and/or hydroxide degradation products which could act also as CAs.

Recently, Imaz et al.[321] have reported the synthesis of colloidal amorphous MOFs by coordination polymerization of Zn^{II} metal ions and 1,4-bis (imidazol-1-yl methyl) benzene. The size of the resulting spherical particles could be varied in a wide range (100−1500 nm) depending on the concentration of the reactants. Iron oxide nanoparticles (10 nm in diameter) could be successfully entrapped inside these spheres during their fabrication procedure, as demonstrated by electron microscopy investigations.[322] Ke et al.[197] has prepared a magnetic MOF nanocomposite, fabricated by incorporating Fe_3O_4 nanorods in nanocrystals of the porous cupper trimesate HKUST-1. Magnetic behavior of the nanocomposites, evaluated at 10 T, showed the saturation magnetization values between 1.54 and 0.92 emu.g^{-1} depending on the Fe_3O_4 content. Moreover, luminescent quantum dots and fluorescent dyes such as fluorescein and rhodamin could be encapsulated by the same procedure. These studies open up possibilities to confer multifunctional capabilities to nanoMOFs.

Optical imaging has emerged over the last years as a powerful imaging modality widely employed mainly for oncological

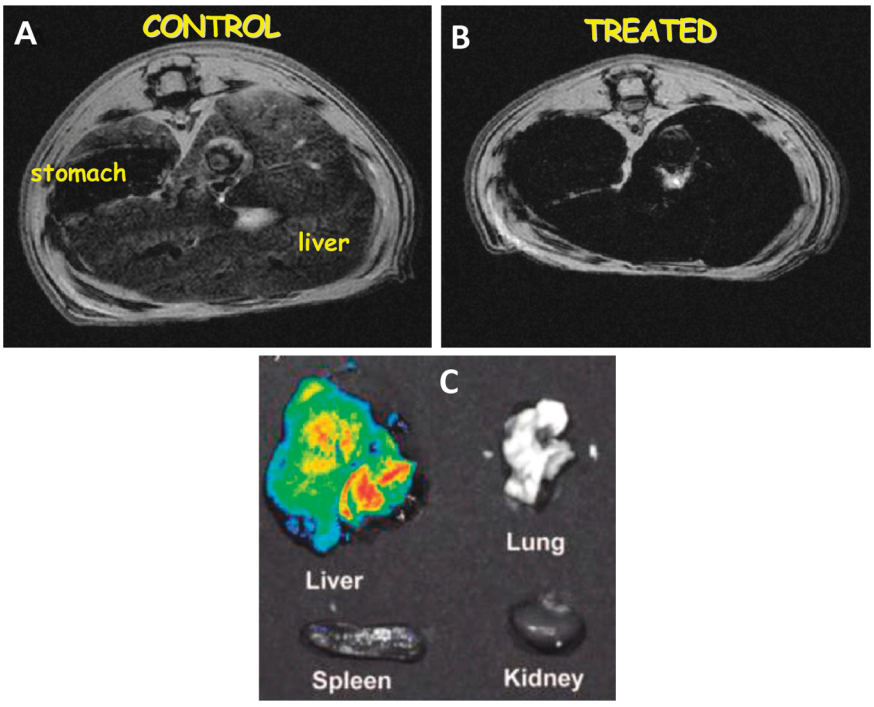

Figure 33. MRI investigations 30 min after injection of isotonic solution (A, control) or MIL-88A nanoparticles (B) in Wistar female rats. Imaging was performed at 300 MHz on a 7T horizontal-bore magnet. Rats were killed (isoflurane over dosage) [adapted from ref 55]. (C) Fluorescent images of tissue samples (liver, spleen, kidney and lung) isolated from mice after intravenous injection of dye doped Gd^{3+} nanoMOFs [adapted from ref 324].

applications, owing to its ability to noninvasively differentiate between diseased (e.g., tumor) and healthy tissues on the basis of differential dye accumulations. Recently, nanoMOFs have been synthesized by using a phosphorescent ruthenium complex as bridging ligand and zinc or zirconium connecting points.[323] The dye loadings reached 78.7% and 57.4%, respectively. The zirconium nanoMOFs were further stabilized with a silica coating and then functionalized with poly(ethylene glycol) (PEG) and a targeting molecule for in vitro optical imaging of cancer cells.

Recently, nanoparticles made of supramolecular coordination polymer networks were obtained from the self-assembly of nucleotides and lanthanide ions in water and could include other functional molecules such as fluorescent dyes, metal nanoparticles, quantum dots, enzymes, and proteins.[324−326] Fluorescence reflectance imaging (Figure 33C) showed that after intravenous administration in mice, fluorescent dye-loaded Gd^{3+} based nanoMOFs were rapidly taken up by liver and were thus not detected in other organs such as lung or kidneys. This was attributed to the recognition of the nanoparticles by RES. As only a negligible effect of the nanoMOFs was observed on the blood levels of aspartate aminotransferase and alanine aminotransferase (enzymes that assess liver function), it was claimed that the nanoparticles were non toxic and could find potential application as imaging agents for liver.[324] Interestingly, the self-assembly of nucleotide monophosphates and lanthanide ions on the surface of the semiconductor nanocrystals (quantum dots) lead to the formation of a supramolecular shell (4−8 nm in thickness) of coordination networks.[326] However, all these studies use lanthanide (essentially Gd^{3+} based nanoMOFs) arising the same toxicity concern as previously discussed.

X-ray computed tomography is a powerful diagnostic tool capable of providing three-dimensional images with excellent spatial resolution to investigate various bodily structures based on their ability to block the X-ray beam. Typical CAs are materials containing elements with a high Z number such as iodine, barium and bismuth. In clinics, iodinated aromatic molecules and barium sulfate have been approved for intravenous and gastrointestinal tract imaging, respectively. The CAs for computer tomography have the same drawbacks as the CAs for MRI, such as a non specific distribution and a fast clearance. For this reason, nanoparticulate nanoMOFs have been developed as carriers for iodinated aromatic molecules.[327] The bridging ligands were tetraiodobenzenedicarboxylic acids and the metal connecting points were Cu^{II} or Zn^{II}. The potential of the resulting iodinated nanoMOFs for computed tomography has been clearly demonstrated in phantom studies.

All the above presented studies highlight the potential of nanoscale coordination polymers as a novel platform for MRI, optical imaging or X-ray computed tomography.

9. CONCLUSION/OUTLOOKS

MOFs or coordination polymers through their tunable composition, structure, pore size, and volume, easy functionalization, flexible network and/or accessible metal sites, possess many advantages for the adsorption and release of biomolecules compared to other carriers such as inorganic porous solids (zeolites or mesoporous silica) or organic polymers. Their biodegradable character can also be modified through an adequate choice of the metal, linker and structure which results in a degradation in body fluid from a few minutes up to weeks. Among them, MOFs based on endogenous linkers are of great interest even if real porous "BioMOFs" are still scarce. An alternative method of releasing high amounts of drugs consists in making a bioactive MOF based on the drug itself as the linker and release it through the degradation of the MOF itself, or use a bioactive metal (Ag, Zn, Ca, Mn, Gd, Fe, ...) as the inorganic cation, to introduce additional properties such as antibacterial activity or imaging properties.

The formulation of MOFs particles is a crucial step for their administration. The synthesis at the nanometric scale of MOFs through various techniques such as microwave assisted hydro or solvothermal conditions, sonothermal methods, reverse emulsion techniques, ..., allows numerous administration routes (intravenous, ocular, etc.), as well as facilitates other formulations. Indeed, many other potentially interesting dispositives have been developed, including pellets, thin films, gels, composites and more. Although the surface modification of MOFs nanoparticles is still at its infancy, this is particularly interesting since it can easily modulate MOFs biodistribution (bioadhesion, stealth, targeting, etc) together with improving their stability.Toxicity studies of MOFs, still very scarce, have shown at the preclinical level using rats that several porous iron carboxylates nanoMOFs are non toxic after i.v. administration at very high doses.

MOFs have shown so far the highest loading capacities of therapeutic molecules (drugs, cosmetics, or biological gases) associated, in most cases, to the possibility of controlling the release of their cargo. Record amounts of highly challenging drug or biogas molecules have therefore been successfully entrapped and in vitro released from non toxic porous MOFs in a controlled manner. The presence of crystalline frameworks also makes easier the analysis of the host−guest interactions and systematic encapsulation/release studies of model drugs combined to modeling techniques represents a promising method to develop predicting models.

However, despite important advantages, there is still a lot to do prior to the practical use of MOFs in biomedecine. First, several critical issues need to be addressed, such as the understanding of the mechanism of degradation of the MOF (or the drug loaded MOF) and the kinetics of delivery for a given pair of drug molecule−MOF structure. Indeed, very large differences in terms of kinetics of release have been observed so far either when changing the drug for a given MOF or using different MOFs for the same biomolecule. It is currently admitted that delivery is controlled mainly by host−guest interactions and diffusion but in the case of MOFs, their degradation in the body fluid leads to an acceleration of the release of the drug molecule. Second, partially because of their degradable character, the synthesis of stable and monodisperse formulations of MOFs nanoparticles represents still a major issue. The same problem occurs for the surface modification of MOFs nanoparticles. If first results seem promising, one has still to evaluate the stability of the surface modification as well as the final stealth, addressing or bioadhesive properties of the resulting surface-engineered nanoparticles. Similar issues are important in the design of MOFs for the controlled-release of medical gases such as NO. If no sign of toxicity at the preclinical level has been demonstrated for a few selected iron carboxylate MOFs, it will be required both to assess the toxicity of other MOFs as well as pursuing the analysis up to the biodistribution of the material, including the cellular transit, degradation, excretion mechanisms, physiological barrier penetration, chronic toxicity, ..., once administered in the body through the different routes. In vivo studies of the pharmacokinetics and efficiency of the drug nanoMOF will be the major next steps to evaluate the real performances of the MOFs in biomedicine.

Finally, the remarkable intrinsic properties of the nanoMOFs as contrast agents either in MRI, optical imaging or X-ray computed tomography allows following both detection of the drug-loaded nanoparticles and efficacy of a given therapy. This multifunctionality opens up challenging perspectives for "theranostics" or the personalized therapy.

In conclusion, MOFs for biomedical applications are of a great interest with many very promising results, indicating that these porous solids exhibit several advantages over existing systems. Despite many issues still to be addressed, considering the huge number of remaining existing encapsulation problems such as the controlled release of the drug molecules that have not been commercialized because of their poor bioavailability (solubility, stability, ...), this strengthens the interest in further developing bioapplications using MOFs.

AUTHOR INFORMATION

Corresponding Author

*E-mail: horcajada@chimie.uvsq.fr (P.H.); serre@chimie.uvsq.fr (C.S.).

BIOGRAPHIES

Dr Patricia Horcajada, 33 years old, received her grade in pharmacy from the University Complutense de Madrid in 2001. Then, she completed her PhD of pharmacy at the University Complutense de Madrid in November 2005, focusing her work on materials for the bone replacing and the drug controlled release from porous solids. She joined the Porous Solids group in the Institut Lavoisier (University of Versailles, France) firstly as a postdoctoral researcher and later, in 2007, as CNRS permanent researcher. With a background in pharmacy and material chemistry, her main research interests concerns the synthesis of porous metal−organic frameworks, controlling their particle size, as well as their applications, especially on biomedicine (imaging, drug delivery).

Dr Ruxandra Gref is research director at the National Research Center, Paris XI, France. Chemical engineer, she performed her postdoctoral research at MIT, where she elaborated "stealth" nanoparticles for controlled drug release. Her research is focussed on "green" nanotechnologies to address challenges such as the entrapment of labile molecules, unable to bypass natural barriers or inducing resistance.

Dr Tarek Baati, 36 years old, received in 2003 his master degree in Biology in the High Institute of Biotechnology of Monastir then he joined the laboratory of Trace Elements and antioxidants in the Faculty of Medicine of Monastir as engineer. In 2005 he completed his PhD of toxicology at the University Paris 11 (France), focusing his work on toxicity and antioxidant effects of fullerene. He joined in 2009 the Porous Solids group in Institute Lavoisier (University of Versailles, France) as a postdoctoral researcher. With a background in Biology, in vivo experiments and bioanalysis, his main research interests concerns the bioapplication of porous metal−organic frameworks (MOFs), controlling their degradation, as well as their applications on biomedicine.

Phoebe Allan is from Rutland, England. She received her MSci in Natural Sciences from the University of Cambridge in 2008. She is currently pursuing a PhD in the area of materials chemistry including the controlled released of biologically active gases from porous solids, at the University of St Andrews, U.K., under the supervision of Professor Russell Morris.

Guillaume Maurin, 36 years old, received a PhD in Physical Chemistry from Université Montpellier 2 (France) in 2001. After a Post-Doctoral Marie Curie Fellowship at the Royal Institution of Great Britain in London (U.K.) in the group of Pr. CRA Catlow, he became Lecturer in 2002 at the Université Provence (France) and later at the Université Montpellier 2 where he received his "Habilitation to Direct Research" in 2006. He is currently Professor at the Université Montpellier 2, head of the "Dynamics & Adsorption in Materials with Porosity" Group in the Institut Charles Gerhardt Montpellier since 2011. His research interests include the development and applications of advanced molecular simulations techniques to model the adsorption and diffusion of guest molecules (gas and drug) confined in inorganic and hybrid nanoporous materials.

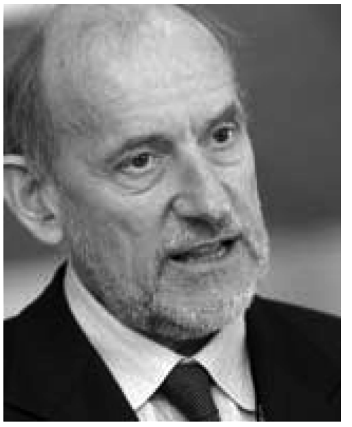

Professor Patrick Couvreur is Full Professor of Pharmacy at the Paris-Sud University and holder of the chair of "Innovation Technologique" (2009-2010) at the prestigious Collège de France. He is appointed as a Senior Member of the "Institut Universitaire de France". He is the recipient of an "ERC Advanced Grant" (2009). His contributions in the field of drug delivery and targeting are highly recognized around the world. His research is interdisciplinary, at the interface between Physico-Chemistry of Colloids, Polymer Chemistry, Material Science and Pharmacology. His overall research has led to the funding of two start-up companies (Bioalliance and Medsqual). His major scientific contribution was recognized through to the prestigious "Host Madsen Medal" (Beijin, 2007) and the Prix Galien 2009. His appointment as a member of four academies (Académie des Technologies, Académie de Médecine and Académie de Pharmacie in France as well as Académie Royale de Médecine in Belgium) is another recognition of his major scientific and scholarly contributions.

Professor Gérard Férey is internationally renowned in the area of solid chemistry and particularly for its contribution to the field of Metal Organic Frameworks, from their synthesis, structure solution,

modelling and applications. He was the creator of Institut Lavoisier in 1996 and at the head of the Porous Solid Group up to 2009. He is a member of the French Academy of Sciences and was awarded the Gold medal of CNRS in 2010. He also received many national and international distinctions including ENI 2010, Japanese Chemical Society 2008, Gay-Lussac-Humboldt 2004.

Professor Russell Morris studied chemistry at the University of Oxford before undertaking postdoctoral studies at the University of California, Santa Barbara. He returned to the UK in 1995 to the University of St Andrews, where he is now a Professor of Chemistry. His research interests include the synthesis, characterization, and application of porous solids. Highlights of his research include the invention of the ionothermal method of synthesis, the development of chiral induction in porous solids, and gas storage applications of porous materials in medicine.

Dr. Christian Serre, 41 years old, is an engineer from the Ecole Supérieure de Physique et de Chimie Industrielles de Paris. He obtained a PhD in Inorganic Chemistry in 1999. After a postdoctoral fellowship in the U.S.A. in 2000, he moved to a permanent CNRS research position in 2001 in the Porous Solids group in Versailles. He is now director of research since 2009. He is currently at the head of the Porous Solid Group in Versailles. He received the CNRS bronze medal in 2006 and a European research council young researchers' grant in 2008. His research topics deal with the synthesis, structure determination and applications of porous hybrid solids.

ACKNOWLEDGMENT

P.H., T.B., and C.S. thank EU for the funding via the ERC-2007-209241-BioMOFs, UniverSud Paris 2010-25, Pôle de Competitivité Medicen "Nanogalenic" and French-Tunisian CNRS/DGRS cooperation n° 24432, P.H., C.S., G.F., R.G. P.C. for their colleagues from Institut Lavoisier, Université Paris Sud and KRICT (Daejon, Korea). R.E M. and P. K.A. acknowledge the E.P.S.R.C for funding. R.E.M is a Royal Society Wolfson Merit Award Holder. G.M. thanks the Region Languedoc Roussillon for its financial support through the award "Chercheur d'Avenir" 2009. RG acknowledge the European CYCLON grant ITN 237962.

ACRONYMS

MOF	metal−organic framework
nanoMOFs	nanoparticles of metal−organic framework
PEG	poly(ethylene glycol)
LD_{50}	lethal dose 50
CPO	coordination polymer from Oslo
MIL	material from Institut Lavoisier
BioMIL	bioactive material from Institut Lavoisier
UiO	University of Oslo
ZIF	zeolite imidazolate framework
HKUST	Hong Kong University of Science and Technology
UMCM	Université de Moncton
STAM	Saint Andrews University
IRMOF	isoreticular metal−organic framework
STY	space time yields
TCNQ	tetracyanoquinodimethane
PVP	polyvinilpyrrolidone
CTAB	cetyltrimettylammonium bromide surfactant
DMF	dimethylformamide
PBI	poly isobutanol
polyHIPE	monolithic macroporous hydrophilic polymer
SBF	simulated body fluid
PBS	phosphate buffer solution
ADME	absorption−distribution−metabolism−excretion
i.v.	intravenous
API	active pharmaceutical ingredient
BET	Brunauer−Emmett−Teller
NMR	nuclear magnetic resonance
XRPD	X-ray powder diffraction
DFT	density functional theory
Bu	busulfan
Doxo	doxorubicin
AZT-Tp	azidothimidine triphosphate
CDV	cidofovir
AZT	azidothimidine
DSCP	disuccinatocisplatin
AIDS	acquired immune deficiency syndrome
HIV	human immunodeficiency virus
NRTIs	nucleoside reverse transcriptase inhibitors
Br-BODIPY	1,3,5,7-tetramethyl-4,4-difluoro-8-bromomethyl-4-bora-3a,4a-diaza-s-indacene
QSAR	quantitative structure−activity relationship
HPLC	high performance liquid chromatography
AAS	atomic absorption spectroscopy
MTT	3-(4,5-dimethylthiazol-2-yl)-2,5-diphenyltetrazolium bromide
PBMC	peripheral blood mononuclear cells
IC_{90}	inhibitory concentration 90
PRP	human platelet rich plasma
MRSA	methicillin-resistant *Staphylococcus aureus*
iNOS	inducible nitric oxide synthases

sGC	soluble guanylatecyclase
cGMP	cyclic guanosine monophosphate
Hb orhaem	hemoglobin
HbCO	carboxy-hemoglobin
OxHb	oxy-hemoglobin
HO	enzyme hemoxygenase
NADPH	nicotinamide adenine dinucleotide phosphate
MC	methylene chloride
CORMs	carbon monoxide-releasing molecules
RES	reticulo-endothelial system
IL-6	interleukine-6
BBB	brain blood barrier
CPK	creatine phosphokinase
AST	aspartate aminotransferase
ALT	alanine aminotransferase
AP	alkaline phosphatase
SOD	superoxide dismutase activity
GSSG	oxidized glutathione
GSH	reduced glutathione
DMT1	divalent metal transporter 1
MRI	magnetic resonance imaging
CA	contrast agent
T1	longitudinal relaxation time
T2	transverse relaxation time
EPR	enhanced permeability and retention

REFERENCES

(1) Clearfield, A. *Prog. Inorg. Chem.* **1998**, *47*, 371.

(2) Eddaoudi, M.; Moler, D. B.; Li, H.; Chen, B.; Reineke, T. M.; O'Keeffe, M.; Yaghi, O. M. *Acc. Chem. Res.* **2001**, *34*, 319.

(3) Férey, G.; Mellot-Draznieks, C.; Serre, C.; Millange, F. *Acc. Chem. Res.* **2005**, 317.

(4) Férey, G. *Chem. Soc. Rev.* **2008**, *37*, 191.

(5) Some major references in the field: (a) Yaghi, O. M.; O'Keeffe, M.; Ockwig, N. W.; Chae, H. K.; Eddaouddi, M.; Kim, J. *Nature* **2003**, *423*, 705. (b) Rowsell, J. L. C.; Yaghi, O. M. *Angew. Chem., Int. Ed.* **2005**, *44*, 4670. (c) Rao, C. N. R.; Natarajan, S.; Vaidhyanathan, R. *Angew. Chem., Int. Ed.* **2004**, *43*, 1466. (d) Kitagawa, S.; Kitaura, R.; Noro, S.-H. *Angew. Chem., Int. Ed.* **2004**, *43*, 2334. (e) James, S. L. *Chem. Soc. Rev.* **2003**, *32*, 276. (f) Maspoch, D.; Ruiz-Molina, D.; Veciana, J. *Chem. Soc. Rev.* **2007**, *36*, 770. (g) Serre, C.; Millange, F.; Thouvenot, C.; Noguès, M.; Marsolier, G.; Louër, D.; Férey, G. *J. Am. Chem. Soc.* **2002**, *124*, 13519. (h) Férey, G.; Mellot-Draznieks, C.; Serre, C.; Millange, F.; Dutour, J.; Surblé, S.; Margiolaki, I. *Science* **2005**, *309*, 2040. (i) Férey, G.; Serre, C.; Mellot-Draznieks, C.; Millange, F.; Dutour, J.; Surblé, S.; Margiolaki, I. *Angew. Chem., Int. Ed.* **2004**, *43*, 6296. (j) Serre, C.; Mellot-Draznieks, C.; Surblé, S.; Audebrand, N.; Filinchuk, Y.; Férey, G. *Science* **2007**, *315*, 1828. (k) Chui, S.S-Y.; Lo, S.M-F.; Charmant, J. P. H.; Orpen, A. G.; Wiliams, I. D. *Science* **1999**, *283*, 1148.

(6) Hoskins, B. F.; Robson, R. *J. Am. Chem. Soc.* **1989**, *111*, 5962.

(7) See the special issues: *Acc. Chem. Res.*, **2005**, *38*, 215; *J. Solid State Chem.*, **2005**, *178*, 2409; Themed issue: Metal−organic frameworks, *Chem. Soc. Rev.* **2009**, 1201.

(8) Férey, G.; Serre, C.; Devic, T.; Maurin, G.; Jobic, H; Llewellyn, P. L.; De Weireld, G.; Vimont, A.; Daturi, M.; Chang, J.-S. *Chem. Soc. Rev.* **2011**, *40*, 550.

(9) Kitagawa, S.; Kitaura, R.; Noro, S.-I. *Angew. Chem., Int. Ed.* **2004**, *43*, 2334.

(10) Férey, G.; Serre, C. *Chem. Soc. Rev.* **2009**, *38*, 1380.

(11) (a) Eddaoudi, M.; Kim, J.; Rosi, N.; Vodak, D.; Wachter, J.; O'Keeffe, M.; Yaghi, O. M. *Science* **2002**, *295*, 469. (b) Li, J.-R.; Tao, Y.; Yu, Q.; Bu, X.-H.; Sakamoto, H.; Kitagawa, S. *Chem.—Eur. J.* **2008**, *14*, 2771. (c) Devic, T.; Horcajada, P.; Serre, C.; Salles, F.; Maurin, G.; Moulin, B.; Heurtaux, D.; Clet, G.; Vimont, A.; Grenèche, J.-M.; Le Ouay, B.; Moreau, F.; Magnier, E.; Filinchuk, Y.; Marrot, J.; Lavalley, J.-C.; Daturi, M.; Férey, G *J. Am. Chem. Soc.* **2010**, *132*, 1127. (d) Wang, Z.; Tanabe, K. K.; Cohen, S. M. *Inorg. Chem,.* **2009**, *48*, 296. (e) Kaye, S. S.; Long, J. R. *J. Am. Chem. Soc.* **2008**, *130*, 806. (f) Hwang, Y. K.; Hong, D.-Y.; Chang, J. S.; Jhung, S. H; Seo, Y.-K; Kim, J.; Vimont, A.; Daturi, M.; Serre, C.; Férey, G. *Angew. Chem., Int. Ed.* **2008**, *47*, 4144.

(12) Van Der Merwe, D.; Tawde, S.; Pickrell, J. A.; Erickson, L. E. *Cutaneous Ocular Tox.* **2009**, *28* (2), 78.

(13) Dietzel, P. D. C.; Blom, R.; Fjellvag, H. *Eur. J. Inorg. Chem.* **2008**, *23*, 3624.

(14) Horcajada, P.; Surblé, S.; Serre, C.; Hong, D.-Y.; Seo, Y.-K.; Chang, J.-S.; Grenèche, J.-M.; Margiolaki, I.; Férey, G. *Chem. Commun.* **2007**, 2820.

(15) An, J.; Geib, S. J.; Rosi, N. L. *J. Am. Chem. Soc.* **2009**, *131*, 8376.

(16) Vimont, A.; Goupil, J.-M.; Lavalley, J.-C.; Daturi, M.; Surblé, S.; Serre, C.; Millange, F.; Férey, G.; Audebrand, N. *J. Am. Chem. Soc.* **2006**, *128*, 3218.

(17) McKinlay, A. C.; Xiao, B.; Wragg, D. S.; Wheatley, P. S.; Megson, I. L.; Morris, R. E. *J. Am. Chem. Soc.* **2008**, *130*, 10440.

(18) Horcajada, P.; Serre, C.; Vallet-Regí, M.; Sebban, M.; Taulelle, F.; Férey, G. *Angew. Chem., Int. Ed.* **2006**, *45*, 5974.

(19) http://www.drugfuture.com/chemdata/zirconyl-acetate.html (accessed 2011).

(20) http://www.absoluteastronomy.com/topics/Zirconium (accessed 2011).

(21) http://www.imperialinc.com/msds0076160.shtml (accessed 2011).

(22) TOXNET.1975−1986. National library of medicine's toxicology data network. Hazardous Substances Data Bank (HSDB). Public Health Service.National Institute of Health, U. S. Department of Health and Human Services. Bethesda, MD: NLM

(23) http://msds.chem.ox.ac.uk/MA/manganese_II_chloride_tetrahydrate.html (accessed 2011).

(24) http://www.jtbaker.com/msds/englishhtml/F1678.htm (accessed 2011).

(25) http://msds.chem.ox.ac.uk/ZI/zinc_chloride.html (accessed 2011).

(26) http://www.mrdc.com/html/pdf/msds/Magnesium%20Chloride%2064%25%20Soln.%20MSDS.pdf (accessed 2011).

(27) http://msds.chem.ox.ac.uk/CA/calcium_chloride_anhydrous.html (accessed 2011).

(28) Eddaoudi, M.; Kim, J.; Rosi, N.; Vodak, D.; Wachter, J.; O'Keeffe, M.; Yaghi, O. M. *Science* **2002**, *295*, 469.

(29) Devic, T.; Horcajada, P.; Serre, C.; Salles, F.; Maurin, G.; Moulin, B.; Leclerc, H.; Heurtaux, D.; Vimont, A.; Clet, G.; Daturi, M.; Grenèche, J. M.; le Ouay, B.; Moreau, F.; Magnier, E.; Filinchuk, Y.; Marrot, J.; Férey, G. *J. Am. Chem. Soc.* **2010**, *132*, 1127.

(30) Horcajada, P.; Salles, F.; Wuttke, S.; Devic, T.; Heutaux, D.; Maurin, G.; Vimont, A.; Clet, G.; Daturi; M.; David, O.; Magnier, E.; Stock, N.; Filinchuk, Y.; Popov, D.; Rieckel, C.; Férey, G.; Serre, C. *J. Am. Chem. Soc.* **2011**, *133*(44), 17839.

(31) Guillerm V. Synthèse, fonctionnalisation et propriétés d'adsorption de nouveaux solides hybrides poreux. phD Thesis, Université de Versailles St Quentin, 2010, p 108.

(32) Li, H.; Eddaoudi, M.; O'Keeffe, M.; Yaghi, O. M. *Nature* **1999**, *402*, 276.

(33) Banerjee, R.; Furukawa, H.; Britt, D.; Knobler, C.; O'Keeffe, M.; Yaghi, O. M. *J. Am. Chem. Soc.* **2009**, *131*, 3875.

(34) Huang, X.-C.; Lin, Y.-Y.; Zhang, J.-P.; Chen, X.-M. *Angew. Chem., Int. Ed.* **2006**, *45*, 1557.

(35) Zhang, J.-P.; Chen, X.-M. *Chem. Commun.* **2006**, 1689.

(36) Liu, Y.; Kravtsov, V. C.; Laren, R.; Eddaoudi, M. *Chem.Commun.* **2006**, 1488.

(37) Whitfield, T. R.; Wang, X.; Liu, L.; Jacobson, A. J. *Solid State Sci.* **2005**, *7*, 1096.

(38) Cavka, J. H.; Jakobsen, S.; Olsbye, U.; Guillou, N.; Lamberti, C.; Bordiga, S.; Lillerud, K. P. *J. Am. Chem. Soc.* **2008**, *130*, 13850.

(39) Dan-Hardi, M.; Serre, C.; Frot, T.; Rozes, L.; Maurin, G.; Sanchez, C.; Férey, G. *J. Am. Chem. Soc.* **2009**, *131*, 10857.

(40) (a) Keskin, S.; Kizilel, S. *Ind. Eng. Chem. Res.* **2011**, *50* (4), 1799. (b) Imaz, I.; Rubio-Martínez, M.; An, J.; Solé-Font, I.; Rosi, N. L.; Maspoch, D. *Chem Commun.* **2011**, *47*, 7287
(41) Weber, R.; Bergerhoff, G. *Z. Kristallogr.* **1991**, *195*, 878.
(42) Serre, C.; Millange, F.; Surblé, S.; Férey, G. *Angew. Chem., Int. Ed.* **2004**, *43*, 6286.
(43) Serre, C.; Surblé, S.; Mellot-Draznieks, C.; Filinchuk, Y.; Férey, G. *Dalton Trans.* **2008**, 5462.
(44) Rabone, J.; Yue, Y.-F.; Chong, S. Y.; Stylianou, K. C.; Bacsa, J.; Bradshaw, D.; Darling, G. R.; Berry, N. G.; Khimyak, Y. Z.; Ganin, A. Y.; Wiper, P.; Claridge, J. B.; Rosseinsky, M. J. *Science* **2010**, *329*, 1053.
(45) Smaldone, R. A.; Forgan, R. S.; Furukawa, H.; Gassensmith, J. J.; Slawin, A. M. Z.; Yaghi, O. M.; Stoddart, J. F. *Angew. Chem Int. Ed.* **2010**, *122*, 1.
(46) Li, W.; Jin, L.; Zhu, N.; Hou, X.; Deng, F.; Sun, H. *J. Am. Chem. Soc.* **2003**, *125*, 12408.
(47) Rood, J. A.; Noll, B. C.; Henderson, K. W. *Inorg. Chem.* **2006**, *45* (14), 5521.
(48) Ingleson, M. J.; Barrio, J. P.; Bacsa, J.; Dickinson, C.; Park, H.; Rosseinsky, M. J. *Chem. Commun.* **2008**, 1287.
(49) Czaja, A., Leung, E., Trukhan, N., Müller, U., *Metal Organic Frameworks*; Farruseng, D., Ed.; Wiley, 2012 (see industrial MOF synthesis Chapter)
(50) Mueller, U.; Schubert, M.; Teich, F.; Puetter, H.; Schierle-Arndt, K.; Pastre, J. *J. Mater. Chem.* **2006**, *16*, 626.
(51) Sun, S.; Murray, C. B.; Weller, D.; Folks, L.; Moser, A. *Science* **2000**, *287*, 1989.
(52) Mokari, T.; Zhang, M.; Yang, P. *J. Am. Chem. Soc.* **2007**, *129*, 9864.
(53) Peng, X.; Manna, L.; Yang, W.; Wickham, J.; Scher, E.; Kadavanich, A.; Alivisatos, A. P. *Nature* **2000**, *404*, 59.
(54) Manna, L.; Milliron, D. J.; Meisel, A.; Scher, E. C.; Alivisatos, A. P. *Nat. Mater.* **2003**, *2*, 382.
(55) Horcajada, P.; Chalati, T.; Serre, C.; Gillet, B.; Sebrie, C.; Baati, T.; Eubank, J. F.; Heurtaux, D.; Clayette, P.; Kreuz, C.; Chang, J.-S.; Hwang, Y. K.; Marsaud, V.; Bories, P.-N.; Cynober, L.; Gil, S.; Férey, G.; Couvreur, P.; Gref, R. *Nat. Mater.* **2010**, *9*, 172.
(56) Horcajada, P.; Serre, C.; Férey, G.; Gref, R.; Couvreur, P.; Solide hybride organique inorganique a surface modifiee. French patent application 102573/FR filed the 1/10/2007 PCT/FR2009/001367, 01/10/08.
(57) Horcajada P., Serre C., Férey G., Gref R., Couvreur P. Nanoparticules hybrides organiques inorganiques a base de carboxylates de fer, French patent application 100936/FR filed the 1/10/2007, PCT/FR2008/001366, 01/10/08.
(58) Chalati, T.; Horcajada, P.; Gref, R.; Couvreur, P.; Serre, C. *J. Mater. Chem.* **2011**, *21*, 2220.
(59) Hermes, S.; Witte, T.; Hikov, T.; Zacher, D.; Bahnmüller, S.; Langstein, G.; Huber, K.; Fischer, R. A. *J. Am. Chem. Soc.* **2007**, *129*, 5324.
(60) Horcajada, P.; Serre, C.; Grosso, D.; Boissière, C.; Perruchas, S.; Sanchez, C.; Férey, G. *Adv. Mater.* **2009**, *21*, 1931.
(61) Cravillon, J.; Munzer, S.; Lohmeier, S.-J.; Feldhoff, A.; Huber, K.; Wiebcke, M. *Chem. Mater.* **2009**, *21* (8), 1410.
(62) Cho, W.; Lee, H. J.; Oh, M. *J. Am. Chem. Soc.* **2008**, *130*, 16943.
(63) Tsuruoka, T.; Furukawa, S.; Takashima, Y.; Yoshida, K.; Isoda, S.; Kitagawa, S. *Angew. Chem., Int. Ed.* **2009**, *48*, 4739.
(64) Kerbellec, N.; Catala, L.; Daiguebonne, C.; Gloter, A.; Stephan, O.; Bunzli, J.-C.; Guillou, O.; Mallah, T. *New J. Chem.* **2008**, *32*, 584.
(65) Daiguebonne, C.; Kerbellec, N.; Guillou, O.; Bünzli, J.-C.; Gumy, F.; Catala, L.; Mallah, T.; Audebrand, N.; Gérault, Y.; Bernot, K.; Clavez, G. *Inorg. Chem.* **2008**, *47*, 3700.
(66) Rieter, W. J.; Taylor, K. M. L.; An, H.; Lin, W. *J. Am. Chem. Soc.* **2006**, *128*, 9024.
(67) Taylor, K. M. L.; Jin, A.; Lin, W. *Angew. Chem., Int. Ed.* **2008**, *47*, 7722.
(68) Rieter, W. J.; Pott, K. M.; Taylor, K. M. L.; Lin, W. *J. Am. Chem. Soc.* **2008**, *130* (35), 11584.
(69) Taylor, K. M. L.; Rieter, W. J.; Lin, W. *J. Am. Chem. Soc.* **2008**, *130* (44), 14358.
(70) Isomaa, B.; Reuter, J.; Djupsund, B. M. *Arch. Toxicol.* **1976**, *35* (2), 91.
(71) http://msds.chem.ox.ac.uk/HE/hexadecyltrimethylammonium_bromide.html, 2010
(72) https://irmm.jrc.ec.europa.eu/html/reference_materials_catalogue/catalogue/attachements/IRMM-442_msds.pdf, 2011
(73) http://msds.chem.ox.ac.uk/HE/1-hexanol.html, 2011
(74) Fillion, H., Luche, J.-L. In *Synthetic Organic Sonochemistry* Luche, J.-L., Ed.; Plenum Press: New York, 1998; p 91.
(75) *Ultrasound: Its Chemical, Physical, and Biological Effects*; S. Suslick, K., Ed.; VCH: Weinheim, Germany, 1988.
(76) Haque, E.; Khan, N. A.; Park, J. H.; Jhung, S. H. *Chem.—Eur. J.* **2009**, *16* (3), 1046.
(77) Schlesinger, M.; Schulze, S.; Hietschold, M; Mehring, M. *Microporous Mesoporous Mater.* **2010**, *132*, 121.
(78) Li, Z.-Q.; Qiu, L.-G.; Su, T.; Wu, Y.; Wang, W.; Wu, Z.-Y.; Jiang, X. *Mater. Lett.* **2009**, *63*, 78.
(79) Qiu, L.-G.; Li, Z.-Q.; Wu, Y.; Wang, W.; Xu, T.; Jiang, S. *Chem. Commun.* **2008**, 3642.
(80) Park, S.-E.; Hwang, Y. K.; Kim, D. S.; Jhung, S. H.; Hwang, J. S.; Chang, J.-S. *Catal. Surv. Asia* **2004**, *8*, 91.
(81) Tompsett, G. A.; Conner, W. C.; Yngvesson, K. S. *ChemPhysChem* **2006**, *7*, 296.
(82) Ni, Z.; Maesl, R. I. *J. Am. Chem. Soc.* **2006**, *128*, 12394.
(83) Jhung, S. H.; Lee, J.-H.; Yoon, J. W.; Serre, C.; Férey, G.; Chang, J.-S. *Adv. Mater.* **2006**, *19* (1), 121.
(84) Demessence, A.; Horcajada, P.; Serre, C.; Boissière, C.; Grosso, D.; Sanchez, C.; Férey, G. *Chem. Commun.* **2009**, 7149.
(85) Taylor-Pashow, K. M. L.; Della Rocca, J.; Xie, Z.; Tran, S.; Lin, W. *J. Am. Chem. Soc.* **2009**, *131*, 14261.
(86) http://msds.chem.ox.ac.uk/DI/N,N-dimethylformamide.html, 2011
(87) http://msds.chem.ox.ac.uk/PY/pyridine.html, 2011
(88) http://msds.chem.ox.ac.uk/ME/methyl_alcohol.html, 2011
(89) Ferreira, A. F. P.; Santos, J. C.; Plaza, M. G.; Lamia, N.; Loureiro, J. M.; Rodrigues, A. E. *Chem. Engin. J.* **2011**, *167*, 1.
(90) Cavenati, S.; Grande, C. A.; Rodrigues, A. E.; Kiener, C.; Muller, U. *Ind. Eng. Chem. Res.* **2008**, *47*, 6333.
(91) Müeller, U.; Lobree, L.; Hesse, M.; Yaghi, O.; Eddaoudi, M.; Shaped bodies containing metal—organic frameworks. U.S. Patent 2003/0222023 A1 (US 10/157182), filed on 30/05/2002, published on 04/12/2003.
(92) Müeller, U.; Lobree, L.; Hesse, M.; Yaghi, O.; Eddaoudi, M.; Shaped bodies containing metal—organic frameworks, BASF. U.S. Patent 6893564 B2 (US 10/157182) filed on 30/05/2002, published on 17/05/2005.
(93) Hesse, M.; Mueller, U.; Yaghi, O. Shaped bodies containing metal—organic frameworks. U.S. Patent 20090155588, filed 17/02/2009, published 18/06/2009
(94) Aguado, S.; Canivet, J.; Farrusseng, D. *Chem. Commun.* **2010**, 7999.
(95) Finsy, V.; Ma, L.; Alaerts, L.; De Vos, D. E.; Baron, G. V.; Denayer, J. R. M. *Microporous Mesoporous Mater.* **2009**, *120*, 221.
(96) Car, A.; Stropnik, C.; Peinemann, K.-V. *Desalination* **2006**, *200*, 424.
(97) Küsgens, P.; Zgaverdea, A.; Fritz, H-G; Siegle, S.; Kaskel, S. *J. Am. Ceram. Soc.* **2010**, *93* (9), 2476.
(98) Aleman, J.; Chadwick, A. V.; He, J.; Hess, M.; Jones., Horie K. *Pure Appl. Chem.* **2007**, *79*, 1801.
(99) Lohe, M. R.; Rose, M.; Kaskel, S. *Chem. Commun.* **2009**, 6056.
(100) Westcott, A.; Sumby, C. J.; Walshaw, R. D.; Hardie, M. J. *New J. Chem.* **2009**, *33*, 902.
(101) Huang, J.; He, L.; Zhang, J.; Chen, L.; Cheng-Yong, S. *J. Mol. Catal. A Chem.* **2010**, *317*, 97.
(102) Zhang, J. Y.; Wang, X.; He, L.; Chen, L.; Cheng-Yong, S.; James, S. L. *New J. Chem.* **2009**, *33*, 1070.

(103) Luisi, B. S.; Rowland, K. D.; Mouton, B. *Chem. Commun.* **2007**, 2802.
(104) Cho, C. Y.; Lo, J. S. *Dermatol. Clin.* **1998**, *16*, 25.
(105) Demessence, A.; Boissière, C.; Grosso, D.; Horcajada, P.; Serre, C.; Férey, G.; Soler-Illia, G. J. A. A.; Sanchez, C. *J. Mater. Chem.* **2010**, *20*, 7676.
(106) Liu, Y.; Ng, Z.; Khan, E. A.; Jeong, H-K; Ching, C-B; Lai, Z. *Microporous Mesoporous Mater.* **2009**, *118*, 296.
(107) Yoo, Y.; Lai, Z.; Jeong, H.-K. *Microporous Mesoporous Mater.* **2009**, *123*, 100.
(108) Guo, H. L.; Zhu, G. S.; Hewitt, I. J.; Qiu, S. L. *J. Am. Chem. Soc.* **2009**, *131*, 1646.
(109) Ranjan, R.; Tsapatsis, M. *Chem. Mater.* **2009**, *21*, 4920.
(110) (a) Bux, H.; Liang, F. Y.; Li, Y. S.; Cravillon, J.; Wiebcke, M.; Caro, J. *J. Am. Chem. Soc.* **2009**, *131*, 16000–16001. (b) Buxa, H.; Chmelikb, C.; Krishnac, R.; Caro, J. *J. Membr. Sci.* **2011**, *369*, 284.
(111) Venna, S. R.; Carreon, M. A. *J. Am. Chem. Soc.* **2010**, *132*, 76.
(112) McCarthy, M. C.; Varela-Guerrero, V.; Barnett, G. V.; Jeong, H.-K. *Langmuir* **2010**, *26*, 14636.
(113) Li, Y.-S.; Bu, H.; Feldhoff, A.; Li, G.-L.; Yang, W.-S.; Caro, J. *Adv. Mater.* **2010**, *22*, 3322.
(114) Li, Y.; Liang, F.; Bux, H.; Yang, W.; Caro, J. *J. Membr. Sci.* **2010**, *354*, 48.
(115) Bae, T.-H.; Lee, J. S.; Qiu, W.; Koros, W. J.; Jones, C. W.; Nair, S. *Angew. Chem., Int. Ed.* **2010**, *49*, 9863. (b) Huang, A.; Caro, J. *Angew. Chem., Int. Ed.* **2011**, *50*, 4979.
(116) Zornoza Martinez-Joaristi, A.; Serra-Crespo, P.; Tellez, C.; Coronas, J.; Gascon, J.; Kapteijn, F. *Chem. Commun.* **2011**, *47*, 9522.
(117) Perez, E. V.; Balkus, K. J.; Ferraris, J. P.; Musselman, I. H. *J. Membr. Sci.* **2009**, *328*, 165.
(118) Zhang, Y. F.; Musseman, I. H.; Ferraris, J. P.; Balkus, K. J. *J. Membr. Sci.* **2008**, *313*, 170.
(119) Car, A.; Stropnik, C.; Peinemann, K. V. *Desalination* **2006**, *200*, 424.
(120) Adams, R.; Carson, C.; Ward, J.; Tannenbaum, R.; Koros, W. *Microporous Mesoporous Mater.* **2010**, *131*, 13.
(121) Schwab, M. G.; Senkovska, I.; Rose, M.; Koch, M.; Pahnke, L.; Jonschker, G.; Kaskel, S. *Adv. Eng. Mater.* **2008**, *10*, 1151.
(122) Müeller, U.; Schubert, M.; Teich, F.; Puetter, H.; Schierle-Arndt, K.; Pastré, J. *J. Mater. Chem.* **2006**, *16*, 626.
(123) Küsgens, P.; Siegle, S.; Kaskel, S. *Adv. Eng. Mater.* **2009**, *11*, 93.
(124) Rose, M.; Böhringer, B.; Jolly, M.; Fischer, R.; Kaskel, S. *Adv. Engin.Mater.* **2011**, *13* (4), 356.
(125) Gref, R.; Minamitake, Y.; Peracchia, M. T.; Trubetskoy, V.; Torchilin, V.; Langer, R. *Science* **1994**, *263*, 1600.
(126) Rowe, M. D.; Thamm, D. H.; Kraft, S. L.; Boyes, S. G. *Biomacromolecules* **2009**, *10* (4), 983.
(127) Rowe, M. D.; Chang, C. C.; Thamm, D. H.; Kraft, S. L., Jr.; Harmon, J. F.; Vogt, A. P.; Sumerlin, B. S.; Boyes, S. G. *Langmuir* **2009**, *25* (16), 9487.
(128) Good, D. J.; Rodriguez-Hornedo, N. *Cryst. Growth. Des.* **2009**, *9*, 2252.
(129) Bis, J. A.; Vishweshwar, P.; Weyna, D.; Zaworotko, M. J. *Mol. Pharm.,.* **2007**, *4*, 401.
(130) Childs, S. L.; Wood, P. A.; Rodriguez-Hornedo, N.; Reddy, L. S.; Hardcastle, K. I. *Cryst. Growth. Des.* **2009**, *9*, 1869.
(131) Ma, Z.; Hopson, R.; Cai, C.; Han, S.; Moulton, B. *Cryst. Growth. Des.* **2010**, *10*, 2376.
(132) Xie, Y.; Yu, Z.; Huang, X.; Wang, Z.; Niu, L.; Teng, M.; Li, J. *Chem.—Eur. J.* **2007**, *13*, 9399.
(133) Rabone, J.; Yue, Y.-F.; Chong, S. Y.; Stylianou, K. C.; Bacsa, J.; Bradshaw, D.; Darling, G. R.; Berry, N. G.; Khimyak, Y. Z.; Ganin, A. Y.; Wiper, P.; Claridge, J. B.; Rosseinsky, M. J. *Science* **2010**, *329*, 1053.
(134) Srivatsana, S. G.; Parvezb, M.; Vermaa, S. *J. Inorg. Biochem.* **2003**, *97*, 340.
(135) Mantion, A.; Massüger, L.; Rabu, P.; Palivan, C.; McCusker, L. B.; Taubert, A. *J. Am. Chem. Soc.* **2008**, *130*, 2517.
(136) Yua, L.-C.; Chen, Z.-F.; Zhoua, C.-S.; Lianga, H.; Li, Y. *J. Coord. Chem.* **2005**, *58*, 1681.
(137) Wang, S.; Qin, J.; Wang, X.-L.; Qin, C.; Li, T.-T.; Su, Z.-M. *CrystEngCom* **2011**, *13*, 325.
(138) Miller, S. R.; Heurtaux, D.; Baati, T.; Horcajada, P.; Grenèche, J.-M.; Serre, C. *Chem. Commun.* **2010**, *46*, 4525.
(139) Miller, S. R.; Horcajada, P.; Serre, C. *Cryst. Eng. Comm.* **2011**, *13*, 1894.
(140) Agostoni V., Baati T., Ben-Yahia, Chalati T., Clayette P., Couvreur P., Cuhna, D., Eubank J. F., Gueutin C., Gref R, Miller S. R., Hillaireau H., Horcajada P., Kerkeni A., Maurin, G, Miller, S., Najjar F., Nefati F., Nejim L., Roger-Kreuz C., Serre C., Zakhama A. Unpublished work.
(141) Allan P. K., Ashbrook S. E., Chapman, K. W., Dawson D., Day S., Duren T., Eubank J. F., Griffin, J. M., Horcajada P., Hriljac J. A., McKinlay A. C., Mercer D., Mohideen M. I. H., Miller S. R., Morris, R. E., Morris Teat S. J., Serre C., Vimont A., Wheatley P., Williams J., Xiao B. Unpublished work.
(142) Moellmera, J.; Celerc, E. B.; Luebkeb, R.; Cairnsb, A. J.; Staudta, R.; Eddaoudi, M.; Thommes, M. *Microporous Mesoporous Mater.* **2010**, *129* (3), 345.
(143) Tsai, W.-J.; Shiao, Y.-J.; Lin, S.-J.; Chiou, W.-F.; Lin, L.-C.; Yang, T.-H.; Teng, C.-M.; Wu, T.-S.; Yang, L.-M. *Bioorg. Med. Chem. Let.* **2006**, *16*, 4440.
(144) Badawi, A. M.; Azzam, E. M. S.; Morsy, S. M. I. *Bioorg. Med. Chem.* **2006**, *14*, 8661.
(145) Kawahara, K.; Tsuruda, K.; Morishita, M.; Uchida, M. *Dental Materials* **2000**, *16*, 452.
(146) Fromm, K. M. *Coord. Chem. Rev.* **2008**, *252*, 856.
(147) Belser, K.; VigSlenters, T.; Pfumbidzai, C.; Upert, G.; Mirolo, L.; Fromm, K. M.; Wennemers, H. *Angew. Chem., Int. Ed.* **2009**, *48*, 3661.
(148) Dorn, T.; Fromm, K. M.; Janiak, C. *Aust. J. Chem.* **2006**, *59*, 22.
(149) Slenters, T. V.; Sagué, J. L.; Brunetto, P. S.; Zuber, S.; Fleury, A.; Mirolo, L.; Robin, A. Y.; Meuwly, M.; Gordon, O.; Landmann, R.; Daniels, A. U.; Fromm, K. M. *Materials* **2010**, *3*, 3407.
(150) Atmaca, S.; Gül, K.; Çiçek, R. *J. Med. Sci.* **1998**, *28*, 595.
(151) Mainardes, R. M.; Silva, L. P. *Curr. Drug Targets* **2004**, *5*, 449.
(152) Davis, M. E.; Chen, Z; Shin, D. M. *Nat Rev Drug Discovery* **2008**, *7*, 771.
(153) Peer, D; Karp, J. M.; Hong, S; Farokhzad, O. C.; Margalit, R; Langer, R. *Nature Nanotechnol.* **2007**, *2*, 751.
(154) Couvreur, P.; Tulkens, P.; Roland, M.; Trouet, A.; Speiser, P. *FEBS Lett.* **1977**, *84*, 323.
(155) Couvreur, P.; Vauthier, V. *Pharm. Res.* **2006**, *23*, 1417.
(156) Fattal, E.; Youssef, M.; Couvreur, P.; Andremont, A. *Antimicrob. Agents Chemother* **1989**, *33*, 1540.
(157) Qiu, L. Y.; Bae, Y. H. *Pharm. Res.* **2006**, *23* (1), 1.
(158) Samad, A.; Sultana, Y.; Aqil, M. *Current Drug Delivery* **2007**, *4* (4), 297.
(159) See special issue and references related. *Adv. Drug Deliv.Rev.*, **2008**, *60*.
(160) Peer, D.; Karp, J. M.; Hong, S.; Farokhzad, O. C.; Margalit, R.; Langer, R. *Nature Nanotechnol.* **2007**, *2*, 751.
(161) Dyer, A.; Morgan, S.; Wells, P.; Williams, C. *J. Helminthology* **2000**, *74* (2), 137.
(162) Horcajada, P.; Márquez-Alvarez, C.; Rámila, A.; Pérez-Pariente, J.; Vallet-Regi, M. *Solid State Sci.* **2006**, *8* (12), 1459.
(163) Arruebo, M.; Fernández-Pacheco, R.; Irusta, S.; Arbiol, J.; Ibarra, M. R.; Santamaría, J. *Nanotechnology* **2006**, *17*, 4057.
(164) Uglea, C. V.; Albu, I; Vatajanu, A; Croitoru, M; Antoniu, S; Panaitescu, L; Ottenbrite, R. M. *J. Biomater. Sci. Polym. Ed.* **1994**, *12*, 633.
(165) Pavelic, K; Hadzija, M; Bedrica, L; Pavelic, J; Dikic, I; Katic, M; Kralj, M; Bosnar, M. H.; Kapitanovic, S; Poljak-Blazi, M; Krizanac, S; Stojkovic, R; Jurin, M; Subotic, B; Colic, M *J. Mol. Med.* **2001**, *78*, 708.
(166) Levy, M. H.; Wheelock, E. F. *J Immunology* **1975**, *115*, 41.
(167) Vallet-Regi, M.; Ramila, A.; del Real, R. P.; Perez-Pariente, J. *Chem. Mater.* **2001**, *13*, 308.
(168) Slowing, I. I.; Trewyn, B. G.; Giri, S.; Lin, V. S.-Y. *Adv. Funct. Mater.* **2007**, *17*, 1225.

(169) Manzano, M.; Colilla, M.; Vallet-Regí, M. *Exp. Opin. Drug Delivery* **2009**, *6* (12), 1383.
(170) Rosenholm, J. M.; Sahlgren, C.; Lindén, M. *Nanoscale* **2010**, *2*, 1870.
(171) He, Q.; Shi, J. *J. Mater. Chem.* **2011**, *21*, 5845.
(172) Ambrogio, M. W.; Thomas, C. R.; Zhao, Y.-L.; Zink, J. I.; Stoddart, J. F. *Acc. Chem. Res.* **2011**, DOI: 10.1021/ar200018x.
(173) Liu, T.; Li, L.; Teng, X.; Huang., X.; Liu, H.; Chen, D.; Ren, J.; He, J.; Tang, F. *Biomater.* **2011**, *32*, 1657. Hudson, S. P.; Padera, R. F.; Langer, R.; Kohane, D. S. *Biomater.* **2008**, *29* (30), 4045. Xie, G.; Sun, J.; Zhong, G.; Shi, L.; Zhang, D. *Arch. Toxicol.* **2010**, *84* (3), 183.
(174) Nishimori, H.; Masuo, K.; Katsuhiro, I.; Shin-Ichi, T.; Yasuo, T.; Kiyohito, Y. *Eur. J. Pharm. Biopharm.* **2009**, *72*, 496.
(175) He, Q. J.; Zhang, Z. W.; Gao, F.; Li, Y. P.; Shi, J. L. *Small* **2011**, *7*, 271. Lu, J.; Liong, M.; Li, Z.; Zink, J. I.; Tamanoi, F. *Small* **2010**, *6*, 1794.
(176) Férey, G.; Serre, C.; Mellot-Draznieks, C.; Millange, F.; Surblé, S. *Angew. Chem., Int. Ed.* **2004**, *116*, 6456.
(177) Serre, C.; Millange, F.; Thouvenot, C.; Noguès, M.; Marsolier, G.; Louër, D.; Férey, G. *J. Am. Chem. Soc.* **2002**, *124*, 13519.
(178) Bourrelly, S.; Llewellyn, P. L.; Serre, C.; Millange, F.; Loiseau, T.; Férey, G. *J. Am. Chem. Soc.* **2005**, *127*, 13519.
(179) Llewellyn, P. L.; Horcajada, P.; Maurin, G.; Devic, T.; Rosenbach, N.; Bourrelly, S.; Serre, C.; Vincent, D.; Sorea-Serna, S.; Filinchuk, Y.; Férey, G. *J. Am. Chem. Soc.* **2009**, *131*, 13002.
(180) Millange, F.; Serre, C.; Guillou, N.; Férey, G.; Walton, R. I. *Angew. Chem., Int. Ed.* **2008**, *47*, 4100.
(181) Trung, T. K.; Trens, P.; Tanchoux, N.; Bourrelly, S.; Llewellyn, P. L.; Loera-Serna, S.; Serre, C.; Loiseau, T.; Fajula, F.; Férey, G. *J. Am. Chem. Soc.* **2008**, *130* (50), 16926.
(182) Horcajada, P.; Serre, C.; Maurin, G.; Ramsahye, N. A.; Vallet-Regí, M.; Sebban, M.; Taulelle, F.; Férey, G. *J. Am. Chem. Soc.* **2008**, *130*, 6774.
(183) Yang, B. B.; Abel, R. B.; Uprichard, A. C. G.; Smithers, J. A.; Forgue, S. T. *J. Clin. Pharmacol.* **1996**, *36*, 623.
(184) Vassal, G.; Gouyette, A.; Hartmann, O.; Pico, J. L.; Lemerle, J. *Cancer Chemother. Pharmacol.* **1989**, *24*, 386.
(185) Nashyap, A.; Wingard, J.; Cagnoni, P.; Roy, J.; Tarantolo, S.; Hu, W.; Blume, K.; Niland, J.; Palmer, J. M.; Vaughan, W.; Fernandez, H.; Champlin, R.; Forman, S.; Andersson, B. S. *Biol. Blood Marrow Transplant.* **2002**, *8*, 493.
(186) Baron, F.; Deprez, M.; Beguin, Y. *Haematologica* **1997**, *82*, 718.
(187) Layre A., Gref R., Richard J., Requier D., Couvreur P., Nanoparticules polymériques composites FR 04 07569, 7 july 2004
(188) Layre, A.; Couvreur, P.; Chacun, H.; Richard, J.; Passirani, C.; Requier, D.; Benoit, J. P.; Gref, R. *J. Controlled Release* **2006**, *111*, 271.
(189) Chalati, T.; Horcajada, P.; Couvreur, P.; Serre, C.; Maurin, G.; Gref, R. *Nanomedicine* **2011**, DOI: 10.2217/NNM.1169.
(190) Li, X.; Chan, W. K. *Adv. Drug Delivery Rev.* **1999**, *39*, 81.
(191) Kukhanova, M.; Krayevsky, A.; Prusoff, W.; Cheng, Y. C. *Curr. Pharm. Des.* **2000**, *6*, 585.
(192) Loke, S. L.; Stein, C A; Zhang, X H; Mori, K; Nakanishi, M; Subasinghe, C; Cohen, J S. *Proc. Natl. Acad. Sci. U.S.A.* **1989**, *86*, 3474.
(193) Hillaireau, H.; Le Doan, T.; Appel, M.; Couvreur, P. *J. Contr. Release* **2006**, *116*, 346.
(194) Xiaoling, L.; Chan, W. K. *Adv. Drug Delivery Rev.* **1999**, *39*, 81.
(195) Thierry, A. R.; Vige, D; Coughlin, S. S.; Belli, J. A.; Dritschilo, A; Rahman, A *The FASEB J.* **1993**, *7*, 572.
(196) Bennis, S.; Chapey, C.; Couvreur, P.; Robert, J. *Eur. J. Cancer* **1994**, *30A*, 89.
(197) Ke, F.; Yuan, Y.-P.; Qiu, L.-G.; Shen, Y.-H.; Xie, A.-J.; Zhu, J.-F.; Tian, X.-Y.; Zhang, L.-D. *J. Mater. Chem.* **2011**, *21*, 3843.
(198) Alaerts, L.; Kirschhock, C. E. A.; Maes, M.; van der Veen, M. A.; Finsy, V.; Depla, A.; Martens, J. A.; Baron, G. V.; Jacobs, P. A.; Denayer, J. F. M.; De Vos, D. E. *Angew. Chem., Int. Ed* **2007**, *46*, 4293.
(199) Lam, A.; Sierra, L. R.; Rojas, G.; Rivera, A.; Rodriguez-Fuentes, G.; Montero, L. A. *Microporous Mesoporous Mater.* **1998**, *23*, 247.
(200) Lam, A.; Rivera, A.; Rodriguez-Fuentes, G. *Microporous Mesoporous Mater.* **2001**, *49*, 157.
(201) Lam, A.; Rivera, A. *Microporous Mesoporous Mater.* **2006**, *91*, 181.
(202) Nunes, C. D.; Vaz, Pedro D.; Fernandes, Ana C.; Ferreira, P.; Romao, C. C.; Calhorda, M. J. *Eur. J. Pharm. Biopharm.* **2007**, *66*, 357.
(203) Mohanambe, L.; Vasudevan, S. *J. Phys. Chem. B* **2005**, *109*, 15651.
(204) Babarao, R.; Jiang, J. *J. Phys. Chem. C* **2009**, *113*, 18297.
(205) Mellot-Draznieks, C. *J. Mater.Chem.* **2007**, *17*, 4348.
(206) Salles, F.; Maurin, G.; Serre, C.; Llewellyn, P. L.; Knofel, C.; Choi, H. J.; Long, J. R.; Filinchuk, Y.; Férey, G. *J. Am. Chem. Soc.* **2010**, *132*, 13782.
(207) Salles, F.; Ghoufi, A.; Maurin, G.; Bell, R. G.; Mellot-Draznieks, C.; Férey, G. *Angew. Chem., Int. Ed.* **2008**, *47*, 8487.
(208) Férey, G.; Serre, C.; Devic, T.; Maurin, G.; Jobic, H.; Llewellyn, P. L.; De Weireld, G.; Vimont, A.; Daturi, M.; Chang, J. S. *Chem. Soc. Rev.* **2011**, *40*, 550.
(209) Walker, A. M.; Civalleri, B.; Slater, B.; Mellot-Draznieks, C.; Cora, F.; Zicovich-Wilson, C. M.; Roman Perez, G.; Soler, J. M.; Gale, J. D. *Angew. Chem., Int. Ed.* **2010**, *49*, 7501.
(210) Manzano, F.; Cauda, V.; Colilla, M.; Delgado, M. R.; Vallet-Regi, M. *Chem. Eng. J.* **2008**, *137*, 30.
(211) Rosenholm, J. M.; Linden, M. *J. Controlled Release* **2008**, *128*, 157.
(212) Vallet-Regi, M.; Collila, M.; Gonzalez, B. *Chem. Soc. Rev.* **2011**, *40*, 596.
(213) Do, D. Q.; Rowe, R. C.; York, P. *Int. J. Pharm.* **2008**, *351*, 194.
(214) Obiol-Pardo, C.; Gomis-Tena, J.; Sanz, F.; Saiz, J.; Pastor, M. *J. Chem. Inf. Model* **2011**, *51*, 483.
(215) Varnek, A.; Gaudin, C.; Marcou, G.; Baskin, I.; Pandey, A. K.; Tetko, I. V. *J. Chem. Inf. Model* **2009**, *49*, 133.
(216) Burello, E.; Rothenberg, G. *Int. J. Mol. Sci.* **2006**, *7*, 375.
(217) Leflaive, P.; Pirngruber, G.; Faraj, A.; Martin, P.; Baron, G. V.; Denayer, J. F. M. *Microporous Mesoporous Mater.* **2010**, *132*, 246.
(218) Goulon, A.; Faraj, A.; Pirngruber, G.; Jacquin, M.; Porcheron, F.; Leflaive, P.; Martin, P.; Baron, G. V.; Denayer, J. F. M. *Catal. Today* **2011**, *159*, 74.
(219) Kim, D.; Kim, J.; Jung, D. H.; Lee, T. B.; Choi, S. B.; Yoon, J. H.; Kim, J.; Choi, K.; Choi, S.-H. *Catal. Today* **2007**, *120*, 317.
(220) Gaudin, C.; Paula de Cuhna, D.; Ivanoff, E.; Horcajada, P.; Serre, C.; Maurin, G. *Microporous Mesoporous Mater.* **2011**, DOI: 10.1016/j.micromeso.2011.06.011.
(221) Fromm, K. M. *Coord. Chem. Rev.* **2008**, *252*, 856.
(222) Belser, K.; VigSlenters, T.; Pfumbidzai, C.; Upert, G.; Mirolo, L.; Fromm, K. M.; Wennemers, H. *Angew. Chem., Int. Ed.* **2009**, *48*, 3661.
(223) Dorn, T.; Fromm, K. M.; Janiak, C. *Aust. J. Chem.* **2006**, *59*, 22.
(224) Slenters, T. V.; Sagué, J. L.; Brunetto, P. S.; Zuber, S.; Fleury, A.; Mirolo, L.; Robin, A. Y.; Meuwly, M.; Gordon, O.; Landmann, R.; Daniels, A. U.; Fromm, K. M. *Materials* **2010**, *3*, 3407.
(225) Wang, R. *FASEB J.* **2002**, *16*, 1792.
(226) Ignarro, L. J.; Buga, G. M.; Wood, K. S.; Byrns, R. E.; Chaudhuri, G. *Proc. Natl. Acad. Sci. U.S.A.* **1987**, *84*, 9265.
(227) Palmer, R. M. J.; Ferrige, A. G.; Moncada, S. *Nature* **1987**, *327*, 524.
(228) Morris, R. E.; Wheatley, P. S. *Angew. Chem. Int. Ed.* **2008**, *47*, 4966.
(229) Smith, D. J.; Chakravarthy, D.; Pulfer, S.; Simmons, M. L.; Hrabie, J. A.; Citro, M. L.; Saavedra, J. E.; Davies, K. M.; Hutsell, T. C.; Mooradian, D. L.; Hanson, S. R.; Keefer, L. K. *J. Med. Chem.* **1996**, *39*, 1148.
(230) Keefer, L. K. *Nat. Mater.* **2003**, *2*, 357.
(231) Wheatley, P. S.; Butler, A. R.; Crane, M. S.; Rossi, A. G.; Megson, I. L.; Morris, R. E. *Molecular Sieves: from Basic Research to Industrial Applications, Pts A and B* **2005**, *158*, 2033.
(232) Xiao, B.; Wheatley, P. S.; Morris, R. E. In *From Zeolites to Porous MOF Materials—The 40th Anniversary of International Zeolite Conference*; Xu, R., Gao, Z., Chen, J., Yan, W., Ed.; Elsevier: 2007; p 902.
(233) Wheatley, P. S.; Butler, A. R.; Crane, M. S.; Fox, S.; Xiao, B.; Rossi, A. G.; Megson, I. L.; Morris, R. E. *J. Am. Chem. Soc.* **2006**, *128*, 502.

(234) Wheatley, P. S.; Butler, A. R.; Crane, M. S.; Rossi, A. G.; Megson, I. L.; Morris, R. E. In *Molecular Sieves: from Basic Research to Industrial Applications, Pts a and B*; Cejka, J., Zilkova, N., Nachtigall, P., Eds., 2005; Vol. 158, p 2033.
(235) Mowbray, M.; Tan, X. J.; Wheatley, P. S.; Morris, R. E.; Weller, R. B. *J. Invest. Dermatol.* **2008**, *128*, 352.
(236) Fox, S.; Wilkinson, T. S.; Wheatley, P. S.; Xiao, B.; Morris, R. E.; Sutherland, A.; Simpson, A. J.; Barlow, P. G.; Butler, A. R.; Megson, I. L.; Rossi, A. G. *Acta Biomater.* **2001**, *6*, 1515.
(237) McKinlay, A. C.; Morris, R. E.; Horcajada, P.; Férey, G.; Gref, R.; Couvreur, P.; Serre, C. *Angew. Chem., Int. Ed.* **2010**, *49*, 6260.
(238) Bordiga, S.; Regli, L.; Bonino, F.; Groppo, E.; Lamberti, C.; Xiao, B.; Wheatley, P. S.; Morris, R. E.; Zecchina, A. *Phys. Chem. Chem. Phys.* **2007**, *9*, 2676.
(239) Dietzel, P. D. C.; Panella, B.; Hirscher, M.; Blom, R.; Fjellvåg, H. *Chem. Commun* **2006**, 959.
(240) Dietzel, P. D. C.; Morita, Y.; Blom, R.; Fjellvåg, H. *Angew. Chem., Int. Ed.* **2005**, *44*, 6358.
(241) Xiao, B.; Wheatley, P. S.; Zhao, X. B.; Fletcher, A. J.; Fox, S.; Rossi, A. G.; Megson, I. L.; Bordiga, S.; Regli, L.; Thomas, K. M.; Morris, R. E. *J. Am. Chem. Soc.* **2007**, *129*, 1203.
(242) Yoon, J. W.; Seo, Y-K; Hwang, Y-K; Chang, J.-S.; Leclerc, H.; Wuttke, S.; Bazin, P.; Vimont, A.; Daturi, M.; Bloch, E.; Llewellyn, P. L.; Serre, C.; Horcajada, P.; Grenèche, J.-M.; Rodrigues, A. E.; Férey, G. *Angew. Chem., Int. Ed.* **2010**, *49*, 5949.
(243) Loiseau, T.; Serre, C.; Huguenard, C.; Fink, G.; Taulelle, F.; Henry, M.; Bataille, T.; Férey, G *Chem.—Eur. J.* **2004**, *10*, 1373.
(244) Hinks, N. J.; McKinlay, A. C.; Xiao, B.; Wheatley, P. S.; Morris, R. E. *Microporous Mesoporous Mater.* **2010**, *129*, 330.
(245) Ingleson, M. J.; Heck, R.; Gould, J. A.; Rosseinsky, M. J. *Inorg. Chem.* **2009**, *48*, 9986.
(246) Nguyen, J. G.; Tanabe, K. K.; Cohen, S. M. *Cryst. Eng. Comm.* **2010**, *12*, 2335.
(247) Xiao, B.; Byrne, P. J.; Wheatley, P. S.; Wragg, D. S.; Zhao, X. B.; Fletcher, A. J.; Thomas, K. M.; Peters, L.; Evans, J. S. O.; Warren, J. E.; Zhou, W. Z.; Morris, R. E. *Nat. Chem.* **2009**, *1*, 289.
(248) Allan, P. K.; Xiao, B.; Teat, S. J.; Knight, J. W.; Morris, R. E. *J. Am. Chem. Soc.* **2010**, *132*, 3605.
(249) Allan, P. K.; Teat, S. J.; Hriljac J. A.; Chapman, K. W.; Morris, R. E. **2011**, submitted
(250) Shimomura, S.; Higuchi, M.; Matsuda, R.; Yoneda, K.; Hijikata, Y.; Kubota, Y.; Mita, Y.; Kim, J.; Takata, M.; Kitagawa, S. *Nature Chem.* **2010**, *2*, 633.
(251) Mohideen, M. I. H.; Xiao, B.; Wheatley, P. S.; McKinlay, A. C.; Li, Y.; Slawin, A. M. Z.; Aldous, D. S.; Cessford, N.; Duren, T.; Zhao, X. B.; Gill, R.; Thomas, K. M.; Griffin, J. M.; Ashbrook, S. E.; Morris, R. E. *Nat. Chem.* **2011**, *3*, 304.
(252) Dietel, P. D. C.; Johnsen, R. E.; Blom, R.; Fjellvag, H. *Chem.—Eur. J.* **2008**, *14*, 2389.
(253) Zhou, W.; Wu, H.; Yildrim, T. *J. Am. Chem. Soc.* **2008**, *130*, 15286.
(254) Morris, R. E. *Nat. Chem.* **2011**, *3*, 347.
(255) Shibuya, N.; Mikami, Y.; Kimura, Y.; Nagahara, N.; Kimura, H. *J. Biochem.* **2009**, *146* (5), 623.
(256) Kimura, Y.; Goto, Y. I.; Kimura, H. *Antioxid. Redox Signaling* **2010**, *12*, 1.
(257) Kimura, Y.; Dargusch, R.; Schubert, D.; Kimura, H. *Antioxid. Redox Signaling* **2006**, *8*, 661.
(258) Blackstone, E.; Morrison, M.; Roth, M. B. *Science* **2005**, *308*, 518.
(259) Drew, K. L.; Rice, M. E.; Kuhn, T. B.; Smith, M. A. *Free Radical Biol. Med.* **2001**, *31*, 563.
(260) Carey, H. V.; Andrews, M. T.; Martin, S. L. *Physiol. Rev.* **2003**, *83*, 1153.
(261) Papapetropoulos, A.; Pyriochou, A.; Altaany, Z.; Yang, G. D.; Marazioti, A.; Zhou, Z. M.; Jeschke, M. G.; Branski, L. K.; Herndon, D. N.; Wang, R.; Szabo, C. *Proc. Natl. Acad. Sci. U.S.A.* **2009**, *106*, 21972.
(262) Whiteman, M.; Bhatia, M.; Moore, P. K. *Inflammation Res.* **2005**, *54*, S200.
(263) Bhatia, M.; Sidhapuriwala, J. N.; Sparatore, A.; Moore, P. K. *Inflammation Res.* **2005**, *54*, S185.
(264) Chen, Y. H.; Wu, R.; Geng, B.; Qi, Y. F.; Wang, P. P.; Yao, W. Z.; Tang, C. S. *Cytokine* **2009**, *45*, 117.
(265) Li, L.; Hsu, A.; Moore, P. K. *Pharmacol. Therap.* **2009**, *123*, 386.
(266) Johansen, D.; Ytrehus, K.; Baxter, G. F. *Basic Res. Cardiol.* **2006**, *101*, 53.
(267) Hamon, L.; Leclerc, H.; Ghoufi, A.; Oliviero, L.; Travert, A.; Lavalley, J. C.; Devic, T.; Serre, C.; Férey, G.; De Weireld, G.; Vimont, A.; Maurin, G. *J. Phys. Chem. C* **2011**, *115*, 2047.
(268) Hamon, L.; Serre, C.; Devic, T.; Loiseau, T.; Millange, F.; Férey, G.; De Weireld, G. *J. Am. Chem. Soc.* **2009**, *131*, 8775.
(269) Barthelet, K.; Marrot, J.; Riou, D.; Férey, G. *Angew. Chem., Int. Ed.* **2002**, *41*, 281.
(270) Petit, C.; Mendoza, B.; Bandosz, T. J. *Chem. Phys. Chem.* **2010**, *11*, 3678.
(271) Allan, P. K.; Wheatley, P. S.; Aldous, D. W., Mohideen, M. I.; Tang, C.; Hriljac, J. A.; Megson, I. L.; Chapman, K. W., De Weireld, G.; Vaesen S.; Morris, R. E. **2011**, submitted
(272) Emsley, J. *Molecules of Murder: Criminal Molecules and Classic Cases*; RSC Pub.: Cambridge, U.K., 2008.
(273) Foresti, R.; Motterlini, R. *Free Radical Res.* **1999**, *31*, 459.
(274) Gorman, D.; Drewry, A.; Huang, Y. L.; Sames, C. *Toxicology* **2003**, *187*, 25.
(275) Piantadosi, C. A. *Antioxid. Redox Signaling* **2002**, *4*, 259.
(276) Berk, P. D.; Rodkey, F. L.; Blaschke, T. F.; Collison, H. A.; Waggoner, J. G. *J. Lab. Clin. Med.* **1974**, *83*, 29.
(277) Maines, M. D. *Annu. Rev. Pharmacol. Toxicol.* **1997**, *37*, 517.
(278) Motterlini, R.; Clark, J. E.; Foresti, R.; Sarathchandra, P.; Mann, B. E.; Green, C. J. *Circ. Res.* **2002**, *90*, E17.
(279) Alberto, R.; Motterlini, R. *Dalton Trans.* **2007**, 1651.
(280) Nakao, A.; Choi, A. M. K.; Murase, N. *J. Cell. Mol. Med.* **2006**, *10*, 650.
(281) Chavan, S.; Vitillo, J. G.; Groppo, E.; Bonino, F.; Lamberti, C.; Dietzel, P. D. C.; Bordiga, S. *J. Phys. Chem. C* **2009**, *113* (8), 3292.
(282) Banerjee, R.; Phan, A.; Wang, B.; Knobler, C.; Furukawa, H.; O'Keeffe, M.; Yaghi, O. M. *Science* **2008**, *319*, 939.
(283) Seo, Y.-K.; Yoon, J. W.; Lee, J. S.; Hwang, Y. K.; Chang, J.-S.; Wuttke, S.; Vimont, A.; Bourrelly, S.; Llewellyn, P.; Daturi, M.; Horcajada, P.; Serre, C.; Férey, G.; *Adv. Mater.* **2011**, accepted for publication.
(284) Soma, C. E.; Dubernet, C.; Barratt, G.; Benita, S. *J. Controlled Release* **2000**, *68*, 283.
(285) Chouly, C.; Pouliquen, D.; Lucet, I.; Jeune, J. J.; Jallet, P. J. *Microencapsulation* **1996**, *13*, 245.
(286) Owens, D. E.; Peppas, N. A. *Int. J. Pharm.* **2006**, *307*, 93.
(287) Weir, M. P.; Gibson, J. F.; Peters, T. J. *Cell Biochem.Funct.* **1984**, *2*, 186.
(288) Damade, R.; Rosenthal, E.; Cacoub, P. *Ann Med Interne* **2000**, *151*, 169.
(289) Bloom, W., Fawcett, D. W. *a Text Book of Histology*, 11 ed.; Saunders, Philadelphia, 1986.
(290) Moghimi, S. M. H.; A., C.; Murray, J. C. *Pharmacol. Rev* **2001**, *53*, 283.
(291) Okon, E.; Pouliquen, D.; Okon, P.; Kovaleva, Z. V.; Stepanova, T. P.; Lavit, S. G.; Kudryavtsev, B. N.; Jallet, P. *Lab. Invest.* **1994**, *71*, 895.
(292) Anthony, S.; Tavill, B. R. B. *Hepatology* **1986**, *6*, 142.
(293) Bassett, M. L.; Halliday, J. W.; Powell, L. W. *Hepatology* **1986**, *6*, 24.
(294) Bourrinet, P.; Bengele, H. H.; Bonnemain, B.; Dencausse, A.; Idee, J. M.; Jacobs, P. M.; Lewis, J. M. *Invest. Radiol.* **2006**, *41*, 313.
(295) Baati T., Horcajada P., David O., Gref R., Couvreur P., Serre C., 2011, submitted.
(296) Baati, T.; Horcajada, P.; Gref, R.; Couvreur, P.; Serre, C. *J. Pharm. Biomd. Anal.* **2011**, *56*, 758.
(297) Briley-Saebo, K.; Bjornerud, A.; Grant, D.; Ahlstrom, H.; Berg, T.; Kindberg, G. M. *Cell Tissue Res.* **2004**, *316*, 315.
(298) Puntarulo, S. *Mol. Aspects Med.* **2005**, *26*, 299.

(299) Mehta, S. H.; Webb, R. C.; Ergul, A.; Tawak, A.; Dorrance, A. M. *Am. J. Physiol. Regul. Integr. Comp. Physiol.* **2004**, *286*, R283.
(300) Bassett, M. L.; Halliday, J. W.; Powell, L. W. *Hepatology* **1986**, *6*, 24.
(301) Shi, H.; Bencze, K. Z.; Stemmler, T. L.; Philpott, C. C. *Science* **2008**, *320*, 1207.
(302) Hentze, M. W.; Muckenthaler, M. U.; Andrews, N. C. *Cell* **2004**, *117*, 285.
(303) TWth, V., Helm, L., Merbach, A. E. In *The Chemistry of Contrast Agents in Medicinal Magnetic Resonance Imaging*; Merbach, A. E., TWth, V., Eds.; Wiley: Chischester, U.K., 2001; p 45.
(304) Aime, S., Botta, M., Fasano, M. Terreno, E. In *Protein-Bound Metal Chelates in Chemistry of Contrast Agents in Medical Magnetic Resonance Imaging*; Merbach, A. E., TWth, V., Eds.; Wiley: Chichester, U.K., 2001, 193.
(305) Torchilin, V. P. *Curr. Pharm. Biotechnol.* **2000**, *1*, 183.
(306) Aime, S.; Botta, I. M.; Fedeli, F.; Gianolio, E.; Terreno, E.; Anelli, P. *Chem.—Eur. J.* **2001**, *7*, 5261.
(307) Zhang, Z.; Greenfield, M. T.; Spiller, M.; McMurry, T. J.; Lauffer, R. B.; Caravan, P. *Angew. Chem., Int. Ed.* **2005**, *44*, 6766.
(308) Sosnovik, D. E.; Weissleder, R. *Curr.Opin.Biotechnol.* **2007**, *18*, 4.
(309) Erdogan, S.; Roby, A.; Sawant, R.; Hurley, J.; Torchilin, V. *J. Liposome Res.* **2006**, *16*, 45.
(310) Mulder, W. J.; Strijkers, G. J.; van Tilborg, G. A.; Griffioen, A. W.; Nicolay, K. *NMR Biomed.* **2006**, *19*, 142.
(311) Othman, M; Bouchemal, K; Couvreur, P; Gref, R *Int. J. Pharm.* **2009**, *379*, 218.
(312) Morawski, A. M.; Lanza, G. A.; Wickline, S. A. *Curr. Opin. Biotechnol.* **2005**, *16*, 89.
(313) Holz, M. *Magn. Reson. Chem.* **1993**, *31*, S154.
(314) Della Rocca, J.; Liu, D.; Lin, W. *Acc. Chem. Res.* **2011**, *44* (10), 957.
(315) Rowe, M. D.; Thamm, D. H.; Kraft, S. L.; Boyes, S. G. *Biomacromolecules* **2009**, *10* (4), 983.
(316) Rowe, M. D.; Chang, C. C.; Thamm, D. H.; Kraft, S. L., Jr.; Harmon, J. F.; Vogt, A. P.; Sumerlin, B. S.; Boyes, S. G. *Langmuir* **2009**, *25* (16), 9487.
(317) Aime, S.; Caravan, P. *J. Magn. Reson. Imaging* **2009**, *30*, 1259.
(318) Holler, C. J.; Muller-Buschbaum, K. *Inorg. Chem.* **2008**, *47* (21), 10141.
(319) Pereira, G. A.; Peters, J. A.; Paz, F. A.; Rocha, J.; Geraldes, C. F. *Inorg. Chem.* **2010**, *49* (6), 2969.
(320) Gref, R.; Domb, A.; Quellec, P.; Blunk, T.; Müller, R. H.; Verbavatz, J. M.; Langer, R. *Adv. Drug Delivery Rev.* **1995**, *16*, 215.
(321) Imaz, I.; Hernando, J.; Ruiz-Molina, D.; Maspoch, D. *Angew. Chem., Int. Ed.* **2009**, *48*, 2325. Imaz, I.; Rubio-Martinez, M.; Garcia-Fernandez, L.; Garcia, F.; Ruiz-Molina, D.; Hernando, J.; Puntes, V.; Maspoch, D. *Chem.Commun.* **2010**, *46*, 4737.
(322) Imaz, I.; Hernando, J.; Ruiz-Molina, D.; Maspoch, D. *Angew. Chem., Int. Ed.* **2009**, *48*, 2325.
(323) Liu, D.; Huxford, R. C.; Lin, W. *Funct. Coord. Polym.* **2011**, *50* (16), 3696.
(324) Nishiyabu, R.; Hashimoto, N.; Cho, T.; Watanabe, K.; Yasunaga, T.; Endo, A.; Kaneko, K.; Niidome, T.; Murata, M.; Adachi, C.; Katayama, Y.; Hashizume, M.; Kimizuka, N. *J. Am. Chem. Soc.* **2009**, *131*, 2151.
(325) Nishiyabu, R.; Aime, C.; Gondo, R.; Noguchi, T.; Kimizuka, N. *Angew. Chem., Int. Ed.* **2009**, *48*, 9465.
(326) Nishiyabu, R.; Aime, C.; Gondo, R.; Kaneko, K.; Kimizuka, N. *Chem. Commun.* **2010**, *46*, 4333.
(327) Dekrafft, K. E.; Xie, Z. G.; Cao, G. H.; Tran, S.; Ma, L.; Zhou, O. Z.; Lin, W. *Angew. Chem., Int. Ed.* **2009**, *48*, 9901.